UNIVERSITÀ DI PARMA

UNIVERSITY OF PARMA

Ph.D. IN BIOTECHNOLOGY AND LIFE SCIENCES

CYCLE XXXIV

Hyperoxia-exposed preterm rabbit BPD models biomolecular characterization

Coordinator:

Chiar.mo Prof. Marco Ventura

Tutor:

Chiar.mo Prof. Simone Ottonello

Ph.D. student: Matteo Storti

Academic years 2018/2021

Abstract

Bronchopulmonary dysplasia (BPD) is a chronic lung disease that represents the most common complication in preterm babies with adverse consequences in adulthood. BPD is a complex and multifactorial disease, and its development relies on several prenatal and postnatal causal factors which alter alveolar growth, pulmonary vascular development, and inflammation. This complex etiology, and the scarcity of human pathology specimens available, hamper the development of effective therapies, therefore BPD animal models are key tools to investigate the precise mechanisms leading to BPD. The preterm rabbit model incorporates the positive aspects of both small (mice and rats) and large animal (baboons and lambs) models used to study BPD pathophysiology so far. Continuous exposure to high oxygen concentration (95% O_2) for 7 days induces functional and morphological lung changes in preterm rabbits that resemble those observed in BPD-affected babies. To date, the molecular characterization of the BPD onset in this model is missing, therefore the main aim of this thesis was to characterize the 95% hyperoxia exposed preterm rabbit model for 7 days (post-natal day = PND7) by a multi-disciplinary approach to i) characterize the histological and molecular changes during BPD development and ii) confirm the translational potential of the preterm rabbit as BPD model for new therapeutic strategies development. We found hyperoxia exposure induced the arrest of lung and vasculature development and lung injury compared to normoxia at day 7. Moreover, several processes have been found dysregulated by hyperoxia exposure. Inflammatory and cell death processes were up-regulated whereas lung and vasculature development ones were down-regulated. We have also identified 42 genes as strongly correlated with BPD development, whose signature would be useful for future evaluations of new pharmacological treatments' therapeutic effects.

An extended version (up to 14 days) of the PND7 preterm rabbit model has been set up and validated in Chiesi Farmaceutici, using 70% of oxygen instead of 95%. This long-term BPD model would

bypass the high oxygen concentrations (O_2> 40%) no longer used in the Neonatal Intensive Care Unit (NICU). Additionally, the short experimental timeframe of the PND7 BPD model impedes testing any therapeutic treatments, since a preventative approach is the only feasible. For these reasons, we characterized the histological features and gene expression patterns of the previously selected 42 genes on day 14. The histological and gene expression analysis showed that normoxic preterm pups, and even more those hyperoxia-exposed, have a lung growth delay when compared to their age-matched controls born at term. Moreover, comparison analyses have been performed in order to highlight the different phenotypes between days 7 and 14 models. Both histology and gene expression analysis revealed that the PND14 model has a milder phenotype than the PND7 one, and we identified a preterm influence on lung development in PND14 pups that was missed in the PND7 one.

The overall of these analyses demonstrated the high translational value of our preterm rabbit models to study BPD development and pathophysiology. Finally, deep molecular characterization of both animal models will be crucial for identifying new targets and pathways that can be used to build novel BPD preventative and therapeutic treatments.

Table of Contents

1. Introduction

1.1 The different stages of human lung development

The physiological period of gestation starts with the fertilization of the egg cell and lasts 40 weeks or 9 months [1]. It can be divided into 3 main periods: zygote (from egg cell fertilization up to the end of the 2nd week), embryonic (from the 3rd up to the 8th week), and fetal period (from the 9th up to the 40th week) (Figure 1).

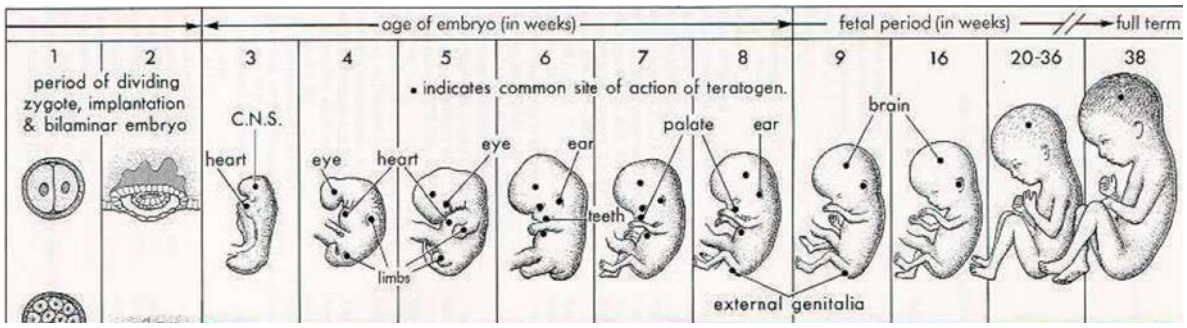

Figure 1. Embryo development phases (image adapted from Moore KL. et al [1])

Lung development is a finely orchestrated process that occurs through five phases during physiological fetal growth, starting from small anterior foregut endoderm cells, in the embryonic period, to a more complex structure composed of different cell populations, in the alveolar period [2]. The development of the lung parallels the pulmonary circulation one [3] (Figure 2):

Embryonic period (from the 4th to the 6th week): the embryonic period is essential for organogenesis and organ development. In the beginning, the lung appears as a prominence in the primitive oesophagus. The trachea develops from the epithelial cells of the foregut endoderm and branches into the right and left main bronchi, and then into lobar and segmental bronchi [4]. The vasculogenesis and angiogenesis start in this period around airways bud [5].

Pseudoglandular period (from the 6th to the 16th week): during this stage, the branches undergo a process of morphogenesis, resembling exocrine glands [5,6]. At the end of this stage, all the

conducting airways and terminal bronchioles are formed, and pre-acinar structures, including pulmonary arteries and veins, appear on the respiratory tree [5].

Canicular period (from the 16th to the 24th week): the respiratory tree starts to expand in length and diameter, along with vascularization and angiogenesis which are important for the future air-blood barrier formation, and the terminal bronchioles divide into respiratory bronchioles and alveolar ducts [6]. Furthermore, the alveolar epithelium differentiates into type 1 and type 2 epithelial cells with lamellar bodies by the end of the 20th week [7]. Type 1 cells line the alveolar surface to form the blood-air barrier and maintain the physiological structure of the lung tissue. Type 2 cells are crucial for normal lung development since they are devoted to the production and secretion of surfactant, which allows the alveoli expansion during inspiration and avoids the alveoli collapse during expiration [8].

Saccular period (from the 24th to the 36th week): at the beginning of this phase, the terminal airways form clusters of thin-walled terminal saccule, which in turn will generate the alveolar sacs during the last lung development phase [3]. Furthermore, the secretory activity of alveolar surfactant by type 2 alveolar cells increases in this phase, along with the vascular system expansion [9]. This latter allows the capillary network to form a double vascular layer in the walls between the sacs [3].

Alveolar period (from the 36th week of gestation to the 2nd postnatal year): alveolarization is the final stage of lung development and it is predominantly a postnatal event [6]. In this stage, the thin-walled terminal saccules shape the last generation of airways: alveolar ducts and alveolar sacs. Septation is another process that occurs during the alveolar period, which is pivotal to subdivide the airspaces and to form the alveoli. At the same time, it occurs a remodelling of the double capillary network, which gradually merges as a single capillary layer [5]. This period starts at the end of gestation and continues until the second year of life [4].

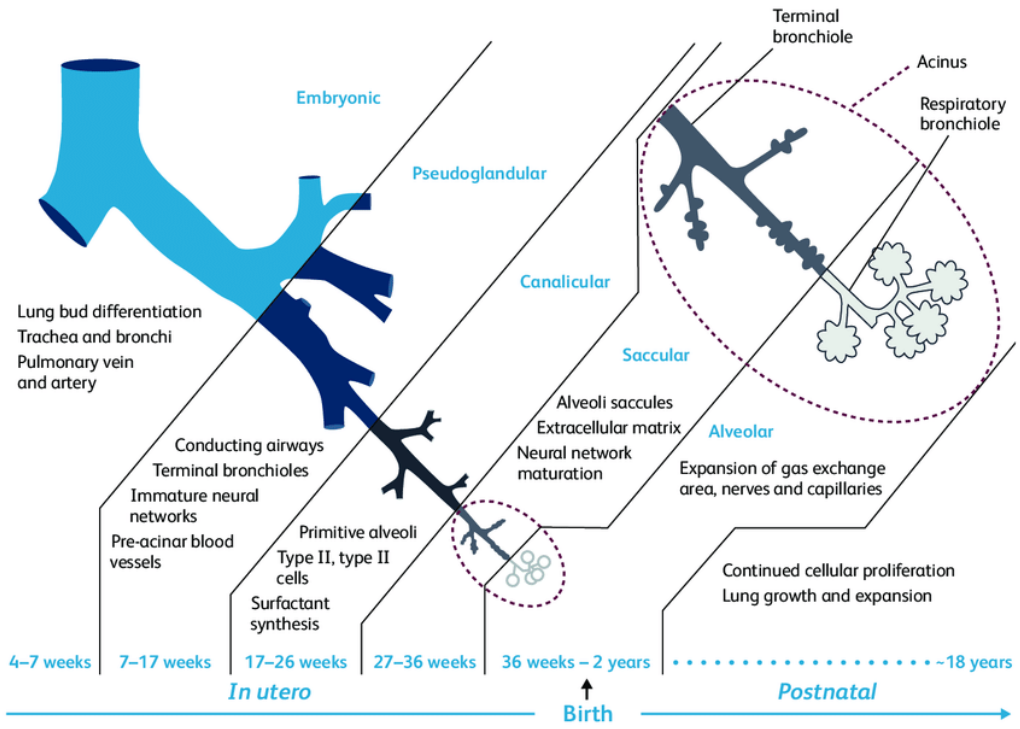

Figure 2. Stages of lung development (image adapted from Kajekar et al [10])

1.2 Prematurity and current strategies

Preterm birth is commonly defined as birth before the 37th week of gestation [7]. Preterm birth is the main cause of neonatal mortality all over the world and it has become an important social and health problem, with a global incidence of approximately 15 million per year [11]. Infants born preterm can fall into four different categories of preterm infants, based on their gestational age (GA) [12]:

- Late preterm (34 to 37 weeks of gestation)
- Moderate preterm (32 to 34 weeks of gestation)
- Very preterm (28 to 32 weeks of gestation)
- Extremely preterm (less than 28 weeks of gestation)

Even if the events leading to preterm birth remain unclear, preterm birth could be associated with several factors [13]. The main clinical risks are related to maternal aspects: (a) nutritional status such as tobacco, drugs and alcohol consumption, medical disorders, stress, and psychological characteristics; (b) pregnancy history such as previous preterm delivery, the interpregnancy interval of less than six

months, and genetic predisposition; (c) sociodemographic characteristics such as the absence of health insurance, ethnicity, male gender, and poor antenatal care; (d) current pregnancy characteristic like intrauterine infection, fetal malformation, and multiple gestations [11,13,14].

Preterm infants are delivered during the late canalicular, saccular, or early alveolar normal lung maturation phase, the most vulnerable stages of lung development. Preterm delivery disrupts the alveolar epithelial cells' differentiation, thus impairing endogenous surfactant production. Moreover, perinatal exposure to infection, mechanical ventilation, inflammation, and high oxygen concentration may lead to additional insult to the immature lung [15]. Prematurity and post-natal factors could lead to the two main preemies respiratory complications: neonatal respiratory distress syndrome (nRDS) and bronchopulmonary dysplasia (BPD). Other prematurity-linked pathologies are intraventricular hemorrhage (IVH) and necrotizing enterocolitis (NEC) [16,17]. The incidence and severity of these morbidities increase with decreasing GA at birth [18]. For instance, nRDS ranges from 2%, at 34–36 weeks of gestation, to more than 50% in extremely low gestational age infants [19]. Respiratory distress is one of the most common reasons for infants to be admitted into neonatal intensive care units (NICUs) to support their breathing at birth. In fact, lungs of preterm infants are not mature and thus they require oxygen supplementation and ventilation support. Mechanical ventilation is an invasive technique, requiring an endotracheal tube, that once applied to a premature lung could lead to inflammation, hyperoxia, volutrauma, barotrauma, oral-pharyngeal abrasion, and lacerations of the oropharynx [16,18,20]. Nowadays, thanks to progress in medical care, assisted ventilation has become less invasive. Nasal continuous positive airway pressure (nCPAP) has become the most used system of non-invasive ventilation after birth. nCPAP has decreased respiratory failure, thus reducing complications and mortality [21]. However, preterm infant lungs lack in surfactant production and the ventilation alone is not often enough to support their recovery. For those reasons, preterm babies are commonly treated with non-invasive exogenous surfactant replacement therapy (SRT), such as LISA

catheter, InSurE (INtubate SURfactant Extubate), and laryngeal mask techniques, coupled with non-invasive ventilation system [22–24].

In the last decades, the progression in medical care has significantly improved the survival rate of extremely preterm infants. However, these infants are often affected by long-term diseases. Among these, BPD is the most common chronic morbidities impairing premature neonatal lung development [25,26].

1.3 Bronchopulmonary dysplasia (BPD)

BPD is a long-term complication of prematurity resulting from complex processes that compromise the physiological lung development of premature babies [27]. In 1967, Dr. Northway defined for the first time the BPD as a chronic lung disease caused by aggressive ventilation with high oxygen levels for at least 7 days in nRDS babies, now known as "Old BPD" [28]. Since this first description, the phenotype of BPD has evolved in parallel with advances in medical care [29,30]. Nowadays, this definition has been replaced by the "New BPD", as a consequence of the introduction of new standard care practices [23]. "Old BPD" manifestations are represented by pulmonary fibrosis and abnormal arterial vascularization, whereas the "New BPD" is characterized by lung arrest development, alveolar hypoplasia, decreased septation, dysregulated development of pulmonary vasculature, and abnormalities in respiratory function [28,31]. Despite the increase in the survival rate of preterm infants and the critical care management progress over the years, the BPD incidence is broadly stable at around 40% worldwide [32]. In addition, a 0.2% increment of global BPD cases is expected for the period 2017-2028, with more than 14000 cases in the USA for the year 2030 [33].

The National Institute of Child Health and Human Development defines BPD patients as those infants born before the 32nd week of gestation that need supplemental oxygen therapy for at least 28 postnatal days or 36 weeks postmenstrual age (PMA) [34]. Moreover, they defined a BPD severity scale, divided into mild, moderate, and severe BPD, based on pathology severity and the required respiratory

support [29]. Mild BPD is diagnosed in those babies who breathe autonomously up to 36 weeks PMA, the moderate BPD infants need a supplemental oxygen therapy with less than 30% O_2 up to 36 weeks PMA, whereas the severe BPD is diagnosed in those infants who need more than 30% oxygen supplementation and/or positive pressure respiratory support up to 36 weeks PMA [33,35]. However, this definition has several limitations because it is based only on baby management and not on the disease pathophysiology.

In the last decades, several studies have shown that BPD is correlated with timing and duration of exposure to several specific risk factors, differentiated into prenatal and postnatal ones, in association with prematurity of lung (Figure 3) [36–39].

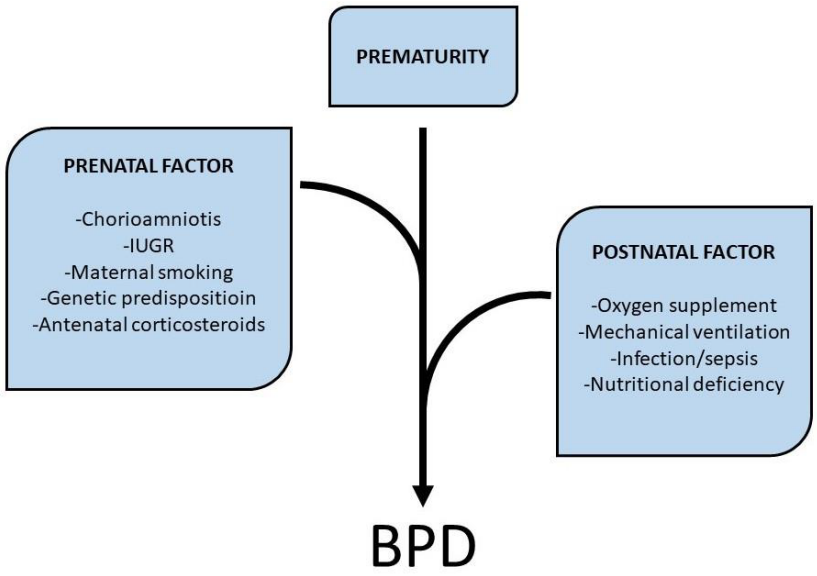

Figure 3. Prenatal and postnatal risk factors for BPD development

1.3.1 Prenatal factors

Prenatal insults such as inflammation, antenatal corticosteroids administration, environment, and genetic predisposition could potentially change the physiological lung development in the prenatal period and affect the development of BPD [40,41].

Inflammation

Chorioamnionitis (CA) is an in-utero inflammation, caused by intrauterine bacterial infection, by *Ureaplasma or Mycoplasma* species, that commonly promotes inflammation processes of fetal membranes, chorion, and amnion [42,43]. Several clinical and pre-clinical studies showed that CA has a dual effect on the fetus [44]. It promotes a temporary lung development burst with an increased surfactant production, partially protecting infants from nRDS [45,46]. Vice versa, intrauterine inflammation can trigger BPD developing [29,37,44,47–50].

Intrauterine Growth Restriction

Intrauterine Growth Restriction (IUGR) consists in the failure of the fetus to reach its growth potential during pregnancy [51], due to the limited levels of oxygen and nutrients in utero. The deficiency of several growth factors leads to IUGR, impairing lung growth [52]. Nowadays IUGR is associated with an increased risk for BPD and it is recognized as an independent risk factor [37,53].

Maternal smoking

Maternal smoking promotes preterm birth and lowers birth weight that can determine abnormalities in pulmonary functions [54]. Nicotine interacts with neonatal lung receptors impairing alveolarization and abnormal airway function [29,52,55].

Genetic predisposition and environment

Genetic predisposition and environment are also involved in BPD [56]. And several studies highlighted potential dysregulated candidates that are components of innate immune and antioxidant defenses, and also modulators of vascular and lung remodeling, including matrix remodeling and surfactant proteins [57].

Antenatal corticosteroids

Administration of antenatal corticosteroids reduces infant mortality and the incidence of nRDS, stimulating the production of surfactant and lung maturation [58]. However, numerous studies have shown that corticosteroids have several targets across the body leading to a plethora of undesirable systemic side effects [59]. For instance, they favor the remodeling of the lung parenchyma, thus improving gas exchange but they also cause fewer and larger alveoli formation. Antenatal corticosteroids treatment can suppress lung inflammation but it could also alter the immune cell function, increasing the risk of early-onset sepsis [42,44]. Despite this evidence, antenatal corticosteroids are widely used in NICUs since they efficiently reduce the complications of preterm birth, but not the incidence of BPD in infants [59].

1.3.2 Postnatal factors

Several post-natal factors could also affect the normal alveolarization, the airways structure, and pulmonary vascular development, intensifying inflammatory response in the lungs. In particular, oxygen supplementation therapy, mechanical ventilation along with postnatal infections and nutritional deficiency can increase lung injury [29,60,61].

Mechanical ventilation and oxygen administration

Mechanical ventilation and oxygen therapy can impinge lung development in preemies. Ventilation-induced lung injuries (VILIs) are associated with proinflammatory mediators release and the disruption of alveolar epithelial cells [62,63]. Barotrauma, caused by high inspiratory pressure, and volutrauma, due to excessive tidal volume, are forms of VILI [52]. Currently, the aim of clinicians is to reduce airways damage attributed to ventilator supports, preferring non-invasive ventilations (e.g. nCPAP) instead of mechanical ones [29,44].

Oxygen therapy, as well mechanical ventilation, can also interfere with lung development [44], since the high level of oxygen exposure, or prolonged oxygen therapy, increases the oxidative stress in

preterm lungs [53]. Reactive oxygen species (ROS) produced by hyperoxia exposure, directly affect cell growth compromising alveolar and angiogenesis maturity [28,60], thus leading to BDP development [28,29,50].

Infection

Preterm babies are more susceptible to infections, such as sepsis, since their immune system is not fully developed [15]. Sepsis is caused by common infectious agents, such as *Streptococci and Staphylococci* species or gram-negative bacteria, causing the impairment of epithelial alveolar cells and BPD onset [29,41,64]. Early-onset sepsis occurs within the first 3 days of life, whilst it has a late-onset within 3-7 days [65,66].

Nutritional deficiency

Adequate nutritional management is crucial for BPD prevention in preemies. Malnutrition affects physiological lung development by disrupting alveolarization and affecting bronchiolar epithelium [67]. *In vivo* studies demonstrated that malnutrition aggravates the effect of hyperoxia on alveolarization and extra-cellular matrix deposition in the lungs [67]. Optimization of the diet is crucial for lung function and development in preterm infants [68], reducing pulmonary disorders onset and consequently lowering moderate and severe BPD incidence [69].

1.3.3 Pathophysiology of BPD

Pathophysiology of BPD has significantly changed over the past decades due to the improvements in the respiratory management of preterm babies [52]. However, the BPD pathophysiology has not been fully understood yet. BPD is a multifactorial disease, leading to high variability among clinical cases with heterogeneous phenotypes. As mentioned before, these latter are known to be triggered by preterm birth and promoted by prenatal and postnatal factors (Figure 4) [70]. Overall, they induce a significant pulmonary inflammatory response, leading to abnormal lung function and structural changes persisting also in childhood and adulthood [15,36]. This inflammatory response is mostly due

to the accumulation of neutrophils and macrophages in airways and pulmonary tissue, affecting the alveolar capillary unit and tissue integrity [71]. Indeed, alveolar macrophages produce diverse pro-inflammatory cytokines which, in turn, increase the levels of chemotactic proteins that attract inflammatory cells (i.e. neutrophils and leukocytes) into the lung. Instead, neutrophils secrete plenty of proteases which lead to pulmonary tissue damage, cellular apoptosis, and surfactant inactivation [71]. To aggravate this situation, the inflammatory process occurs on developing lungs and the degree of these alterations depends on the developmental stage at which preterm babies are born. Altogether, these events lead to alveolar and pulmonary vascular simplification characterized by gas exchange and respiratory system abnormalities [52]. Nevertheless, the pathophysiology of BPD is not fully investigated to study since is a multifactorial disease with a non-homogeneous phenotype among the preterm population. Moreover, the increase of patient survival rate and ethical constraints have reduced the pathologic human specimens available, hampering the investigation of the BPD pathophysiological mechanisms. In this scenario, the histological and -omic data that come from BPD animal models are crucial to characterize the pathophysiology of BPD and to identify new therapeutic targets. Even if phenotype and symptoms differ among BPD-affected preterm infants, the majority of them have shown three common hallmark features: lung parenchymal alterations, pulmonary vasculature disease, and respiratory function abnormalities [29,52].

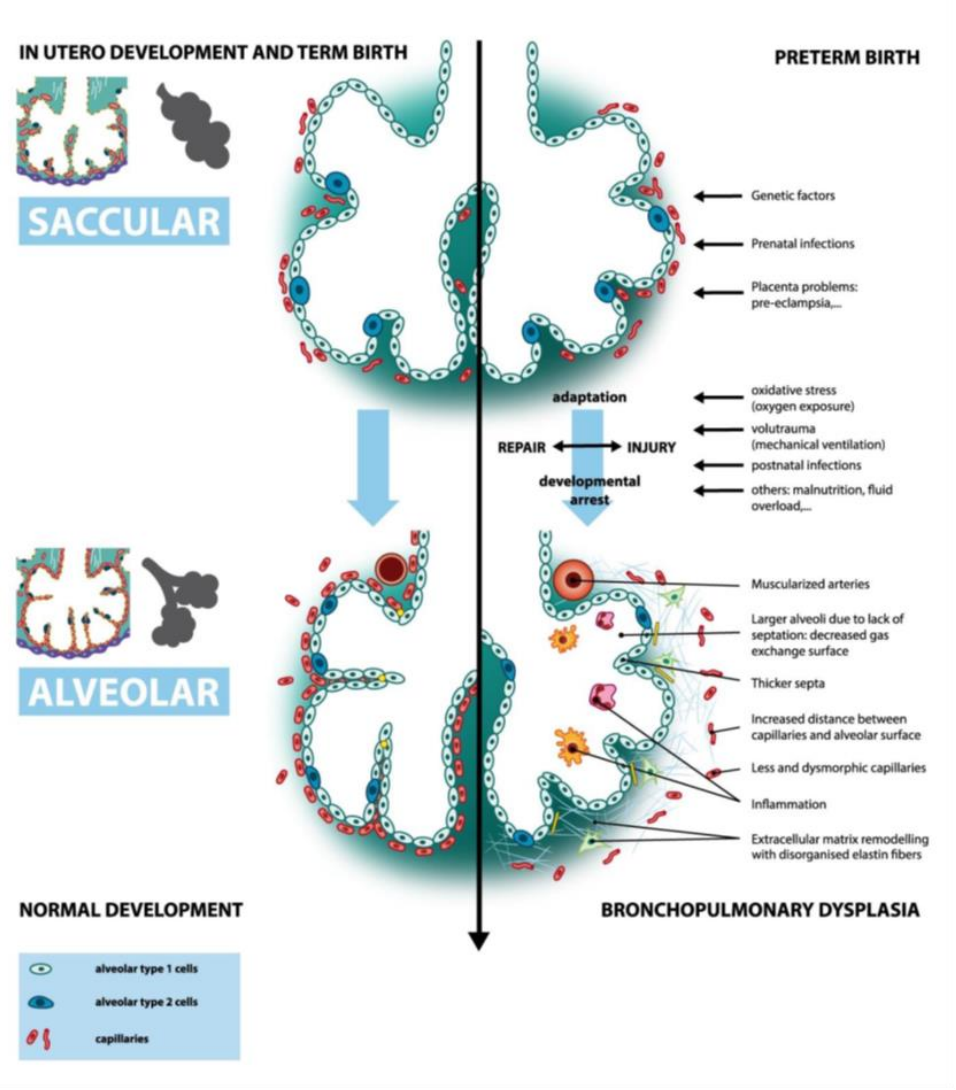

Figure 4. Pathophysiology of human BPD (image from Salaets et al [72])

1.3.3.1 Lung parenchymal structure alterations

The physiologic formation of the alveolar structure creates the appropriate interface with the developing capillary bed, allowing an adequate gas exchange [73]. The lung architecture of BPD preterm babies is characterized by a dysregulated expression and organization of elastin fibers and collagen, leading to enlarged alveolar units and reduced alveolarization [73,74]. The degree of these alterations depends on the developmental stage at which preterm birth occurs, being more serious in preterm babies born in the late canalicular-early saccular phases compared to ones in the late saccular-early alveolar phases [74,75]. The arrest of lung development is primarily attributed to oxygen toxicity. High levels of ROS interfere with cell growth pathways causing alveolar epithelial cells injury, or

necrosis if hyperoxia exposure is prolonged [76], which is associated with modification in density and disposition of extracellular matrix (ECM) components. The lung parenchymal damage starts with inflammatory cells infiltration in the lung tissue. Thereafter, neutrophils and macrophages augment recruiting of leucocytes and contribute to damage ECM, due to leucocytes proteases releasing [29]. Several *in vivo* studies demonstrated that the inflammatory response reduces the number of alveoli and capillary growth, increases the thickness of septa, and alters the expression of ECM components [36,73,77,78].

Physiologically, elastin is involved in the formation of secondary septa, and collagen increases during lung development permitting normal septation [79]. During BPD onset, irregularly deposed-elastic fibers become thicker, tortuous. Moreover, the immature fetal lung is characterized by thickened collagen around the saccule walls, a widened interstitium, and by an increase of larger interstitial collagen fibers [80]. The delay in the deposition process of elastic fibers decreases the elasticity of the neonatal lung making it more vulnerable to tissue damage related to VILI [81].

1.3.3.2 Pulmonary vascular alterations

Premature birth and postnatal lung injuries impact pulmonary circulation, other than impairing alveolar development [36]. Oxidative stress and inflammation inhibit angiogenesis, disrupting capillary growth and inducing smooth muscle proliferation, which increase media thickness of small pulmonary arteries. Alterations in pulmonary vessel structures, defined as “dysmorphic” [36], impair gas exchange, increase vascular resistance and reduce compliance, leading to the development of pulmonary hypertension (PH) [67–70]. PH is a severe complication of BPD, leading to increased oxygen demand, hospital readmission, and mortality of premature infants [71].

1.3.3.3 Airway injury

Infants affected with BPD have abnormal respiratory system mechanics. Preterm babies exposed to prolonged supplemental oxygen show airway hyperreactivity [82]. Moreover, pulmonary edema,

interstitial fibrosis, and tissue overdistension due to mechanical positive pressure ventilation worsen lung function [29,83]. These factors can lead to airways obstruction, increased airway resistance, reduction of lung compliance and functional volume. Lung mechanics abnormalities in BPD-affected babies manifest as an increase of breathing work, tachypnea, and intercostal retractions [84], leading also to long-term consequences, such as asthma and other reactive airway diseases [52,82,83].

1.3.3.4 Long-term outcomes

Extremely preterm babies, who survived in the "non-invasive era", are now reaching childhood and early adulthood, thus the long-term outcomes are still poorly characterized [27,28]. Several studies showed that about 50% of children with BPD are re-hospitalized within the first year of life because of nRDS, BPD, and respiratory tract infections. Moreover, 70-80% of BPD-affected patients require home oxygen therapy [28,29,83,84] and, at the end of the alveolarization phase (2 years old), a small percentage still necessitates oxygen supplementation [83]. Hospital recovery for respiratory illness decreases drastically at 4-5 years of life [29,73,84]. Furthermore, BPD survivals show visible neonatal impairment of alveolar development in these first years of life, which might persist into childhood and adulthood [85]. Indeed, specific functional tests show abnormalities compared to healthy age-matched controls [83,86]. Clinical manifestations include exercise intolerance, asthma-like symptoms, airway hyper-reactivity, and PH. Furthermore, premature BPD babies have a compromised immune system, thus they are more susceptible to infection during childhood, causing severe pulmonary complications [27,87]. Impaired lung function is considered also a risk factor for developing progressive airflow limitations, known as chronic obstructive pulmonary disease (COPD) [80]. Several studies highlighted that prenatal factors as prematurity, maternal behavior, and early lung development disruption are recognized as factors contributing to COPD [88]. Beyond the impact on respiratory health, BPD survivors show also a high risk of long-term neurodevelopmental disorders [83,87,89]. Oxidative stress, inflammation, malnutrition, and antenatal/postnatal corticosteroids treatments are well-recognized risk factors for brain injury. They lead to reduce overall brain volume, with an

evident decrease in both gray and white matter, increasing the risk for cognitive impairment in childhood and adolescence [90]. Moreover, other neurological disorders linked to BPD pathophysiology include delayed motor, academic, cognitive performance, and behavioral problems [87,91].

1.4 BPD prevention and treatments

Several improvements in neonatal medical care have been performed, including non-invasive ventilation, less invasive surfactant administration, and reduction of inspired fraction of oxygen but none of them showed a positive impact on the BPD incidence rate in preterm infants [92]. As previously described, BPD arises from several pathological factors, and its prevention and treatment require a multi-pronged approach [83,93]. In the last decades, limited therapies have evidenced some significant positive effects: caffeine, vitamin A, postnatal steroid treatments, mesenchymal stem cells, and the insulin-like growth factor-1 [94].

1.4.1 Caffeine

Caffeine is a methylxanthine derivative commonly used for the treatment of apnea in preterm infants [27]. It stimulates breathing through competitive inhibition of adenosine, an endogenous inhibitor of the respiratory system in the central nervous system [95]. Several studies demonstrated that caffeine significantly reduces BPD development and improves neurodevelopmental outcomes in preterm babies [27], by stimulating the respiratory centers and decreasing pro-inflammatory cytokines production, improving lung function and inflammation, and pulmonary mechanics [96,97]. Animal studies showed that administration of caffeine, combined with surfactant, reduced airway resistance and improved lung compliance [98]. The timing of treatment is crucial because earlier treatment is associated with increased benefits. Indeed, caffeine therapy within the first three days of life results in a lower BPD incidence compared to a delayed administration [98,99].

1.4.2 Postnatal steroids therapy

Benefits derived from steroid treatments are mainly related to improved lung compliance, decreased airway resistance, and early weaning from mechanical ventilation [100]. Systemic dexamethasone administration within the first eight days of life reduces the risk of BPD in very preterm babies [101]. Similarly, dexamethasone administration after the third week of life accelerates extubation time, but it does not have an impact on BPD severity [27]. However, postnatal steroid therapy can also cause multiple systemic side effects [102]. The early use of dexamethasone increases the rate of gastrointestinal perforation, neurological disorders (e.g. cerebral palsy), and hypertrophic cardiomyopathy. For these reasons, systemic corticosteroid therapy is not recommended in very preterm infants [101,103–105]. In order to reduce systemic side effects, steroids can be delivered directly to neonatal lungs through inhalation or intra-tracheal instillation [103,106]. Early administration (within the first week of life) of inhaled corticosteroids, in extremely preterm infants, is associated with a significant reduction of BPD rate even if its long-term effects on neurological development are not clearly established [27,103,107]. Inhaled steroids require a high dosage to allow sufficient drug deposition into the lungs [27,103,108] thus, to overcome their possible side effects, steroids can be mixed with exogenous surfactant and delivered through intra-tracheal injection [103,109,110], to improve their delivery and distribution throughout the lung epithelium [110–112]. Nonetheless, a few studies have demonstrated that this mixture facilitates early extubation, decreases BPD incidence, and improves pulmonary outcomes without significant side effects [106].

1.4.3 Vitamin A

Vitamin A is the collective term for a group of nutritionally fat-soluble retinoids that are essential for physiological growth and maturation of the respiratory epithelium [113,114]. This group includes retinoic acid, retinol, retinal, and retinyl esters that are required for surfactant synthesis as well as epithelial cells differentiation, and proliferation [115–117]. Physiologically, the expression of vitamin A occurs in the fetus during the third trimester. Diverse studies showed that preterm infants have reduced hepatic

stores of retinol-binding proteins, as well as in the plasma, that can contribute to lung development arrest and consequently BPD development [115,118]. Conversely, vitamin A supplementation seems to have positive effects on BPD-affected babies by reducing the inflammatory response and improving the alveolar septation process [94,115,118,119]. Vitamin A can be administrated in several ways. Vitamin A administration via enteral feeding does not permit adequate adsorption owing to immaturity of gastrointestinal function. The parenteral administration of vitamin A is an invasive procedure and can increase the risk of infections [115,119]. Currently, the intramuscular route is preferred in clinical practice [27,92,106,119]. However, the vitamin A supplementation benefits are controversial because the reduction in BPD development can be only observed in extremely low-weight infants [120]. Moreover, vitamin A administration does not reduce the duration of mechanical ventilation need or length of hospital stay, and it does not improve neurodevelopmental outcomes [27].

1.4.4 Cell therapy

A new and promising therapeutic field in BPD prevention is the use of stem cells [93]. Stem cells and stem-cells derived exosomes are emerging tools for treating or preventing BPD in the neonatal population [121]. In the last decades, researchers' attention has been mainly focused on the mesenchymal stem cells (MSC). This interest is related to their multipotent and anti-inflammatory proprieties, low immunogenicity, the ability of self-renewing, and easiness to be extracted [93,122]. MSC are commonly isolated from several sources including bone marrow, adipose tissue, lung, placenta, and umbilical cord [123]. Studies showed that the administration of bone marrow-derived MSC has shown a survival improvement and a reduction of lung inflammation and lung vascular damage, in rodent models with hyperoxia-induced lung damage [124]. The potential therapeutic applications of stem cells are not only related to their regenerative capacity but also their potential paracrine properties [121]. The paracrine effects act via secretion of subcellular organelles, such as exosomes, which can protect pulmonary epithelial and microvascular endothelial cells from oxidative stress and prevent alveolar developmental impairment induced by hyperoxia. Moreover, they decrease macrophages and

neutrophils infiltration and repair the lung by stimulating bronchioalveolar stem cells. Thus, MSC treatment seems to be very encouraging for the prevention of BPD [122,125]. Nevertheless, several questions regarding the best timing and method of administration continue to be unclear. Finally, since that premature infants have an immature immune system, some precautions should be taken, avoiding the risk of stem cells anomalous proliferation in clinical trials [122,124,125].

1.4.5 Insulin-like growth factor-1 therapy

Insulin-like growth factor-1 (IGF-1) is an important regulator of fetal growth and lung angiogenesis and development [126]. IGF-1 levels mainly increase during the second and third trimester of pregnancy, and then rapidly decrease after birth [127]. Low serum levels of IGF-1 in preterm neonates have being associated with an increased risk of BPD [126]. Consistently, IGF-1 administration to neonatal rodent model seems to reduce lung injury in response to hyperoxia. Clinical studies demonstrated that treatment with recombinant human IGF, in combination with its binding protein, reduces the number of preterm neonates with severe BPD and shifted the disease severity to milder BPD [127,128].

1.5 Translation of BPD phenotype in animal models

During the last years, numerous therapeutic strategies have been clinically investigated, but only the ones described above seem to be effective in reducing the incidence of BPD. As mentioned before, since the increased patient survival rate led to a paucity of human pathological specimens, the large part of data on new therapeutic strategies derives from *in vivo* studies [36,39]. The use of non-invasive ventilation strategies, SRT efficacy, antenatal steroids, and retinoids' key role in reducing BPD have been first established in animal models, providing the rationale for clinical trials [39,129]. Animal models allowed to investigate key-player mechanisms leading to BPD onset and progression, but a standardized preclinical model does not exist yet, since the heterogeneity of lung pathology of BPD in human infants cannot be fully recapitulated by animal models. The identification and validation of

a research-fit animal model with a good translational power for testing novel strategies to prevent or treat BPD is an unmet need [39].

As previously discussed, BPD phenotype in humans is characterized by alveolar developmental arrest, obstructive airways, and pulmonary vascular alterations that are extremely difficult to mimic in animal models, thus hampering the preclinical development of new drug candidates [72,130]. In the last decades, two classes of animal models have been developed: small and large animal models (Figure 5). Both models have some advantages and limitations which should be carefully considered [72]. Small animal models are suitable to investigate the molecular pathways involved in specific aspects of BPD, revealing those mechanisms that impact the immature lung. Conversely, large animal models are useful for physiological studies of evolving BPD and for the transnationality potential of innovative therapeutic strategies to the NICUs [72,75].

Hyperoxia and additional insults (e.g. mechanical ventilation and perinatal inflammation) are mainly used to mimic BPD-like lung injury and to better reproduce the clinical scenario [72,131]. Specifically, the exposure to high levels of oxygen (fraction of inspired oxygen > 80%) in these animal models leads to alveolarization arrest with decreased the number of alveoli and increased alveolar septal wall thickness, which are two key histopathological characteristics of BPD [131]. Aside from hyperoxia and external insults, the animal model birth has to occur in the same lung development stage as in premature infants to better mimic the structural and functional lung immaturity of human BPD, that is from the late canalicular to the early saccular stage. Animal models, in which preterm birth is combined with mechanical ventilation and oxidation-mediated injury, provide an important translational advantage [72].

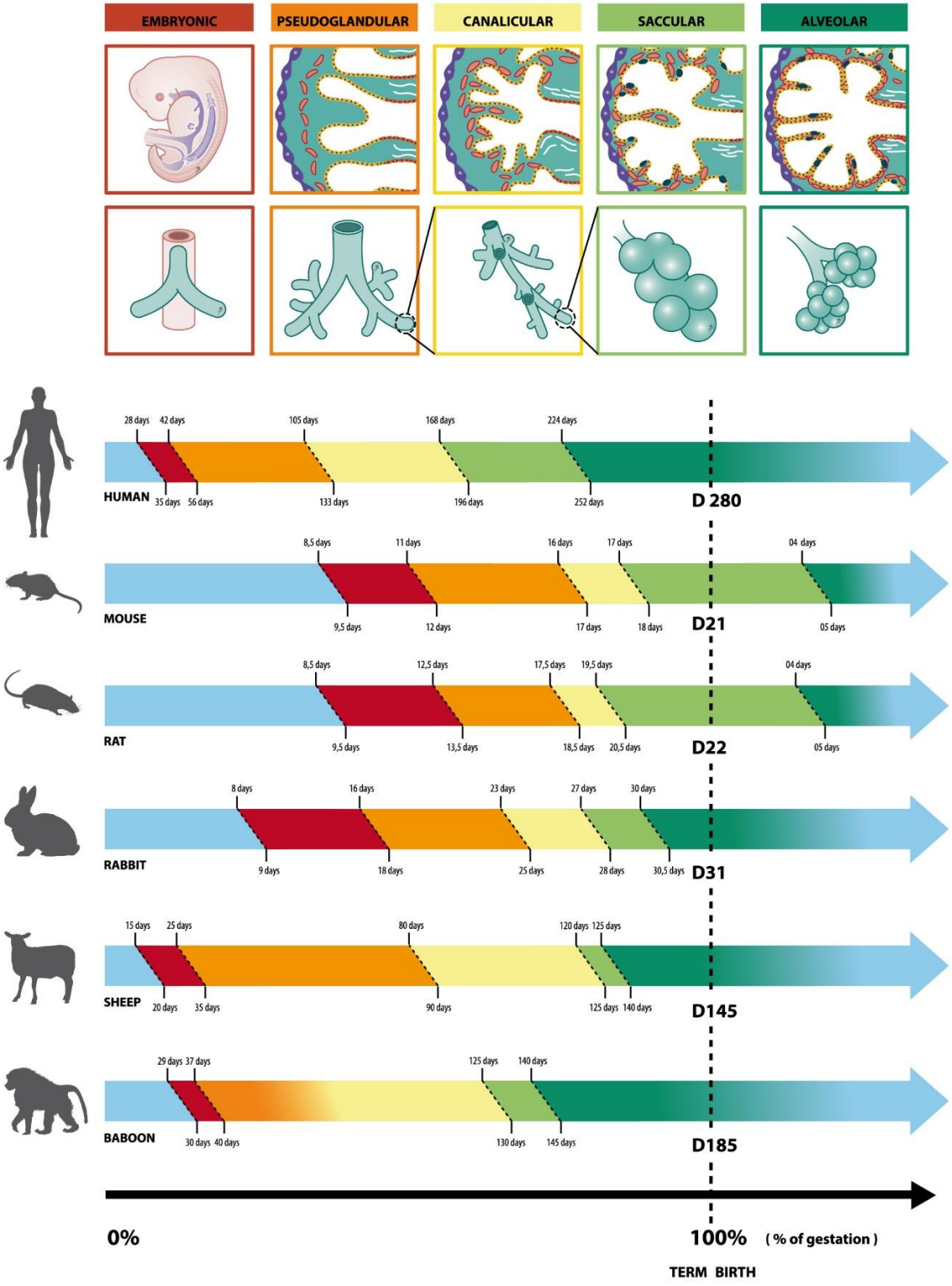

Figure 5. Lung mammalian development (adapted from Salaets et al [72])

1.5.1 Small animal models: Mice and Rats

Term mouse and rat models share similar advantages. They are small and convenient to house with a short gestation (21 days for mice, 22 days for rats) and large availability of reagents and techniques for molecular investigations [72]. However, rodents' physiology and lung structures differ from the human ones, implicating that the same intervention may provide different responses [132]. Mice and rats are physiologically delivered at term in the saccular stage of lung development, which lasts until the post-natal day 5 when they are in the alveolar phase [72]. In this condition, the lung morphology resembles the human one at the 28^{th}-30^{th} gestation week (Figure 5). At birth, their lungs are structurally immature but functionally mature, implicating that newborn pups have no gas exchange limitation, which is however observed in premature infants [72,133]. A widely used BPD rodent model is the rodent pup, born at term, exposed to various degrees of high oxygen levels for a prolonged time. This animal model permits to study lung responsiveness to hyperoxia injury during the saccular stage as it occurs in extremely preterm infants. On the other hand, their lung functional maturity limits the extrapolation of findings from rodents to humans [72,133,134]. For practical reasons, rodent models are useful to study pathogenic mechanisms involved in BPD development [72,75,133,134], but the lack of prematurity, the levels of oxygen utilized, and the unfeasibility to perform long-term mechanical ventilation experiments do not allow to accurately mimic the clinical neonatal scenario [72,134].

1.5.2 Large animal models: Baboons and Lambs

Premature lambs and baboons are widely used for physiological studies of BPD pathogenesis and to investigate new therapeutic strategies [72,75,78]. They are born at term in the alveolar phase of lung development and they present airway anatomy similar to human [72] (Figure 5). Their size permits repeated blood sampling, catheterization, and the employment of standard care strategies, similar to NICUs scenario [72,78]. Moreover, their offspring can be prematurely delivered, mimicking the BPD airway pathology as in preterm infants, since they require prolonged invasive mechanical ventilation with oxygen supplementation [72,75,78]. The main advantages of the preterm lamb model, compared to

the baboon one, are mostly related to their larger size and organs that favor postmortem sampling. On the other hand, baboons are phylogenetically closer to humans and newborns are more immature at the time of preterm labor compared to the lamb model (Figure 5) [75,135]. In the last decades, researchers developed several models characterized by different lung insults. In the preterm baboon model, pups delivery usually occurs at the 125th day of gestation (185-day at term) and they are stabilized by SRT and artificial ventilation. Regarding lamb models, their delivery is between 125 and 132 days of gestation (145-day at term) to study the effects of different ventilation modalities [72]. Moreover, researchers set-up several baboons and lambs models characterized by in utero injection of the most common preterm babies infecting agents such as *Ureaplasma and Mycoplasma* organisms [135]. However, these models present several limitations: high cost and intensity of care, small litter size, and ethical limitations. Furthermore, compared to rodent models, the availability of reagents is rather limited [72].

1.5.3 The Preterm Rabbit Model: a practical compromise between small and large models

Rabbits are a practical compromise between small and large animal models. They are easy to house, cost-effective, with a relatively short gestational period (31 days), large litter size, and can be easily manipulated [72,132]. Like baboons and lambs, rabbits' lung development is in the alveolar stage at birth, as the humans one (Figure 5), and continues through the postnatal period [72,132,133]. Moreover, rabbits can be delivered prematurely in contrast to mice and rats. They can be delivered through the caesarian section on the 28th day of gestation, during the saccular phase of lung development, and they can spontaneously breathe. In this way, premature rabbits have a comparable immaturity of the antioxidant and surfactant systems to human preterm babies [72,132,133]. The size of preterm rabbits allows the use of numerous types of manipulations such as SRT, hyperoxia exposure, intra-tracheal injection of drugs, gavage feeding, and short periods of mechanical ventilation [72,77]. Therefore, the preterm rabbit model represents a valid option for investigating innovative strategies for BPD

treatment with high translational power. Despite these positive features, the preterm rabbit model has some limitations; i) it is not commonly used as rodent models, ii) reagents and tools are not large available, iii) long-term ventilation can not be performed because of its small size, and iv) it is less characterize at the molecular level compared to rodent models. Nevertheless, preterm rabbits, as large and small animal models are a valid option for both exploratory and translational research studies. Mataloun *et al* [136] investigated the combination between malnutrition and hyperoxia. Malnutrition leads to lower lung weight and decreased alveolar number, elastic fiber, and collagen deposition. These outcomes are extremely amplified in combination with hyperoxia [132,136]. Recently, Salaets *et al* have demonstrated that prematurity itself causes lung developmental delay, even in absence of high oxygen levels and mechanical ventilation [137]. In this study, rabbits delivered at the 28th day of gestation exhibit thicker septa, less complex airspaces, and increased alveolar size at day 7. Moreover, the mRNA expression of surfactant proteins is lower in preemies than in term pups. Lastly, preterm pups display thicker arterial walls, indicative of increased pulmonary vascular resistance [137,138].

In the last decades, a widely used BPD rabbit model is the hyperoxia-exposed preterm rabbit [77,132]. Several studies have shown that this model summarizes most of the main features of BPD phenotype [77,138,139]. Preterm pups under hyperoxia condition (fraction of inspired oxygen > 95%) for 7 days show several BPD hallmarks, as decreased inspiratory capacity and compliance, and increased lung tissue resistance and elastance, indicative of reduced respiratory capacity and an abnormal tissue structure. Moreover, hyperoxia-exposed preterm rabbis display the first symptoms of PH, as demonstrated by a reduced ratio in pulmonary artery acceleration time (PAAT) and ejection time (PAET), which is indirectly correlated with pressure in the right ventricle of the heart. Furthermore, hyperoxia-exposed preterm rabbits have larger alveolar size, suggestive of a deficit in secondary septation and formation of new alveoli [77,132,138,139]. However, the hyperoxia-exposed animal model presents some limitations. Studies performed so far use high oxygen concentration (fraction of inspired oxygen > 95%) which is no more the standard care in NICUs. 7 days preterm rabbit model can not permit to study long-

term outcomes, as happen in small and large animal models [77,132,138,139], thus it is useful to test preventative drugs and not therapeutic treatments. For this reason, several efforts have been done to extend the hyperoxia exposed preterm rabbit model from day 7 up to day 14. Moreover, delivery at the 28th day of gestation does not closely mimic the prematurity condition of extremely preterm neonates, since most of the pups are able to breathe spontaneously, with no mechanical ventilation support. The induction of preterm delivery at 27th days of gestation has been considered for better mimicking extremely preterm babies, but their management is very challenging and probably not easily feasible for application as a long-term model. Finally, this model does not incorporate prenatal interventions, as antenatal steroids administration, and post-natal ones, as caffeine administration. Ideally, the preterm rabbit model should mimic closely as possible the clinical scenario tackling the limitations exposed above.

1.6 "OMICS" approaches to study BPD

Omics approaches such as genomics, transcriptomics, proteomics, microbiomics, and metabolomics have been extensively used to identify therapeutic targets and diagnostic biomarkers in several human diseases [140]. In the last decades, transcriptomic analysis has been used to deeply characterize genes and pathways that are dysregulated during diseases development, identifying those putative for novel preventive strategies to avoid/reduce the occurrence of BPD [124,141]. Human BPD has a strong genetic predisposition [57,142], but different genome-wide association studies (GWAS) did not identify any BPD-associated single-nucleotide polymorphisms (SNPs) [143–146], that it might be due to the small cohorts analyzed. Several -omics approaches have been performed on urine and blood samples since they are easy to collect, following up BPD patients from disease onset to its progression [143,146–154]. However, the use of these samples has some limitations: they do not allow to evaluate the pathophysiological patterns inside the lungs and often authors focused on a specific cell population or metabolite instead of analyzing the whole sample. To overcome these issues, -omics studies made use of tracheal aspirates (TA) from mechanical ventilated preterm babies, identifying several

activated inflammation patterns [143,146–154]. Oji-Mmuo *et al.* performed mRNA and miRNA analysis on TA from invasive ventilated BPD preterm babies, demonstrating a dysregulation of several pathways, including inflammation, cellular growth, and tissue development [147]. Furthermore, a proteomic study highlighted an over-expression of proteins associated with inflammation and lung epithelium injury in TA from BPD patients [152]. Regarding the metabolomic approach, Piersigilli and colleagues identified that histidine, glutamic acid, citrulline, glycine, acylcarnitine, and isoleucine levels were higher in TA from neonates with BPD compared to aged-matched controls. Authors have suggested that these metabolites could be used as BPD biomarkers [153].

Despite these scientific advances, using lungs samples as matrix for omic-based studies would be of great advantage for investigating BPD pathophysiology. However, thanks to the improvement of clinical care, BPD patients have been reduced. This improvement in NICUs, along with ethical-related constraints, has broadly limited the availability of lungs and tracheal aspirates from preterm babies on which -omic analyses might be performed to unravel pathways and genes dysregulated by BPD. In facing these problems, several transcriptomic studies have been performed on mice and rats BPD animal models, identifying several new BDP candidate genes and pathways [140,155–157]. Inflammatory processes, lung development, and angiogenesis pathways are the most relevant dysregulated pathways in BPD animal models that have shown evidence in human studies [155,158–160]. To date, preterm rabbit is probably the best animal option to mimic clinical BPD. Salaets *et al*. have characterized the bulk transcriptomic profile of the preterm rabbit model exposed to hyperoxia at day 7 [155], showing that the expression of several pro-inflammatory genes, such as IL1A, IL1B, PTGS2, and CCL2 are increased in the lungs of hyperoxia-exposed preterm rabbits. Moreover, hyperoxia exposure dysregulated lung development-related genes such as PPARG, SPP1, CAV1, DKK1, and ACE as well as vasculogenesis genes such as VEGFA, TEK, and TIE1. Although this molecular characterization of the lungs of hyperoxia-exposed preterm rabbits highlights several patterns involved in BPD, authors have only analyzed the condition at the end of the experiment. To date, a

comprehensive bulk transcriptomic analysis of the development of BPD-like phenotype during hyperoxia exposure in preterm rabbits is still lacking. These studies relying on bulk transcriptome analysis permits only to evaluate the whole transcriptome profile within the sample, thus not revealing which cell populations are affected by BPD, as well as the primary effector cells and disease-related cell-cell communication.

2. Aim of the study

BPD is the most common pulmonary chronic disease affecting preterm babies. It is a multifactorial disease with no commercially available medications, making BPD an unmet clinical need. For the development of new treatment therapies, understanding the genes and mechanisms involved in BPD development will be crucial. For this reason, in the last decades, several BPD animal models have been developed and the hyperoxia-exposed preterm rabbit BPD model is the most promising one. However, it is less characterized than the other BPD animal models.

The main aim of this Ph.D. thesis is to demonstrate the translational potential of the hyperoxia-exposed preterm rabbit as a suitable model to mimic BPD, in order to acquire a deeper and comprehensive view of the model and develop innovative therapeutic approaches. Based on this, a whole biomolecular and histopathological characterization was performed on preterm rabbits exposed to hyperoxia (95% oxygen) or normoxia (21% oxygen) conditions for 7 days. These analyses permitted us to understand the most important features that characterize the evolution of the BPD-like phenotype in the model.

Since preterm babies are normally exposed to oxygen levels significantly lower than 95% and 7 days model permit us only to test preventative treatments, the post-natal day 14 preterm rabbit model exposed to 70% of oxygen has been recently set-up and validated in Chiesi Farmaceutici laboratories. This model will permit us to characterize the progression of BPD and test therapeutic drugs after the disease onset. A secondary aim of this thesis was to characterize histological and gene expression profile of this alternative model, highlighting the differences between preterm animals exposed to hyperoxia (70% oxygen) or normoxia (21% oxygen) at day 14 and aged-matched birth at term animals. Finally, these results give us the opportunity to compare the two animal models, demonstrating similarities and differences.

3. Materials and methods

3.1 Custom-made incubators

A neonatal incubator is a device commonly used to maintain an optimal environment for the care of a newborn, in which temperature, humidity, and oxygen levels are monitored. In order to mimic the real clinical scenario for the preterm rabbit management, Okolab company (Naples, Italy) manufactured ad hoc incubators (Figure 6) for rabbit pup litters management. The incubator structure placed under a walk-in aspiration hood (Weiss Technik, Germany), consists of a rigid box-like enclosure equipped with both gas (oxygen and nitrogen) and temperature sensors with a feedback control loop to allow regulation and maintenance of oxygen concentration and temperature inside the chamber.

Figure 6. Ad hoc incubators developed by Okolab

3.2 *In vivo* protocol

Pregnant New Zealand White rabbits were provided by Charles River (Domaine des Oncins, France) and maintained in Chiesi's research facility under specific conditions, with food and water ad libitum, until Caesarean section (C-section) or pups natural delivery. When natural delivery at term (31st GA) was allowed, does were placed in special cages equipped with an external box where to build their nest. The experimental procedure was approved by the local animal ethics committee and met the standard European regulations on animal research (n°744/2017-PR). The delivery procedure and the postnatal handling of the fetuses will be described in the next paragraphs.

3.2.1 C-section and animal randomization

On day 28th of gestation, does (3.8±0.3 kg of body weight) were initially sedated with intramuscular (i.m.) medetomidine 2 mg/kg (Domitor®, Orion Pharma, Finland). Ten minutes later the animals received 25 mg/kg of ketamine (Imalgene®, Merial, France) and 5 mg/kg of xylazine (Rompun®, Bayer, Germany) i.m. After adequate sedation was reached, does were placed in the supine position, shaved on the abdomen, and euthanized with an overdose of 100 mg/kg of pentothal sodium (MSD Animal Health, USA). Right after, the abdomen was opened through a low midline abdominal incision, the uterus was exposed, and all pups were extracted through hysterotomy. Subsequently the delivery, pups were dried, stimulated, and placed in the incubator where temperature, oxygen, and humidity were set according to the experimental conditions. After one hour, the surviving pups were weighed, and placed into the Okolab incubators under normoxia (21% O_2) or hyperoxia (95 % or 70 % O_2) conditions.

3.2.2 Neonatal rabbit care

The preterm rabbits were placed on soft bedding and remained in the incubator except for the feeding. Housing material is changed daily. Pups were fed twice daily via a 3.5 Fr orogastric tube (Vygon, France) placed prior to and removed immediately after the feeding. The feeding consists of a milk

replacer (Day One®, Protein 30%, Fat 50%; FoxValley, Illinois, US) mixed with water (250 mg/ml) according to the manufacturer's directions. Probiotics (25 mg/ml) were added for all the days (Bio-Lapis®; Probiotics International Ltd, UK), whereas additional immunoglobulins (15 mg/ml) only on the day of birth and during the first 2 days (Col-o-Cat®, SanoBest, Netherlands). The feed volume was stepwise increased from a total of 80 ml/kg/day on day 1 of life to 200 ml/kg/day on days 3-7 for the postnatal day (PND) 7 model or on days 3-14 for the PND 14 one. The total volume was divided into 2 daily feeds. Pups were stimulated twice daily to urinate preceding feeds. On day 2, vitamin K was administered intramuscularly (0.25 mg/kg, Izokappa®; Izo s.r.l., Italy). The temperature inside the incubators was maintained to 32 °C. For the 14 days model, the incubator temperature was gradually decreased from day 7 to day 10 from 32°C up to 25°C and then maintained until day 14.

3.2.3 Lung tissue collection

All pups were euthanized with a pentothal sodium overdose before lungs harvesting. Lung samples from the 7 days model were collected from preterm pups exposed to hyperoxia (95% O_2) and normoxia at days 3 (HT3 and NT3), 5 (HT5 and NT5), and 7 (HT7 and NT7). For the 14 days study, lungs were harvested at day 14 from hyperoxia (70% O_2) and normoxia-exposed animals (HT14 and NT14). For physiological lung development, lungs from preterm pups delivered at 28^{th} GA and term pups at 35^{th} and 42^{nd} GA have been collected. The whole lungs from D28 pups were immediately surgically dissected in order to avoid contact with the surrounding environment and gene expression changes caused by respiration. Term rabbits were naturally delivered at 31^{st} GA and were nursed by their dams for 4 or 11 days of postnatal age (corresponding to 35^{th} and 42^{nd} GA) in individual cages at room air. Lungs (n=3, each time point) were removed, weighted, and separated into the right and the left parts. Right lungs were dedicated to RNA-seq and qPCR analysis, while histological analysis was performed on the left ones. The overall study design is shown in figure 7.

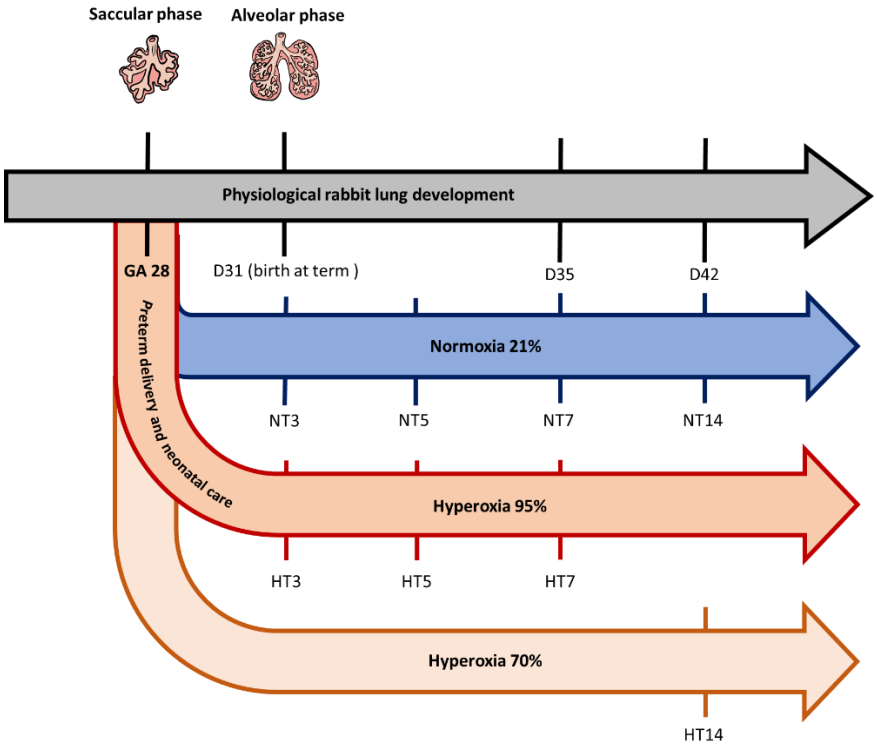

Figure 7. Scheme of the experimental timeline. Preterm rabbits were delivered through C-section on the 28th day of gestation and randomized at birth in hyperoxia (95% or 70% oxygen) or normoxia (21% oxygen) condition (natural birth on the 31^{sh} day of gestation). Pups were maintained in custom-made incubators until lung collection was performed at 3 (NT3 and HT3), 5 (NT5 and HT5), 7 (NT7 and HT7), or 14 (NT14 and HT14) days after preterm birth. Development samples D28 were harvested after preterm delivery, while term pups were naturally delivered at term on the 31st day of gestation and they were maintained with mothers until lung collection at 4 and 11 days (D35 and D42) after a natural delivery.

3.2.4 Histological analysis

The left lungs were fixed in 10% buffered formalin (Sigma-Aldrich, Germany) for at least 4 hours under constant pressure (25 cmH2O) using a custom-made fixation device to ensure homogenous fixation pressures during each experimental session (Figure 8). Hereafter, the lungs were first left in formalin for at least 24h and then transferred to 70% ethanol. The left lungs were embedded in paraffin, cut at 5µm thick with a rotary microtome (Slee Medical, Germany), and stained with eosin and hematoxylin (H&E) following standard histology protocols. Subsequently, several parameters were evaluated: the radial alveolar count (RAC), the septal thickness (ST), the medial thickness of pre- and intra-acinar arteries (MT%), and the acute lung injury score (ALI). Specifically, the RAC

parameter is an indicator of the alveolarization and, hence, of the changes in the alveolar number [161,162]. RAC measurements were performed by dropping a perpendicular line from the center of a respiratory bronchiole to the edge of the septum or pleura and counting the number of alveoli traversed by this line [162]. The ST parameter was directly and manually determined as the mean thickness of all septa intercepted by a test line 2 mm long randomly oriented across the slide, so taking care of excluding all the intercept falling upon bronchi, blood vessels, and pleura [163]. According to Zhenxing et al. [164] all the septa thinner than 0.6μm were considered "thin" because the average thickness of the thin side of the blood-gas barrier in the adult rabbit is 0.53μm. The septa whose thickness was comprised between 0.6 and 1.5μm were designate as "medium", while the septa whose thickness was ≥1.5 μm were divided into two further classes. The ones whose thickness ranged between 1.5 and 3 μm were categorized as "thick", while the septa thicker than 3μm were omitted from the analysis [165]. For the evaluation of MT%, 10 random peripheric muscularized vessels with an external diameter (ED) 100 μm, corresponding in rabbits to the pre- and intra-acinar arteries, were selected for each section. Their external and internal diameter along the shortest axis of the vessel was measured (40X magnification) and MT% was calculated by applying the following formula: MT%=*(ED-ID)/EDx100* [166]. This proportional parameter nullifies the effect of vasodilation, vasoconstriction, and tissue shrinkage. The ALI score was the one proposed by the American Thorax Society [167] in animal models of acute lung injury studies and was measured on five histological findings (i.e. neutrophils in the alveolar space, neutrophils in the interstitial space, hyaline membranes, proteinaceous debris in the airspace, and alveolar septal thickening) [72,139]. Due to the irregular nature of ALI, at least 20 random high-power fields (400X total magnification) were independently scored in a blinded fashion for each condition. Furthermore, at least 50% of each field has to be occupied by lung alveoli; fields that consist predominately of the lumen of large airways or vessels should be rejected. To generate a lung injury score, the sum of each of the five independent variables, specified above, were weighted according to the relevance ascribed to each feature by the

American Thorax Committee [167], and then were normalized to the number of fields evaluated. The resulting injury score was a continuous value between zero and one.

RAC, ST, and ALI score have been considered for the PND 7 model whereas only RAC and ALI have been measured for the 14 days model.

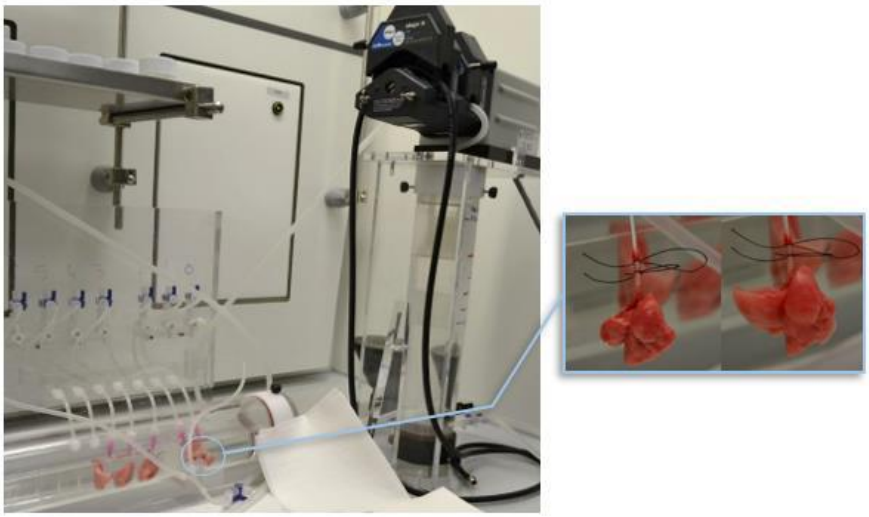

Figure 8. Custom-made device for constant pressure fixation

The histological analysis was presented as mean ± SEM. Data are analyzed with one-way ANOVA followed by Tukey's multiple comparisons test. Statistical analysis is performed using GraphPad software, version 9.0 for Windows (Graph-Pad Software, San Diego, CA, USA).

3.2.5 Transcriptomic analysis on PND 7 animal model

3.2.5.1 RNA isolation, library preparation, and sequencing

Upon removal, the right lungs were immediately transferred to and preserved in RNAlater (Sigma Aldrich, USA) solution at -20 °C until RNA-extraction was performed. Samples were homogenized in QIAzol® Lysis Reagent. mRNA and miRNA were extracted using the miRNeasy Mini Kit protocol (QIAGEN, Germany), using an automated method (QIAcube: QIAGEN, Germany). DNAse I treatment was added following the manufacture's instruction to remove genomic DNA contamination. The RNA concentration and quality were measured using the Qubit 4 fluorometer

(ThermoFisher, USA). The RNA integrity was assessed by electrophoresis and EtBr staining on denaturing 1.5 % agarose-formaldehyde gels, and by the Bioanalyzer RNA 6000 Nano Kit analysis (Agilent, USA). RNA-sequencing has been performed in collaboration with Centro Di Ricerca Interdipartimentale Per Le Biotecnologie Innovative (CRIBI) Sequencing Core, University of Padua, Italy. Libraries for parallel RNA and miRNA sequencing were prepared using the QuantSeq FWD and Small RNA-Seq kits (Lexogen, Austria), and sequenced with the Illumina NexSeq500 platform, allowing to generate at least 20 million reads for each sample. Reads quality analysis was performed with the FastQC tool (Galaxy Software Framework [168]). Transcripts were aligned on the rabbit (*Oryctolagus cuniculus*) genome with the STAR tool (Galaxy Software Framework [168]) and counts were obtained with the HTSeq-count tool (Galaxy Software Framework [168]), using the latest Ensembl available annotation on rabbit (OryCun2.0).

3.2.5.2 Transcriptome data analysis

Principal Component Analysis (PCA) is a statistical procedure that reduces the information inside a large dataset, thus being more easily visualized and analyzed, reducing the loss of information [169]. PCA creates a new set of uncorrelated variables, called principal components (PCs), increasing the variance. The results are commonly displayed by a cartesian graph that shows the first two or three PCs, which represent the experiment variability. In this study, PCA data was generated using the ClustVis tool [170].

Differentially expressed genes (DEGs) were identified for each time-point with the Limma-voom tool (Bioconductor, R package), considering only genes with 10 counts in at least 3 samples. Genes were considered as differentially expressed if the $\log_2$ fold-change ($\log_2$FC) was ≥ 1 or ≤ -1 and the adjusted p-value ≤ 0.05. Pathway enrichment analysis was performed on converted human homologs DEGs' lists using the Metascape software [171]. Only pathways with false discovery rate (FDR) ≤ -4 were considered significantly enriched. Heatmaps and similarity matrix were generated using ClustVis [170] and Morpheus tools (URL: https://software.broadinstitute.org/morpheus).

miRNAs were converted in human homologs and identified using the miRbase database (URL: https://www.mirbase.org/). Differentially expressed miRNAs were identified for each time-point with the Limma-voom tool (Bioconductor, R package), considering only miRNAs with 10 counts in at least 3 samples. miRNAs were measured as differentially expressed if the log_2FC was ≥ 0.5 or ≤ -0.5 and the adjusted p-value ≤ 0.05.

3.2.5.3 Gene Set Enrichment Analysis (GSEA)

Gene Set Enrichment Analysis (GSEA) determines whether members of a gene set S are disposed toward the top (or bottom) of a ranked list L. This analysis reveals if a set of genes from a study in literature are randomly distributed through a list of pre-ranked genes (for example list of DEG ranked based on the log_2 FC values). For each S-L relation, GSEA gives an enrichment score (ES), a normalized enrichment score (NES), and the false discovery rate (FDR). The NES represents the ES normalized for each gene set taking into account their size, while the FDR exemplifies the statistical significance adjusted for multiple hypotheses [172].

In this study, the GSEA tool was used to compare the transcriptional profile obtained in this study with the published dataset by Salaets and colleagues [155]. A list of pre-ranked genes according to log_2 FC was generated by our data and used as GSEA input.

GSEA was used also to correlate transcriptomic and histological results. Firstly, a phenotype label file (or class file) was created, structured as follows:

- The first line contained the text "#numeric", indicating that the file defined continuous labels.
- The rest of the file defined the continuous phenotypes (histological traits). Specifically, for each phenotype the first line defined the name of the phenotype (#RAC, #MLI, #ST, #SC, #MT, #ALI, #LIS), while the second line contained values resulting from histological analysis for each sample (tab separated)

The phenotype label file was used as GSEA input together with our expression dataset, i.e. the matrix containing expression values for each gene (identified by gene symbol) in each sample. GSEA was run selecting the C2 and C5 gene sets (collections of curated gene sets from various sources, including online pathway databases, biomedical literature and Gene Ontology) from the website, in order to obtain gene sets enriched among genes that positively or negatively correlated with histological traits. Parameters were set as default, except for Metric for ranking genes set to Pearson and Seed for permutation set to 149.

3.3 Linguamatics analysis and qPCR validation

Forty-two genes have been selected on day 7 model as biomarkers of BPD. Literature research has been performed in order to identify genes that are relevant in BPD development. Lists of dysregulated genes deriving from transcriptomic studies conducted on BPD patients, BPD animal models, or cellular models were organized in up- or down-regulated genes [155,173–178]. Moreover, the Linguamatics software was also used to retrieve lists of genes involved in BPD. Linguamatics is a natural language processing (NLP) text mining platform, that extracts facts, relationships, and assertions that would otherwise remain hidden in the text of articles or reviews, avoiding to review each paper [179]. RNA-seq transcriptional profiles data of the 95% hyperoxia-exposed rabbit BPD model were matched for the Linguamatics gene lists. Genes significantly dysregulated in at least one time point, with $|FC| \geq 4$, were deemed as suitable for the qPCR-array selection. An easy-to-assay custom RT2 Profiler qPCR array (QIAGEN, Germany) was used for the validation of PND 7 model RNA-seq data. The same RNA samples used for the RNA-seq analysis (NT7 and HT7 groups only) have been used. Moreover, the validated qPCR has been tested on RNA extracted from the right lungs of HT14, NT14, and D42 samples.

Samples were reverse transcribed using RT2 First Strand Kit (QIAGEN, Germany) following the manufacturer's instructions. The reverse transcription reaction was performed with Eppendorf Mastercycler ep Gradient, (Eppendorf, Germany). Then, the cDNA was mixed with RT² SYBR Green

ROX qPCR Mastermix (QIAGEN, Germany) and added into a custom RT2 PCR Array. The plates were analyzed with StepOnePlus^{tm} Real-Time PCR Systems (ThermoFisher Scientific, USA) following the manufacturer's protocol. The melting curve analysis was also performed at the end of each single PCR array.

Since it is not possible to publish the complete list of genes included in the array for intellectual property issue, a scatter plot has been created to compare the Log_2 FC values obtained from qPCR and RNA-seq analyses. Finally, the gene expression of the 42 hyperoxia-induced selected genes has been compared between the PND 7 and 14 models.

4. Results

4.1 Morphological characterization of the 7 days hyperoxia-exposed preterm rabbit BPD model.

Histological analysis was performed on left lungs collected from pups exposed to hyperoxia (95% O_2) or normoxia (21% O_2) conditions for 3, 5, and 7 days. The progressive morphologic and structural changes due to hyperoxic exposure, compared to normoxia, are shown in figure 9. Normoxia samples showed a maturational pattern of the airways from day 3 up to day 7, despite the premature birth. Indeed, the airspaces increased, and the septal thickness decreased. Three days of hyperoxia exposure did not produce significant changes in lung parenchyma compared to the normoxia group (Figures 9 and 10). However, hyperoxic pups depicted a more rudimentary lung structure after day 3. Indeed, in the multiple comparisons between time points, significant differences became detectable on days 5 and 7. Their airspaces become more rounded and less complex with larger and simplified alveoli and thicker septations than same-age pups kept under normoxic conditions. Moreover, an increasing presence of inflammation and alveolar debris were found in hyperoxia-exposed pups.

RAC parameter reflects lung parenchyma maturation, highlighting an increased alveolar size. Normoxia samples showed that RAC values increased from day 3 up to day 7. At this latter timepoint, RAC values were significantly lower in hyperoxia-exposed pups than normoxic samples, demonstrating lower airway complexity (Figure 10A). The ST parameters remained stable in the normoxic pups while it increased in the hyperoxia-exposed ones, reaching the statistical significance only at the last timepoint (Figure 10B). On day 7, the ALI score was used to assess lung parenchymal inflammation. From day 3 to day 7, ALI values raised stepwise in hyperoxic samples than time-matched normoxia samples, reaching the statistical significance at day 7, indicating that high oxygen exposure led to increased inflammation over time (Figure 10C).

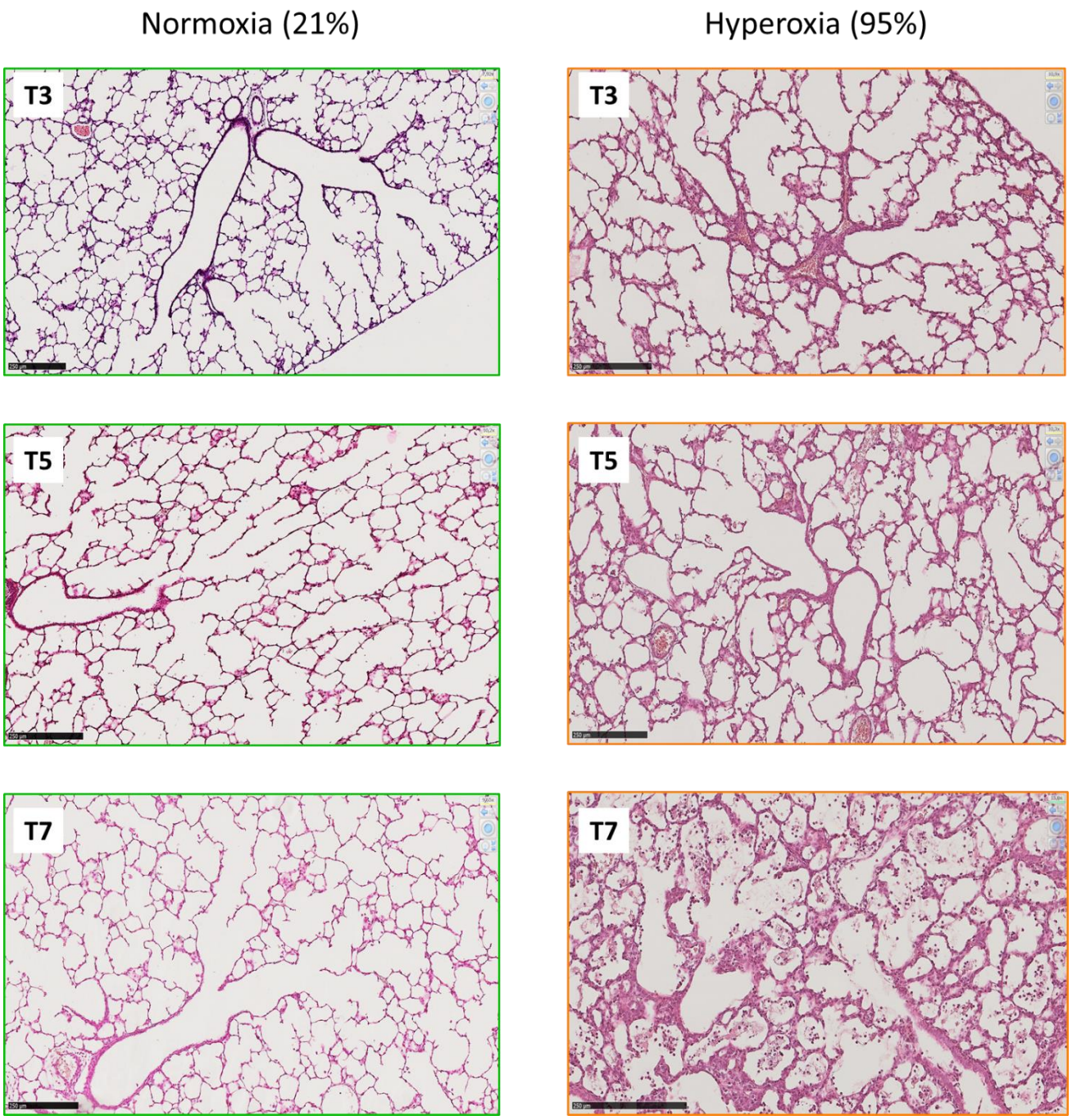

Figure 9. Representative pictures of H&E lung slides from preterm rabbit pups delivered by C-section on day 28th of gestation and kept in normoxia (left line) or hyperoxia (right line) for 7 days (scale bar = 250µm).

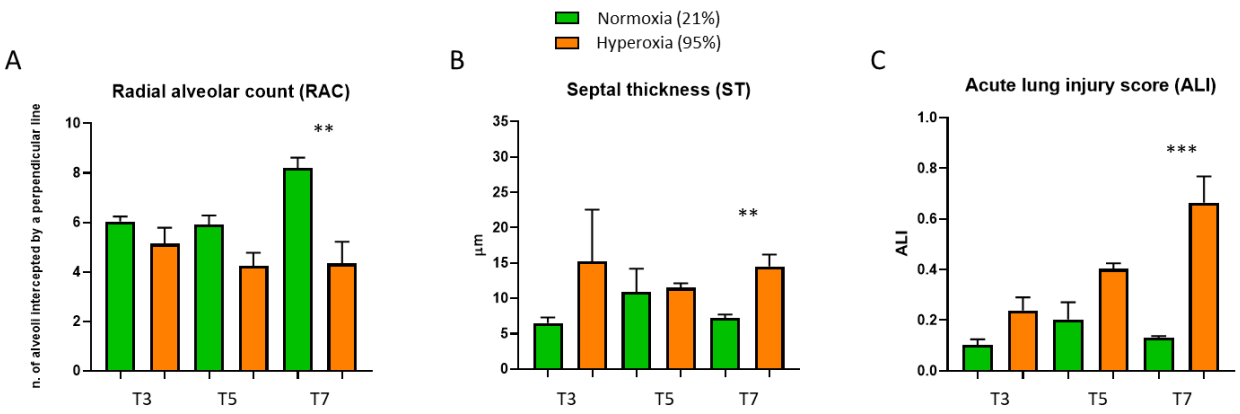

Figure 10. Histomorphometric parameters of preterm rabbits exposed to normoxia (21% O_2) and hyperoxia (95% O_2) for 3 (T3), 5 (T5), or 7 (T7) days ***A.*** *Radial alveolar count (RAC) parameters **p<0.01 HT7 vs NT7.* ***B.*** *Mean septal thickness (ST) parameters **p<0.01 HT7 vs NT7* ***C.*** *Acute Lung Inflammatory Score (ALI) ***p<0.001 HT7 vs NT7. Data are expressed as mean ± SEM and analyzed with one-way ANOVA corrected for multiple comparisons.*

During lung development, alveoli formation occurs in concert with lung microvasculature development to create the air-blood barrier. An arrest in alveolar development leads to an aberrant lung vasculature formation. At the histological level, also the peripheral arterial media thickness was affected by hyperoxia exposure. Indeed, the tunica media progressively thickened in the hyperoxia groups compared to the normoxia ones from day 3 up to day 7 (Figure 11). Consistently, the MT% parameter was significantly higher in hyperoxic pups at day 7 than age-matched normoxic pups (Figure 12). No significant variations in the MT% parameter were found between the hyperoxia and normoxia groups on days 3 and 5.

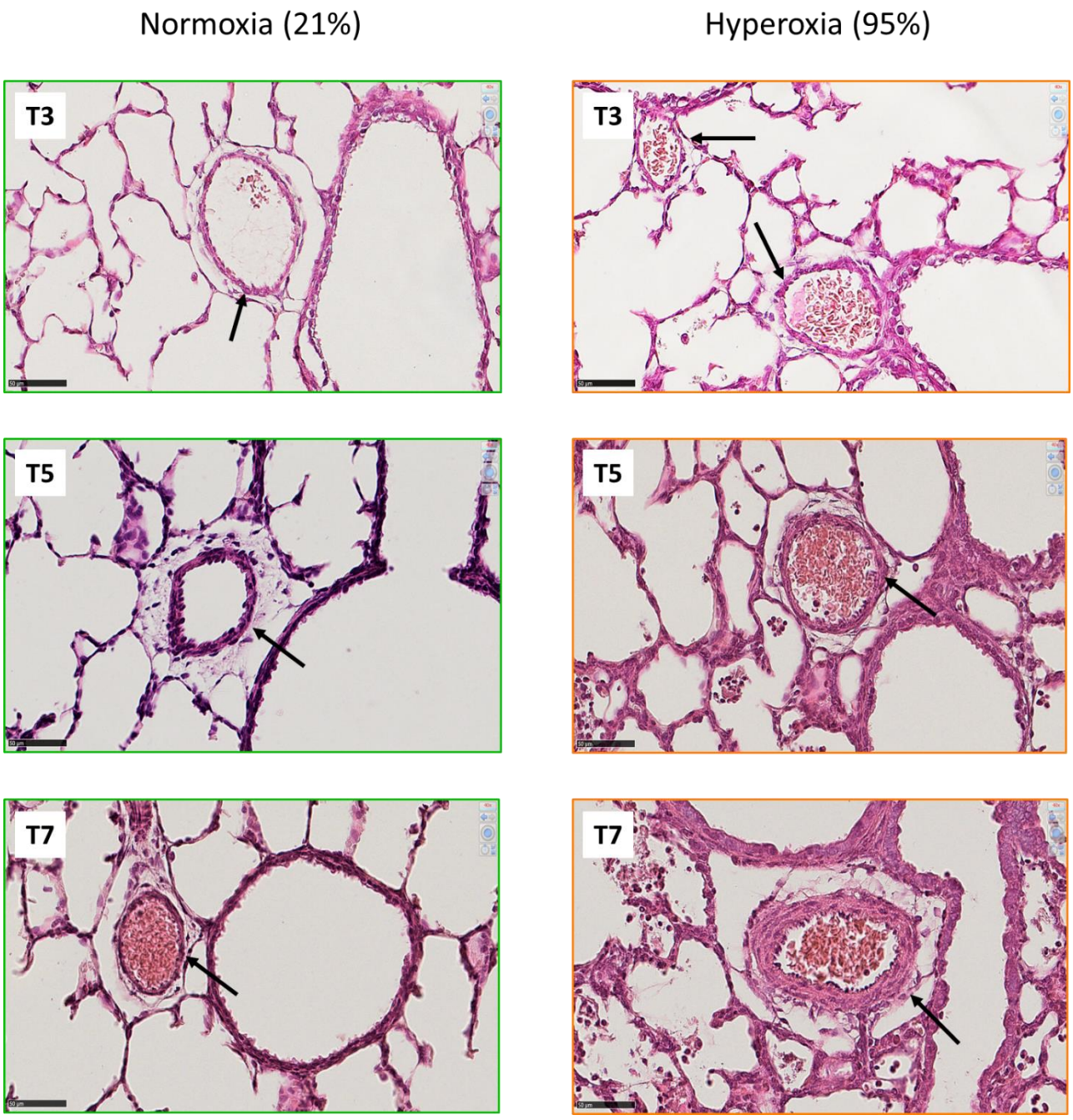

Figure 11. Representative images of lung peripheral arteries, stained with H&E, from preterm rabbit pups delivered by c-section on day 28 of gestation and kept in normoxia (left line) or hyperoxia (right line) for 7 days. Images showed a progressive thickening of tunica media in the hyperoxia group (scale bar = 50µm). Black arrows indicate the pre- and intra-acinar arteries.

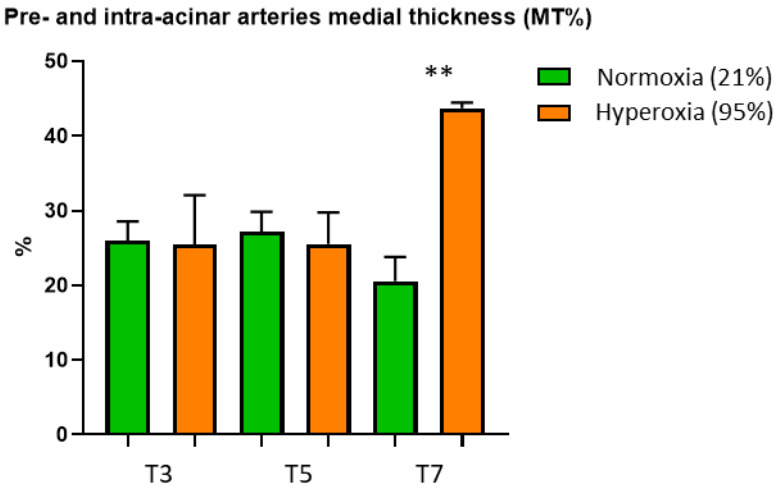

*Figure 12. Percentage Media Thickness of lung peripheral arteries (MT%) of preterm rabbits exposed to normoxia (21% O_2) and hyperoxia (95% O_2) for 3 (T3), 5 (T5), or 7 (T7) days. Data are represented as mean ± SEM **p<0.01 HT7 vs NT7, one-way ANOVA corrected for multiple comparisons*

4.2 Whole transcriptomic analysis of the day 7 days hyperoxia-exposed preterm rabbit BPD model

Transcriptome profiling was performed on right lung samples from preterm pups delivered at 28th GA (D28) and preterm pups exposed to hyperoxia (HT3, HT5, and HT7) and normoxia (NT3, NT5, and NT7), and term pups at 35th GA (D35) (n=3, each time-point). RNA-seq analysis revealed that a total of 12,339 genes were expressed in at least one sample. The PCA showed three major clusters (Figure 13). HT5 and HT7 samples were clearly separated from the other conditions, although the replicates from each condition were not grouped. NT3, NT5, NT7, and D35 samples clustered together with HT3 samples. D35 samples showed a comparable gene expression to this last sample cluster, while D28 samples belonged to a different cluster.

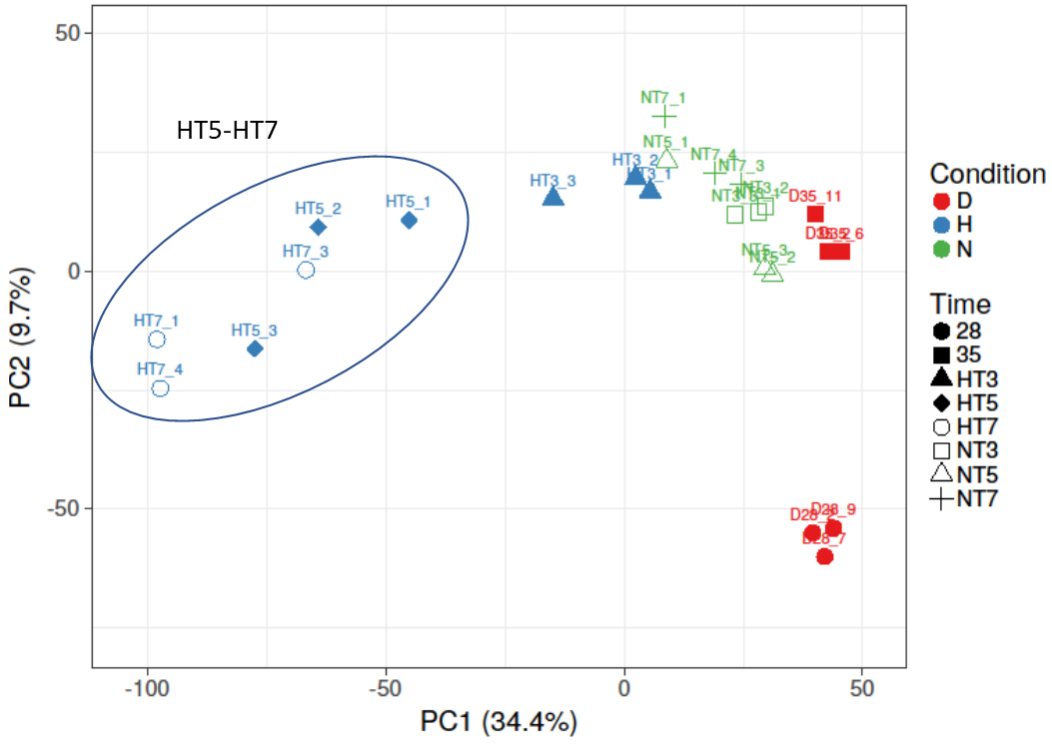

Figure 13. Principal component analysis (PCA) showed specific clusters among samples of the same time point.

4.2.1 Differentially expressed genes (DEGs)

The limma-voom analysis identified a total of 2848 genes as differentially expressed between HT *vs* NT at different time points. The DEGs obtained between D28 *vs* D35 samples were 789 (Figure 14), which of 271 were up-regulated and 518 down-regulated, confirming the results indicated by the PCA plot (Figure 13). On day 3, only 36 genes were differentially expressed (HT3 *vs* NT3 comparison). On day 5, 1592 DEGs were counted (HT5 *vs* NT5), with 971 showing a down-regulation pattern and 621 showing an up-regulation one. Finally, 2370 DEGs were identified at day 7 (HT7 *vs* NT7), of which 1399 were down-regulated and 971 up-regulated.

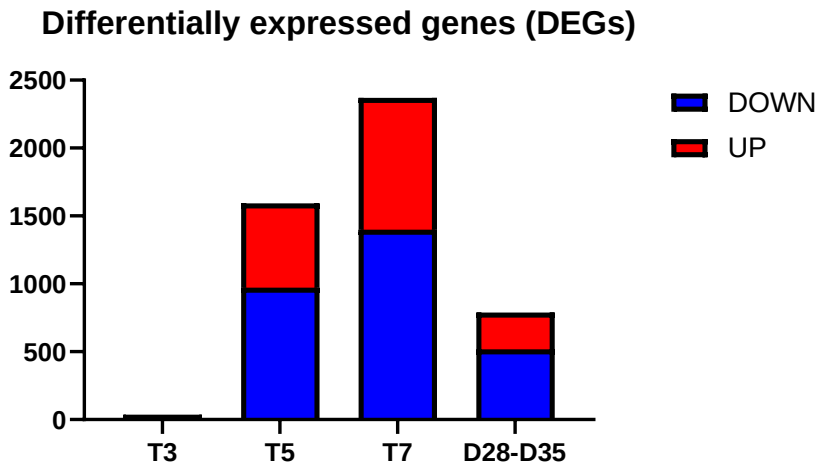

Figure 14. Histogram representation of differentially expressed genes (DEGs) across time points comparing hyperoxia and normoxia groups. Up-regulated genes are shown in red and down-regulated genes are shown in blue. The highest number of DEGs were identified in the HT7 vs NT7 (T7) comparison.

BPD phenotype is characterized by an arrest in lung and microvascular development and by inflammation, and this must be mimicked in the preclinical BPD model. To verify the arrest in lung and microvascular development on the preset set of data, we compared the transcriptional profile of the rabbit BPD model with that of the lung development time-course (D28 and D35). To better observe the transcription profiles, a cluster analysis focused on the 2848 differentially expressed genes between matched H *vs* N time points. A set of genes increased their expression during lung development, from D28 to D35 (marked with a black rectangle in Figure 15). The same up-regulation pattern can be observed in the normoxia samples from day 3 to day 7 (blue rectangle). Instead,

hyperoxia exposure lungs (red rectangle) showed a down-regulation pattern of these genes which reached expression levels at day 7 similar to D28 ones, suggesting their participation in the delay or block in lung development. This set of genes contains part of the hyperoxia down-regulated genes. The other hyperoxia up-regulated genes (gene set A) were characterized by similar expression levels in D28 and D35 samples from preterm rabbits under normoxic conditions, and by a progressive up-regulation in hyperoxia-exposed samples. Similarly, hyperoxia down-regulated genes (gene set B) showed similar expression levels in D28 and D35 lungs as well as in normoxic ones, while the hyperoxia exposure induced a gene down-regulation. Of note, genes in both set A and set B showed a progressive down- or up-regulation during hyperoxia exposure from day 3 to day 7, suggestive that their levels were specifically altered by hyperoxia in a time-dependent fashion.

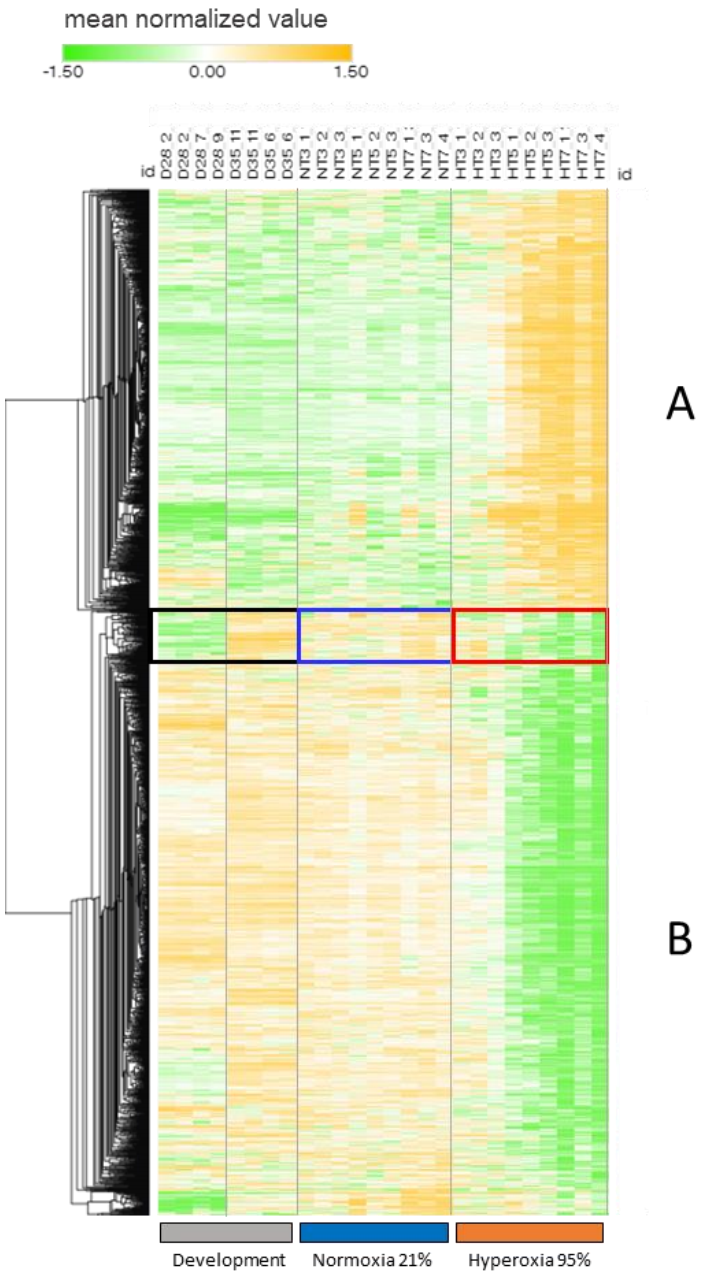

Figure 15. Comparison of T3, T5, and T7 DEG transcription profiles between the rabbit BPD model experiment and the lung development experiment. The black and blue rectangle highlighted a set of DEGs with a comparable expression between development and normoxia samples. On the contrary, the red rectangle showed that hyperoxia genes had a similar expression between HT7 and D28. Gene set A highlighted up-regulated genes in the hyperoxia samples. Gene set B highlighted down-regulated genes in the hyperoxia samples. Over- and under-expressed genes are respectively in orange and green, respectively.

4.2.2 Pathway enrichment analysis and histological correlation

The functional analysis conducted on the above described DEGs' lists, revealed several pathways involved in hyperoxia exposure damage. Enrichment pathways analysis showed that hyperoxia

exposure up-regulated pro-inflammatory pathways were significantly enriched in up-regulated genes at day 5 and day 7, such as TNFα signaling via NFKB, inflammatory response, interleukin 10, positive regulation of MAPK cascade, interferon-gamma response, response to oxygen level, and positive regulation of cytokine production. Apoptotic-related pathways such as positive regulation of programmed cell death, ferroptosis were also up-regulated at day 5 and day 7. Response to molecule of bacterial origin was found up-regulated at days 5 and 7, highlighting response to bacterial infection. Surprisingly, the hypoxia pathway was found mainly up-regulated at day 7 (Figure 16A).

Conversely, hyperoxia treatment induced a downregulation in genes involved in pathways related to lung development at day 5 and day 7, such as tissue and cell morphogenesis, embryo development, extracellular matrix organization, epithelial and endothelial cell migration, respiratory tube and lung development, and mesenchyme development. Cell cycle and G2M checkpoint pathways were downregulated after 5 days of hyperoxia exposure only. Conversely, angiogenesis and blood vessel development pathways were down-regulated both at day 5 and day 7, even if their downregulation was more evident at day 7, compared to day 5, when the developmental block occurred (Figure 16B).

The GSEA tool has been used to highlight the correlation between transcription profiles and histological results (Figure 16C). The analysis demonstrated that the ALI and ST had a positive correlation with genes involved in the innate immune system, complement activation, response to TNF, ferroptosis, and rRNA modification (Figure 16C). As expected, RAC showed an opposite correlation with the same pathways (Figure 16C).

Genes involved in collagen biosynthesis, vessel development, embryonic development, epithelial tube morphogenesis, and branching showed a negative correlation with ALI and ST, as observed in down-regulated pathways in hyperoxia groups on day 5 and day 7 (Figure 16B). While RAC NES values positively correlated with the same pathways (Figure 16C).

Figure 16. Results of pathway enrichment analysis on HT5 and HT7 and correlation with histological traits. ***A.*** *Up-regulated enriched pathways.* ***B.*** *Down-regulated enriched pathways. Representative terms significantly enriched in one or more time points are shown. Color saturation corresponds to enrichment significance (Log q-values).* ***C.*** *GSEA correlation analysis between pathways and histological parameters. ALI and ST parameters were found anti-correlated to RAC one.*

4.2.3 Comparison with the BPD animal model by Salaets et al. study

We assessed the consistency of our transcriptomic analysis by comparing our results with those described by Salaets and colleagues on transcriptomic profile of preterm rabbits exposed to hyperoxia (95% O_2) for 7 days [155]. We performed the GSEA analysis to compare the two datasets at day 7, using a ranked list based on log_2FC. GSEA analysis demonstrated robust significant NES values between our model and that described by Salaets et al. (Figure 17). NES values were 3.99 for the up-regulated list and -3.56 for the down-regulated one. Moreover, NES values were statistically significant (FDR<0.001) for both the up-regulated and down-regulated lists.

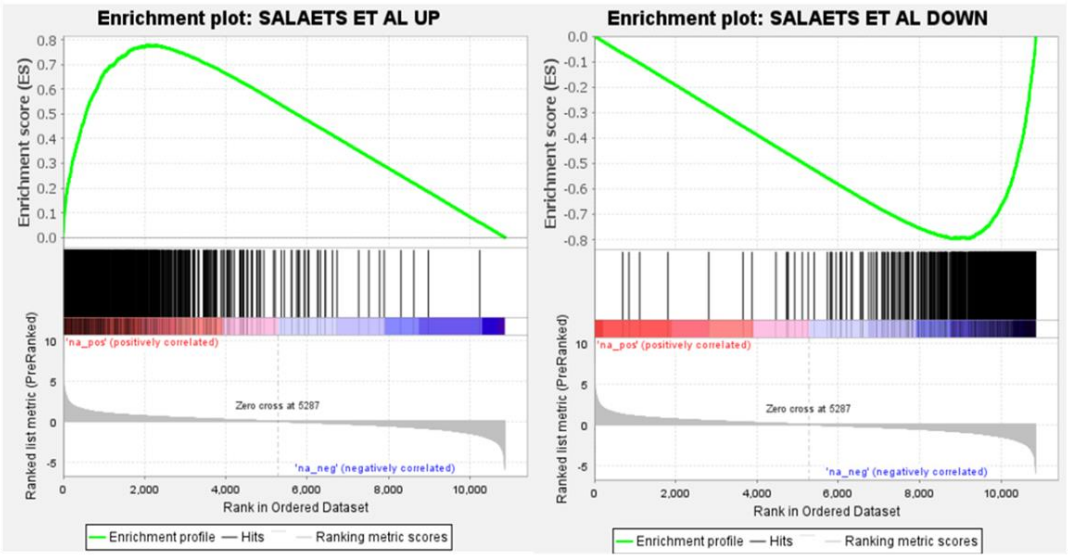

GS follow link to MSigDB	GS DETAILS	SIZE	ES	NES	NOM p-val	FDR q-val	FWER p-val	RANK AT MAX
SALAETS ET AL UP	Details ...	795	0.78	3.99	0.000	0.000	0.000	2094

GS follow link to MSigDB	GS DETAILS	SIZE	ES	NES	NOM p-val	FDR q-val	FWER p-val	RANK AT MAX
SALAETS ET AL DOWN	Details ...	691	-0.80	-3.56	0.000	0.000	0.000	2080

Figure 17. Gene Set Enrichment Analysis (GSEA) of the transcription profiles comparison with Salaets et al model. Up- or down-regulated genes obtained by Salaets et al matched with the up- or down-regulated ones described in this study.

4.2.4 RNA-sequencing results validation

A set of 42 genes was selected as representative of the BPD phenotype development in preterm rabbits exposed to hyperoxia for 7 days for RNAseq validation in qPCR and as a potential diagnostic tool.

The selection was based on data available in the literature, using the Linguamatics bioinformatic tool, and on day 7 DEGs and involved in the above described BPD-related pathways, such as TNFα signaling, apoptosis, response to oxidative stress, vasculature development, lung development, response to oxygen levels, response to hypoxia. (see also "Materials and Methods" section). The selected genes will be not included in the dissertation for confidentiality reasons. Results showed a high degree of similarity between PCR and RNA-seq data (Pearson Correlation value = 0.96, Figure 18).

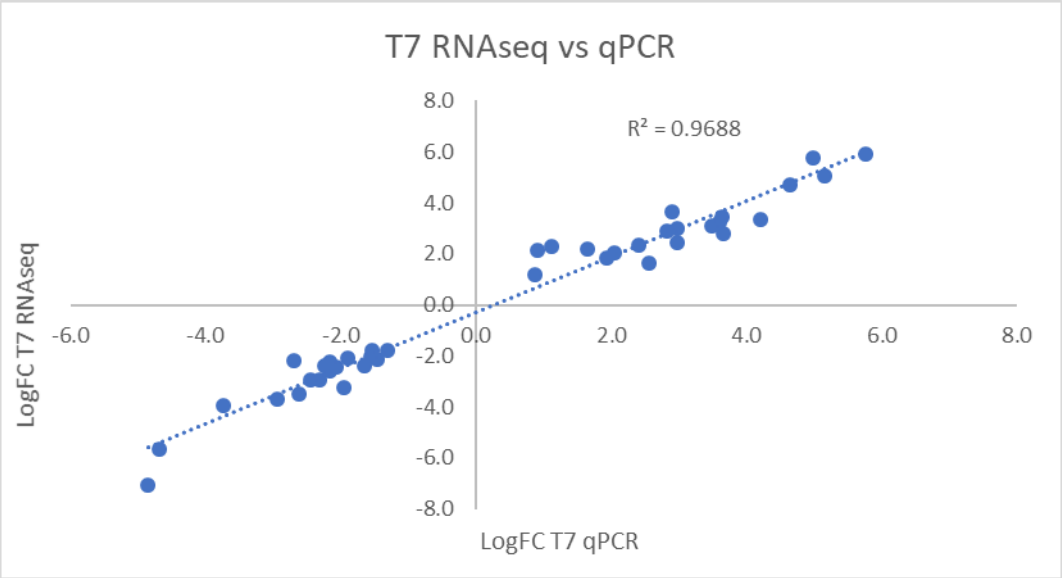

Figure 18. Comparison between the two techniques of RNA quantification.

4.2.5 Hyperoxia-induced miRNAs

Raw RNA-seq reads were initially checked for quality and aligned to the *Oryctolagus cuniculus* genome. Annotated *O. cuniculus* miRNA (a total of 588 genes) were used to calculate read counts. The PCA conducted on transcriptome data of the above-described samples (without D28 and D35 samples), revealed that normoxic samples (NT3, NT5, and NT7) clustered together with HT3 samples. Moreover, PCA revealed that HT5 and HT7 samples were separated from this cluster, suggesting that hyperoxia damage from days 5 to 7 was evident as miRNA signature (Figure 19).

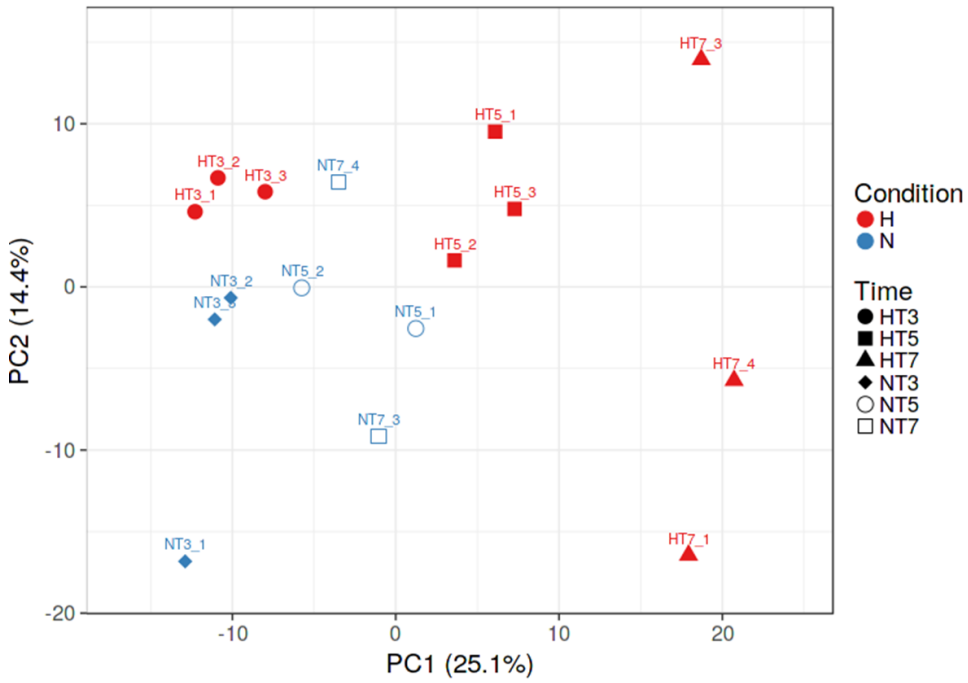

Figure 19. Principal component analysis (PCA) of miRNAs

Forty-one miRNAs were detected as differentially expressed and defined as hyperoxia-specific between HT *vs* NT at the different time points by limma-voom analysis (Figure 20A) ($Log_2FC > 0.5$ or < -0.5, average expression > 5 normalized counts and the adjusted p-value ≤ 0.05). There are no differentially expressed miRNAs between HT3 and NT3 samples. The hyperoxia and normoxia groups diverged starting from day 5. Most of miRNAs were deregulated after 7 days of hyperoxia exposure (Figure 20A) and the top dysregulated ones are listed in figure 20B. Our analysis highlighted miR-21, miR-29a, miR-29b, miR-223, miR-31, and miR34a as the most up-regulated miRNAs by hyperoxia exposure. Conversely, the most down-regulated miRNAs were miR-503-3p, miR181c and miR99a-3p.

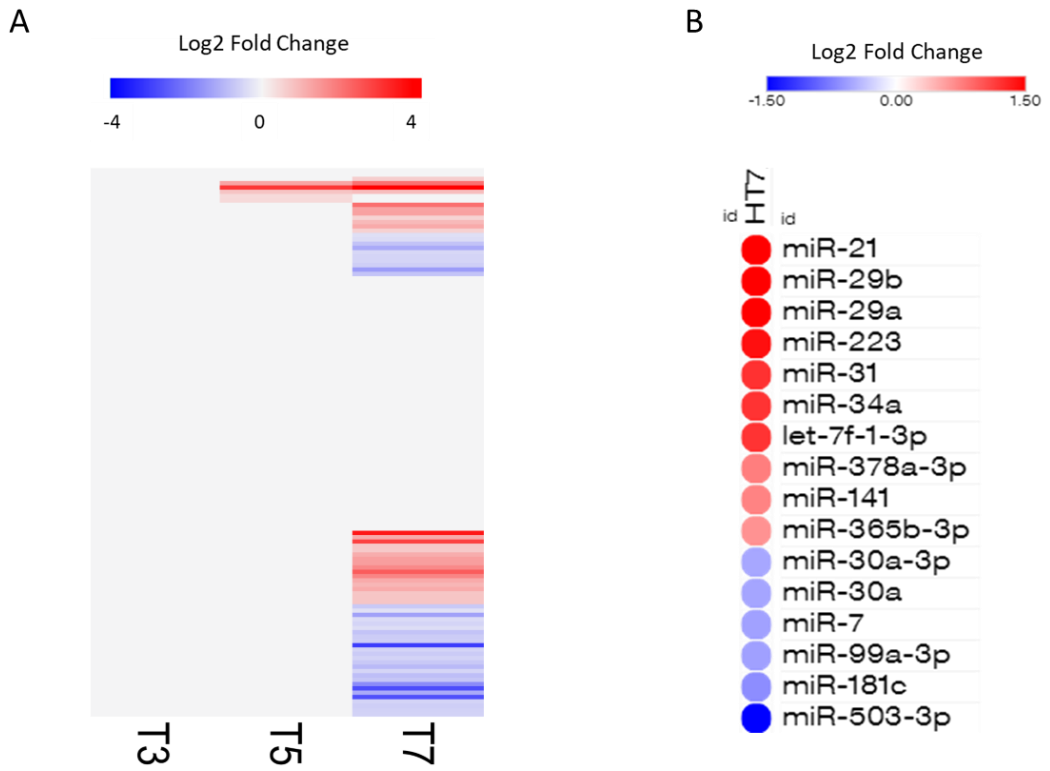

*Figure 20. miRNAs analysis **A.** Simplified heat-map of differentially expressed miRNAs identified at individual time-points. **B.** Top 16 dysregulated miRNAs on day 7. Up-regulated miRNAs are shown in red, while down-regulated genes are presented in blue ($log_2FC \geq 0.5$, adj. p-value ≤ 0.05 and average expression > 5 normalized counts).*

4.3 Characterization of the PND14 (70% O_2) preterm rabbit BPD model

An extended version from days 7 up to 14 has been set up and validated in Chiesi Farmaceutici laboratories, using 70% of oxygen instead of 95%. A long-term model could allow to test therapeutic BPD drug candidates, assessing their effects at later and more relevant time points. In this paragraph, we will focus on molecular and histological characterization of this new animal model. Main findings were then compared between preterm pups exposed to normoxia (21% O_2) and hyperoxia (70% O_2) for 14 days and age-matched term animals (D42).

4.3.1 Morphological characterization

As shown in Figures 21A and 21B, we found a significant decrease in lung alveolarization of premature pups (both hyperoxia and normoxia groups) compared to aged-matched term animals

(Figure 21A). In the lungs of preterm pups under hyperoxia, airspaces were more rounded and less complex, and the septa appeared thicker compared to pups under normoxic conditions and term animals. As expected, RAC values were significantly higher in term pups than in both hyperoxia and normoxia-exposed ones. The 70% O_2-exposed preterm group showed the lowest RAC values. Lung inflammation (ALI score) was increased in both hyperoxia and normoxia groups and it was almost absent in the D42 rabbits born at term (Figure 21C). Hyperoxia-exposed animals displayed the highest level of ALI score values compared to the other groups.

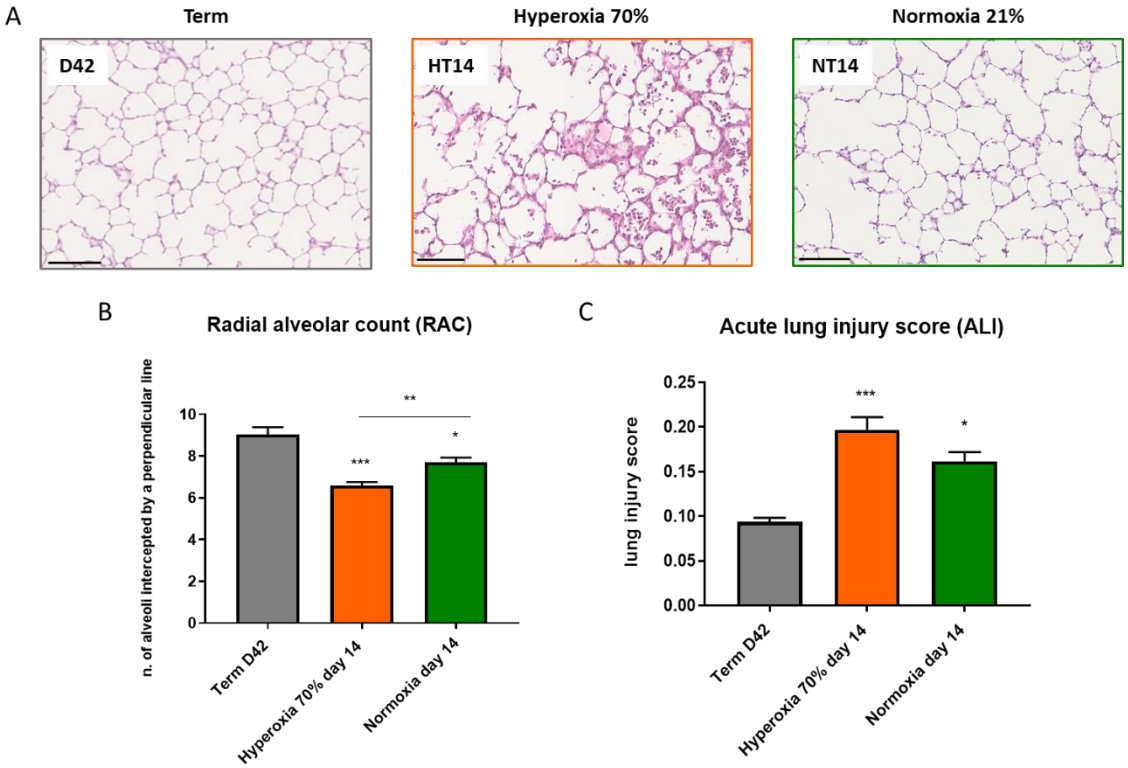

Figure 21. Histological and histomorphometric characterization of preterm rabbit pups delivered by C-section on day 28 of gestation and kept in hyperoxia 70% (HT14) and normoxia (NT14) for 14 days, and from term rabbit nursed by their does up to gestational age 42 (D42). ***A.*** *Representative pictures of lung slides, stained with H&E. Term animals (left picture), hyperoxia 70% (central picture), and normoxia (right picture) (scale bar = 100µm).* ***B.*** *Radial alveolar count (RAC) parameters **p<0.01, ***p<0.001 HT14 vs D42 and *p<0.05 NT14 vs D42.* ***C.*** *Acute Lung Inflammatory Score (ALI) parameters ***p<0.001 HT14 vs D42 and *p<0.05 NT14 vs D42. Data expressed as mean ± SEM and analyzed with one-way ANOVA corrected for multiple comparisons.*

4.3.2 Gene expression analysis on 14 days model

In the first part of this thesis, we have developed and validated a qPCR array containing 42 genes that are representative of the BPD phenotype development in preterm rabbits exposed to 95% of oxygen for 7 days. We have tested the validated qPCR array on three lung samples collected on day 14 for each group in duplicate, to evaluate if the selected genes for the 7 days model are also affected by prematurity and 70% oxygen exposure after 14 days.

Gene expression of the selected 42 genes showed a different pattern between PND 7 and 14 models. Three transcriptional profiles could be identified: hyperoxia-induced genes, prematurity-induced genes, and term-related genes (Figure 22). 10 genes were induced by hyperoxia exposure, being up-regulated only on HT14 samples. 19 genes seemed to be mostly induced by premature birth, since they were up-regulated both in hyperoxia and normoxia groups in a similar fashion, compared to the term one. Finally, 13 genes, belonging to cluster C, were mostly up-regulated in the right lungs of term animals compared to both normoxia- and hyperoxia-exposed preterm rabbits. They were predominantly down-regulated in HT14 lung samples but showed an intermediate phenotype in NT14 lung samples.

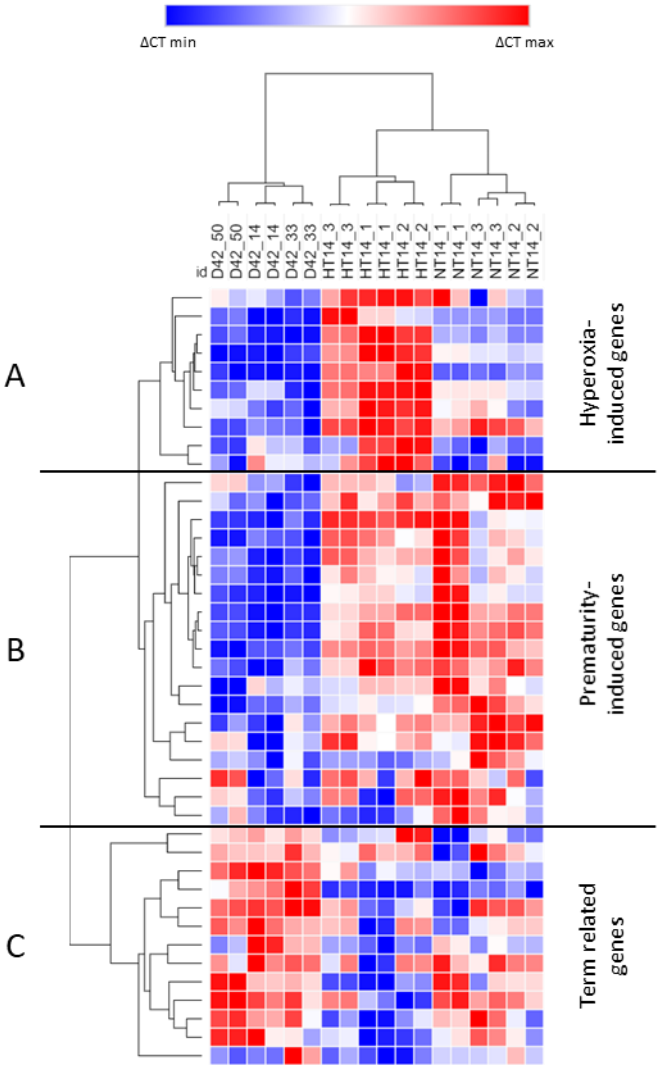

Figure 22. Heatmap of the gene expression results of normoxia (NT14), hyperoxia 70% (HT14), and term (D42) qPCR analysis. The ΔCT values were calculated using PPIB as the housekeeping gene. The results showed three different expression patterns. ***A.*** *The hyperoxia-induced group, where genes are mainly expressed in the hyperoxia-exposed animals.* ***B.*** *The prematurity-induced group, where genes are mainly expressed in preterm animals (hyperoxia and normoxia conditions).* ***C.*** *Term-related group in which genes are mainly expressed in term animals and down-regulated in preterm ones.*

4.3.3 PND7 vs PND14: histological and gene expression comparison

A comparison analysis has been performed to highlight similarities and differences between PND7 and PND14 BPD animal models. The histological comparison did not show any significant differences in RAC values between NT14 and NT7 left lung samples (Figure 23A). RAC values differences between NT7 *vs* HT7 and NT14 *vs* HT14 were confirmed. Moreover, HT7 samples

displayed significantly lower RAC values compared to the HT14 ones. Similarly, the ALI score was comparable between NT14 and NT7 groups. The analysis confirmed the above results in ALI score values between NT7 *vs* HT7 and NT14 *vs* HT14. ALI score was significantly higher in HT7 compared to NT14 (Figure 23B). These results demonstrated a higher lung injury and a lung developmental arrest in HT7 samples compared to the HT14 ones.

Moreover, the gene expression of 42 genes investigated in both the PND7 and PND14 was compared (Figure 23C). Consistently with the previous histological findings, genes from NT14, HT14, and NT7 groups clustered together (although NT7 samples belonged to a sub-cluster), while HT7 samples showed a distinct gene expression profile. In particular, 21 genes showed a similar down-regulation pattern in HT14, NT14 and NT7 samples that resulted up-regulated in the HT7 group. Oppositely, 21 genes showed a down-regulation pattern in the HT7 samples that were up-regulated in HT14, NT14, and NT7 ones. These findings confirmed the histological results and revealed a milder phenotype of the PND14 animal model that should be further characterized through transcriptomic analysis.

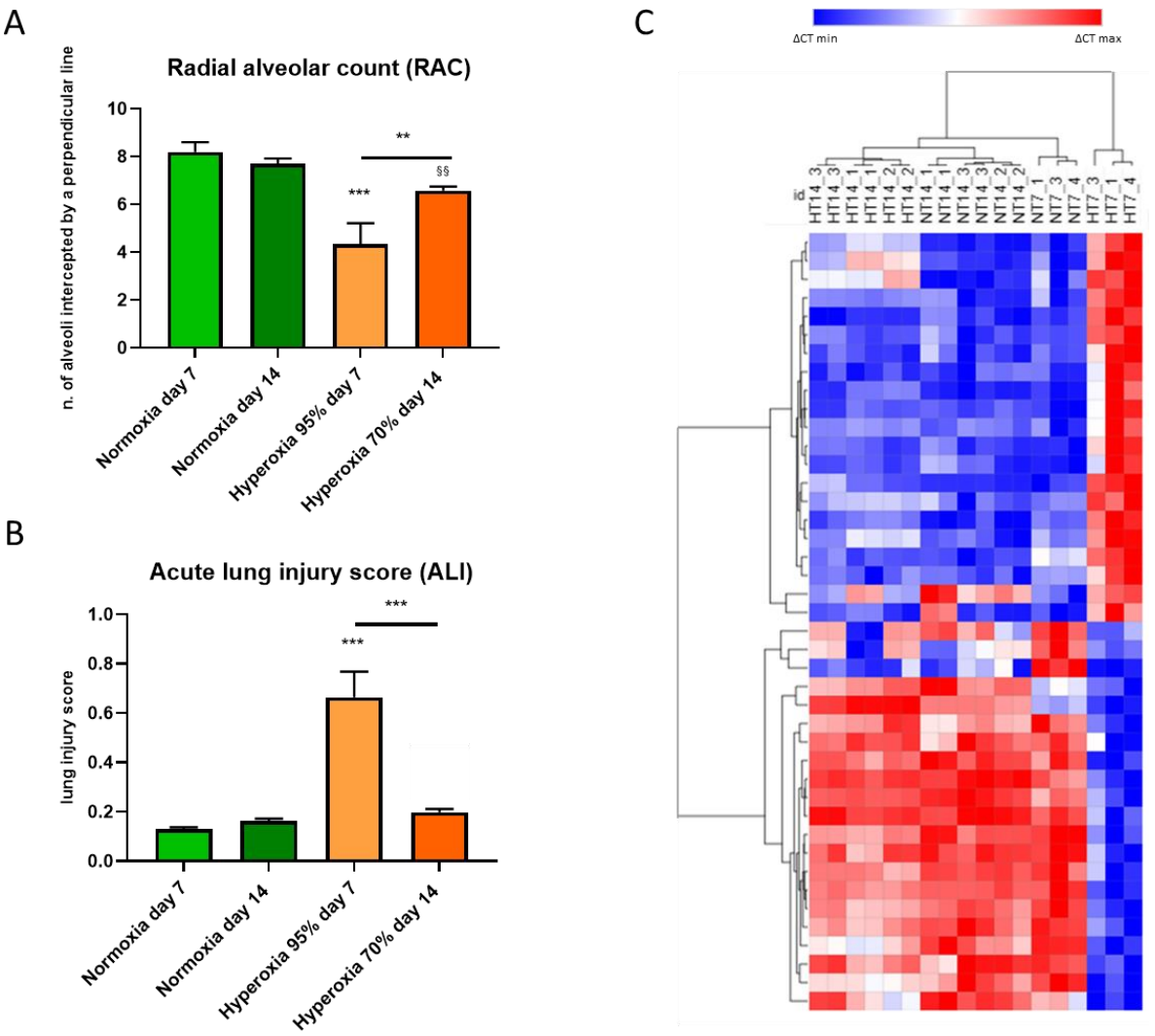

Figure 23. Comparison between PND7 and PND14 BPD animal models. ***A.*** *Radial alveolar count (RAC) parameters **p<0.01, ***p<0.001 NT7 vs HT7 and §§p<0.001 NT14 vs HT14.* ***B.*** *Acute Lung Inflammatory Score (ALI) parameters *** p<0.001 NT7 vs HT7. Data expressed as mean ± SEM and analyzed with one-way ANOVA corrected for multiple comparisons.* ***C.*** *Heatmap of the qPCR gene expression comparison between normoxia (NT14 and NT7), hyperoxia 70% (HT14), and hyperoxia 95% (HT7) qPCR. The ΔCT values were calculated using PPIB as the housekeeping gene.*

5. Discussion

The constant progression in neonatal clinical care has increased the survival of extremely premature infants, but BPD remains the most common complication with adverse long-term outcomes [30,73]. The etiology of BPD consists of a complex interplay between pre- (IUGR, maternal smoking, genetic predisposition, and inflammation) and post-natal (malnutrition, mechanical stretch, inflammation, and oxygen toxicity) factors that compromise the functionality and the structure of immature lungs [43,63], implicating a high variability among clinical cases and heterogeneity in phenotype. In the last decades, several animal models have been developed to mimic BPD phenotype, although they were not completely reliable, making this disease difficult to be deeply investigated [72,129]. A pivotal aspect to be taken into account in order to establish valid BPD models is their translation value considering in particular the need for mimicking a lung development condition. Indeed, mice, rats, rabbits, baboons, and lambs share a similar lung development, but the duration and type of developmental stage at term birth vary greatly between different species [72]. Moreover, most of BPD models have been developed by exposing animals to high oxygen concentrations (O_2>80%), which alone may not be sufficient to recapitulate all the BPD features [72,76,130,133,134,138]. For these reasons, most of the research has been focused on the refinement of available BPD animal models, in order to expand the knowledge on BPD pathophysiology and to test innovative therapeutic strategies [130,136].

The 95% hyperoxia exposed preterm rabbit BPD model has been originally described by Manzano *et al.* and it has been further refined and characterized by Prof. Toelen's research group in Katholieke Universiteit in Leuven, Belgium [138,139,155]. They found that elastance and tissue damping were significantly increased, and total lung capacity and compliance decreased in preterm rabbits exposed to 7 days of hyperoxia (95% O_2) compared to ones exposed to normoxia (21% O_2) [138,139,155]. In our study, we did not test pups' lung functionality since we focused our analysis on the lungs' gene expression profile, which could be altered by this invasive procedure. However, lung function analysis has been performed during the set-up and validation of this model in Chiesi laboratories,

confirming the Prof. Toelen results (data not shown). Moreover, Jimenéz *et al.* found that a hyperoxia-exposed lung had extensive and homogeneous lung damage with interstitial and alveolar edema on day 7 [138]. We found that the hyperoxia and normoxia groups were similar up to day 3 in each histological parameter measured (Figures 9 and 12). In fact, high oxygen exposure did not affect RAC, ST, ALI, and MT% values up to day 3 (Figures 10 and 12), but the two groups started to diverge only from day 5, confirming the results by Jimenéz and colleagues [139]. From day 5, hyperoxia leads to increased alveoli dimensions, with apparently thicker walls, less complex distal airways, and more inflammation than normoxia-exposed pups' lungs (Figures 9, 10, 11, and 12). The increased lung inflammation in hyperoxia-exposed pups' lungs, evaluated by the ALI score parameter, resulted similarly to that shown in Jimenéz *et al.* study (Figures 9 and 10) [139]. Conversely, RAC values were higher in normoxia-exposed pups' lungs compared to the hyperoxia-exposed ones, indicating alveolar simplification characterized by a reduction of alveoli number and enlarged alveolar space in hyperoxia-exposed animals (Figures 9 and 10).

Despite this histological and lung functional characterization, the PND7 hyperoxia-exposed preterm rabbit BPD model lacks of a deep molecular characterization compared to other BPD animal models. To date, only Salaets *et al* have characterized the lung transcriptomic profile of preterm rabbits but focusing only on the final timepoint of postnatal day 7 after either hyperoxia or normoxia exposure [155]. In this study, we performed a longitudinal lung transcriptomic characterization in order to fulfill this evident knowledge gap and to understand which pathways were involved in the BPD onset and development. The analysis of DEGs demonstrated different transcriptomic patterns in hyperoxia animals from day 5 up to day 7, in line with the histological findings (Figure 14). More than 2000 genes were dysregulated at day 7. These data are consistent with those obtained by Salaets and colleagues that found 2217 DEGs at day 7 in the hyperoxia group, compared to the normoxia one [155]. Moreover, GSEA analysis demonstrated that the gene expression profile of the lung exposed to hyperoxia for 7 days was comparable between our study and Salaets work, implying a similar

response to hyperoxia injury despite the different strains used (a hybrid of New Zealand White and Dendermond in the Salaets study *vs* a New Zealand White inbred strain in our study). Contrary to day 7, there were no differences in terms of DEGs between hyperoxia and normoxia condition at day 3, but the two groups started to diverge from day 5 (Figure 14). The gene expression analysis also showed that normoxia (NT3, NT5 and NT7) and physiological lung development samples (F28 and T35) had a comparable expression, suggestive of a similar lung developmental pattern not dependent on prematurity. This data confirmed Jimenéz *et al* and Salaets *et al* main findings [137,138], demonstrating that, other than premature birth, high oxygen exposure is essential to disrupt gene expression and to block lung developmental patterns (at least for this degree of prematurity and triggering conditions).

We performed an enrichment pathways analysis on the DEGs to determine which processes and pathways were dysregulated. We found that hyperoxia exposure increased the expression of a plethora of pro-inflammatory patterns in the lung such as TNFα signaling, inflammatory response, positive regulation of MAPK cascade, interferon-gamma response, response to oxygen level, and positive regulation of cytokine production, which guide human BPD development [141,180–182], halting alveolarization and vascular development processes in the immature lungs of preterm infants [71,182,183]. Several transcriptomic studies performed on BPD animal models showed that hyperoxia exposure stimulates pro-inflammatory pathways [177,184]. We found that TNFα signaling via NFKB was significantly up-regulated from day 5 to day 7 (Figure 16). TNFα is a primary mediator of acute lung inflammation [185,186], while NFKB regulates the cellular response to oxidant stress and inflammation, both contributing to the pathophysiology of BPD [187]. Consistently, Salaets *et al* have shown that inflammatory and ROS metabolism pathways were significantly up-regulated in the preterm rabbit after 7 days of hyperoxia exposure, suggesting their crucial role in the pathogenesis of hyperoxia-induced lung injury [155]. Moreover, interleukin pathways were found to be significantly enriched in our study. Speer *et al* and Todd *et al* demonstrated high levels of pro-inflammatory cytokines such as

IL-1β, IL-6, IL-8, TNF-α, and macrophage inflammatory proteins, in tracheal aspirates from mechanically ventilated preterm infants who develop BPD Pulmonary inflammation and bronchopulmonary dysplasia [188,189]. Furthermore, we found MAPK cascade pathways as significantly up-regulated by hyperoxia exposure (Figure 16). These pathways activate several transcription factors involved in innate immunity, cell growth, stress response, apoptosis, and differentiation [190].

Linked to inflammatory processes, our analysis identified that processes involved into response to bacterial were up-regulated in hyperoxia group on days 5 and 7 (Figure 16). Post-natal sepsis can participate in inflammatory induction. Several studies have demonstrated that preterm babies are susceptible to sepsis after birth occurrence and severity of bronchopulmonary dysplasia and respiratory distress syndrome after a preterm birth [191–194], which is mainly due to an immature immune system or post-natal infections that should be further evaluated. In the last decades, corticosteroids treatments have been developed and used to reduce inflammation in BPD patients. Post-natal corticosteroids administration exhibited considerable beneficial effects on lung function and inflammation in premature infants with lung disease [195]. To date, the intratracheal administration of surfactant and budesonide has shown a reduction of BPD rate in very low birth weight infants [111,196], reducing systemic adverse effects of systemic corticosteroids administration.

Cell death processes are also involved in hyperoxia damage [197]. Our analysis showed that apoptosis pathways were up-regulated in hyperoxia pups at days 5 and 7 (Figure 16). Apoptotic cell death plays an important role in physiological lung development and repair after lung injury and contributes to BPD onset [198,199]. Das *et al* demonstrated that p53 and p21 expression were increased in 125-day and 140-day premature baboons with BPD, demonstrating an increase in apoptosis phenotype in their lung tissues [200]. Similarly, we found p53 related pathways as activated at days 5 and 7 (Figure 16). The MTORC1 pathways were up-regulated in hyperoxia-exposed pups. MTORC1 is a negative regulator of autophagy by modulating the activity of ULK1 complex that is essential for the formation of autophagosomes [201]. Sureshbabu and colleagues reported that mTOR was up-regulated in lung

epithelial cells of hyperoxia-exposed mice for 7 days. They also demonstrated that RPTOR inhibition, a key component of MTORC1, increased autophagy, decreased apoptosis, and improved lung architecture in hyperoxia surroundings [202]. Lastly, ferroptosis was also found to be up-regulated in pups exposed to hyperoxia at day 7. Ferroptosis is a non-apoptotic cell death resulting from an excessive iron-dependent lipid peroxidation caused by high free radical exposure [203]. Recent studies demonstrated that ferroptosis plays a critical role in the pathogenesis of chronic obstructive pulmonary disease, fibrosis, infection, and asthma [204–208]. To date, this pathway has not been described as linked to BPD pathophysiology yet and it might deserve further evaluation.

The hypoxia pathway was mostly up-regulated in hyperoxia lung samples at day 7 (Figure 16), suggesting that hyperoxia damage could favor hypoxic zones formation in the lung parenchyma of the hyperoxia exposed pups. Several studies demonstrated that preterm babies have high intermittent hypoxic spikes as a consequence of immature respiratory control, that could sustain a proinflammatory cascade [209,210], as described herein.

We also showed that hyperoxia exposure down-regulated several pathways involved in physiological lung development. It is known that BPD disrupts lung and vascular development, indeed preterm babies with severe BPD showed alveolar simplification, reduced secondary septation, and markedly abnormal microvascular growth [211,212]. We found that angiogenesis and blood vessel development were the most down-regulated pathways in the lung of day 5 and 7 hyperoxia exposed pups (Figure 16). Salaets *et al* showed similar results, highlighting that vasculogenesis pathways were significantly down-regulated by hyperoxia in preterm rabbits after 7 days [155]. More than 100 vascular-related genes were dysregulated in hyperoxia exposed newborn mice model in Revhaug and colleagues' study [213]. Hurskainen *et al* also showed that hyperoxia reduced general capillary (gCap) cells in a hyperoxia-exposed mouse model (85% O_2 for 14 days): gCap cells are distal lung vascular progenitor cells and their reduction in this hyperoxia mouse model may impair the repair of the injured lung, leading to the development of pulmonary vascular disease [214]. Our results are in line with these studies since we

found both simplification of lung vascular development and block in vascular gene expression patterns (Figures 12 and 16), similar to those observed in BPD patients [133,134]. Hyperoxia-mediated detrimental changes on lung vasculature result also in higher tissue resistance and, consequently, in pulmonary hypertension (PH) in preterm rabbits, as in humans [139,215–217]. Jimenéz J. *et al.* described that newborn rabbits exposed to 95% of oxygen for 7 days have decreased PAAT/PAET ratio, linked to PH onset, when compared to both normoxia and term controls [139]. These results were confirmed during the set-up and validation in Chiesi laboratories (data not shown).

As previously described, alveolarization is the last phase of lung development and it is mainly a post-natal event [3]. Clinical and experimental studies demonstrated alveolarization is disrupted in preterm BPD babies, decreasing the gas exchange surface area of their lungs [15,36,218,219]. We demonstrated that lung airways development was also significantly affected by hyperoxia exposure (Figures 9 and 10). Lung development, tissue morphogenesis, embryo morphogenesis, mesenchyme development, extracellular matrix organization, and developmental growth pathways were significantly down-regulated in the lung of hyperoxia exposed animals at days 5 and 7 compared to the normoxia ones (Figure 16), in line with Salaets *et al.* findings [155].

Epithelial and endothelial cell migration pathway was also found down-regulated mainly at day 7. Akram and colleagues suggested that cell migration is the key driver of the alveologenesis. Indeed, they demonstrated in a precision cut lung slice (PCLS) model that migration inhibitors (i.e. blebbistatin and cytochalasin D) significantly restricted alveologenesis [220]. The present study suggests that hyperoxia damage decreases epithelial cell migration and consequently the alveologenesis process in the hyperoxia-exposed preterm rabbit.

Mesenchymal development pathways are critical for epithelial cell differentiation and vasculogenesis during the lung developmental phases [221], and they resulted significantly inhibited by hyperoxia exposure. Lung-resident MSCs from hyperoxia-exposed lungs show decreased pathways that

promote lung and vascular growth [222]. Moreover, MSCs tracheal aspirates from babies with BPD were reduced, suggesting that their absence contributes to reduced alveolarization [223]. These investigations revealed that BPD can impair the growth function of lung MSCs, hence the development of several MSC-based therapies to prevent BPD [122,125].

Lastly, we also found a common pattern between lung gene expression and histological parameters. The analysis demonstrated a positive correlation between genes involved in lung development-related pathways and RAC values (Figure 16C), both negatively affected by BPD progression in hyperoxia-exposed animals compared to the normoxic ones. Consistently, ALI and ST negatively correlated with RAC values and positively correlate with lung injury pathways, boosted by hyperoxia exposure (Figure 16C).

A secondary aim of this study was the development of a molecular assay, based on selected candidate biomarkers with translational value based on our results and literature analysis. This is an essential tool because it is difficult to applicate molecular approaches to evaluate the BPD development in rabbits such as ELISA, western blot, and immunofluorescence. Indeed, rabbits are not often utilized as laboratory animals so the reagents and antibodies available are scarce. For these reasons, 42 genes have been selected from literature analysis and to be representative of BPD onset in the PND7 model, since they belong to pathways that we have highlighted in this study such as inflammation, vasculature development, apoptosis, lung development, and response to hypoxia. RT2 PCR array confirmed and validated the RNAseq results on the selected genes. This array will be a unique preclinical tool in future experiments for evaluating the therapeutic effect of new pharmacological treatments in the PND7 BPD animal model (Figure 18).

In the last decades, miRNAs have been considered promising candidates for novel therapeutic approaches for BPD treatment [224]. miRNAs are single-stranded sequences of short non-coding RNAs (~21–25 nucleotides) that are transcribed from DNA sequences into precursor miRNAs and finally

processed in mature miRNAs [225]. They can be considered as "gene expression regulators" and they are essential in several cellular processes such as differentiation, development, proliferation, signaling, inflammation, and cell death [225–227]. In this study, hyperoxia exposure dysregulated 45 miRNAs (Figure 20B) and, among them, miR-21 was the most significantly up-regulated one. miR-21 has been described as a potent proliferation promoter and inhibitor of apoptosis [228,229] and Bhaskaran *et al* and Dong *et al* demonstrated its up-regulation in hyperoxia exposed newborn rats and mice [175,230]. Other than miR-21, miR-29a has been described by Dong *et al* as the most up-regulated miRNA[175], supporting our results. Hu *et al* identified GABA1 as the target of miR-29a and its inhibition may impair surfactant protein homeostasis, subsequently predisposing to lung injuries [231,232]. Moreover, it has been suggested that inhibition of miR-29a decreased apoptosis phenotype in a hyperoxia-exposed mouse model [231]. miR-223 was also found to be induced in our dataset. This result is in contrast with Oji-Mmuo and colleagues' findings: they showed that miR-223 was down-regulated in TA from mechanical ventilated preterm babies with BPD [147]. Conversely, miR-223 has been reported to be over-expressed in patients with diverse pathologies, including type II diabetes, acute lung injury (ALI), rheumatoid arthritis, and inflammatory bowel disease [233–236]. Feng *et al* study showed also that patients with acute RDS have a higher level of miR-223 in the bronchial alveolar lavage fluid compared to healthy controls [237], suggesting that the relationship between miR-223 and lung injury should be further investigated. Lastly, miR-34a has been found up-regulated in our dataset. Syed *et al* demonstrated that hyperoxia led to a significant increase of miR-34a, in neonatal mice lungs exposed to hyperoxia via p53 induction, and in type 2 alveolar epithelial cells from preterm neonates with nRDS and BPD. They have also shown that miR-34a deletion decreased cell death and inflammation, ameliorating the pulmonary and PH phenotype [238].
On the other side, among the most down-regulated miRNAs in our dataset, we found miR-503-3p, miR181c, and miR99a-3p. Xing et al. found all of them to be down-regulated in neonatal rat lungs exposed to hyperoxia for 14 days [239,240]. MiR-181c was also significantly down-regulated in lung

tissues from patients with COPD and its over-expression in a COPD mice model (a cigarette smoke model) reduced inflammatory response and ROS production [241]. Consistently, Li *et al* demonstrated that miR-181c over-expression reduced inflammation, down-regulating the TLR4 signaling pathway, in the lungs of a LPS rat model [239]. This evidence is supported by results on our preterm rabbit model showing that inflammation is strongly activated in hyperoxia exposed pups at days 5 and 7. Moreover, this miRNA was found also up-regulated in a neonatal mouse BPD model [175]. Future research should be conducted to determine whether miR-181c activation in the lungs is a compensatory mechanism to contrast inflammatory processes that are critical to BPD formation.

In this study, we demonstrated that based on its transcriptomic and histologic profiles the hyperoxia-exposed PND7 preterm rabbit model could be a valuable tool for testing new pharmacological interventions for the prevention of BPD, but hawse must acknowledge several limitations. In particular, the short experimental duration (7 days) allows testing drugs only as preventative intervention and not as therapeutic treatment. A long-term model could allow to test of BPD drug candidates assessing their effects at later and more relevant time points and offering the possibility of treatment after an already established lung injury. Moreover, the hyperoxia condition (95% O_2) used in this study is quite far from the standard of care in the NICUs [242]. Velten and colleagues have shown that mice exposed to hyperoxia (85% O_2) for 14 days have higher airways resistance and lower compliance compared to normoxia exposed group [243]. In another study, high oxygen exposure (60% O_2) for 4 days in term mice, after a recovery in normoxia up to 8 weeks from birth, have not changed the lung functionality [244]. Similar outcomes have been reported in mice exposed to hyperoxia (70% O_2) for 7 days and then exposed to normoxia for 14 days [245]. Contrary, Menon *et al* have demonstrated that term mice exposed to 70% of oxygen for 15 days and then exposed to normoxia for 6 weeks, developed alveolar and vascular simplification, and PH [246]. This evidence underlined the need to extend the hyperoxia exposed preterm rabbit model beyond day 7. For these reasons, an extended version up to day 14 of the BPD model using 70% oxygen has been set up and validated in Chiesi

laboratories. Firstly, rabbits at 14 days post-birth have an age close to the one at which BPD is diagnosed in neonates (36-38 weeks gestational age) [247]. During the model set-up and validation, preterm rabbits exposed both to hyperoxia (70% oxygen) and normoxia conditions have shown differences in lung functionality compared to age-matched term animals (data not shown). For this reason, in this study, we chose to analyze the histological features and gene expression of the 42 genes selected in PND7 model in both preterm animals, exposed to hyperoxia (70% O_2) and normoxia (21% O_2) at day 14, and age-matched term controls. At day 14, histological results have demonstrated that normoxic pups showed a lung growth delay when compared to their age-matched controls born at term (Figure 21). Taking together, this data indicates that prematurity, in association with artificial diet and care, without exposure to any other insult can already lead to a lung developmental gap compared to age-matched controls born at term. Hyperoxia exposure exacerbated this phenomenon, leading to a reduced alveolarization and increased inflammation, as shown by higher ALI score and lower RAC values compared to normoxia and term animals (Figure 21), indicating that premature birth and 70% oxygen exposure triggered a stronger arrest of lung development in preterm rabbits compared to room-air exposure ones.

The 42 genes selected for the qPCR analysis from the PND7 model have been assayed on the PND14 samples in order to highlight similarities and differences among the two groups. The qPCR highlighted three sets of genes (Figure 22). The first one was enriched with genes up-regulated by hyperoxia exposure only, suggestive of their strong correlation with oxygen damage. The second one included genes mostly up-regulated by prematurity condition rather than hyperoxia. Lastly, the third group consisted of genes down-regulated in the lungs of preterm animals. We could speculate that these set of genes are important for physiological lung development or down-regulated by hyperoxia exposure, but further investigations are required.

Finally, PND7 and PND14 models were compared at histological and gene expression profile levels (Figure 23). Regarding the RAC parameter, most of the differences were accounted for the HT7 and

NT7 groups. As expected, the PND14 model (HT14 *vs* NT14) showed a milder phenotype compared to the PND7 one. Anyhow, we found a significant difference between HT7 and HT14 groups that was not detected in both normoxia groups (NT14 *vs* NT7). The same findings were found analyzing the ALI score parameter. Gene expression confirmed the histological data between PND7 and PND14 models. Indeed, the HT7 group showed a different expression pattern compared to NT14, HT14, and NT7 groups. These findings demonstrated a milder BPD phenotype for the PND14 hyperoxia model compared to the PND7 one, indicating that an RNA-seq approach should be performed to further characterize how premature birth and hyperoxia exposure alter gene expression and pathways.

5.2 Conclusions and future directions

In conclusion, we deeply characterized the histological and transcriptomic profile of the PND7 hyperoxia exposed preterm rabbit BPD model. The gene expression analysis highlighted several pathways that are dysregulated during BPD development, confirming several features of human BPD. Moreover, the PND14 model allows us to observe the preterm impact on lung development that is not evident in the PND7 model, according to histology and gene expression results. All these results demonstrated the high translational value of our preterm rabbit model to study BPD development and pathophysiology. Finally, deep molecular characterization of both animal models will be critical to identify new targets and pathways to develop innovative preventive and therapeutic therapies against BPD.

It must be acknowledged that this study has some limitations. First of all, rabbits are not commonly used as a lab model and there is not a large availability of reagents. For this reason, ELISA, immunohistochemistry, or western blot analysis have not been performed to validate the transcriptomic analysis. Second, we did not compare our results obtained in preterm rabbit lungs with transcriptomic analysis performed on human BPD lungs because these specimens are lacking due to ethical constraints. In fact, studies have been focused only on blood samples and tracheal aspirates, but they are not comparable with lung tissue. In addition, authors often focused on selected cell

populations instead to analyze the whole sample. Moreover, the rabbit genome is less curated than other species and that could have caused a loss of information during our analysis. Another issue is the lack of lung functional analysis of the animals used in this study. As already mentioned, we avoided this analysis because it is an invasive procedure that may cause changes in lung gene expression. Furthermore, we have performed a bulk RNA-seq analysis instead of a single cell one. Finally, the characterization of the day 14 model was performed only at the end of the experiment (day 14) without taking into account the progression of BPD through time, which surely deserves future investigation.

In future studies, we will employ a multi-omics approach to characterize the PND7 hyperoxia exposed preterm rabbit. We will collect lung samples at the same time points to characterize the proteomic profiling. This analysis coupled with transcriptomic and miRNAs ones will permit us to evaluate the correlation between gene expression and protein production and understand the gene expression regulation. Moreover, several bioinformatics tools such as Metascape and Ingenuity Pathways Analysis (IPA®, Qiagen, Germany) will be employed on these datasets in order to identify new BPD biomarkers and targets of interest. These findings will be used to develop new therapeutic treatments. Furthermore, the single-cell RNA-sequencing (scRNA-seq) technology has been recently developed, permitting a high resolution and simultaneous characterization of thousands of cells at the transcriptome level. This approach will be employed to identify which cell populations are mostly impacted by hyperoxia and premature birth, highlighting the main effector cells and disease-associated cell-cell communications. In addition, we are performing several experiments to set-up and validate RNA-in situ hybridization (RNAscope®, ACD, USA). This technique delivers quantitative, sensitive, and specific molecular detection of RNA species on a cell-by-cell basis with morphological context, permitting to overcome the lack of anti-rabbit antibodies.

The whole RNA-seq analysis will be performed on the PND14 hyperoxia-exposed preterm rabbit BPD model on lung samples collected in both hyperoxia and normoxia preterm animals, and aged-

matched term ones. This analysis will allow us to understand the similarities and differences between PND7 and PND14 models. As mentioned before, BPD is a disease with a severity scale from mild to severe. These investigations may reveal a different severity of the two models (moderate-severe for PND7 and mild for PND14), necessitating different pharmacological approaches. Finally, the bulk or single-cell RNA-seq analysis will be performed after pharmacological treatment to fully understand the curative effects on pathways and genes compared to untreated animals.

References

1. Moore KL. *Developing Human : Clinically Oriented Embryology, The*. Saunders; 1988.
2. Pereda J, Sulz L, San Martin S, Godoy-Guzmán C. The human lung during the embryonic period: vasculogenesis and primitive erythroblasts circulation. *J Anat*. 2013;222(5):487-494. doi:10.1111/joa.12042
3. Smith LJ, McKay KO, van Asperen PP, Selvadurai H, Fitzgerald DA. Normal Development of the Lung and Premature Birth. *Paediatr Respir Rev*. 2010;11(3):135-142. doi:10.1016/j.prrv.2009.12.006
4. Burri PH, Tarek MR. A novel mechanism of capillary growth in the rat pulmonary microcirculation. *Anat Rec*. 1990;228(1):35-45. doi:10.1002/ar.1092280107
5. Burri PH. Structural Aspects of Postnatal Lung Development – Alveolar Formation and Growth. *Neonatology*. 2006;89(4):313-322. doi:10.1159/000092868
6. Warburton D, El-Hashash A, Carraro G, et al. Lung Organogenesis. *Curr Top Dev Biol*. 2010;90:73-158. doi:10.1016/S0070-2153(10)90003-3
7. World Health Organization. Preterm birth. https://www.who.int/en/news-room/fact-sheets/detail/preterm-birth. Published 2018.
8. CAMPICHE MA, GAUTIER A, HERNANDEZ EI, REYMOND A. AN ELECTRON MICROSCOPE STUDY OF THE FETAL DEVELOPMENT OF HUMAN LUNG. *Pediatrics*. 1963;32:976-994.
9. Sanders RL, Hassett RJ, Vatter AE. Isolation of lung lamellar bodies and their conversion to tubular myelin figures in vitro. *Anat Rec*. 1980;198(3):485-501. doi:10.1002/ar.1091980310
10. Kajekar R. Environmental factors and developmental outcomes in the lung. *Pharmacol Ther*. 2007;114(2):129-145. doi:10.1016/j.pharmthera.2007.01.011
11. Granese R, Gitto E, D'Angelo G, et al. Preterm birth: seven-year retrospective study in a single centre population. *Riv Ital Pediatr*. 2019;45(1). doi:10.1186/s13052-019-0643-9
12. Glass HC, Costarino AT, Stayer SA, Brett CM, Cladis F, Davis PJ. Outcomes for Extremely Premature Infants. *Survey of Anesthesiology*. 2015;59(6):272-273. doi:10.1097/01.sa.0000471763.32127.3c
13. Beck S, Wojdyla D, Say L, et al. The worldwide incidence of preterm birth: a systematic review of maternal mortality and morbidity. *Bulletin of the World Health Organization (Bulletin De L'Organisation Mondiale De La Sante)*. 2010;88(1):31-38. doi:10.2471/BLT.08.062554
14. Georgiou HM, Di Quinzio MKW, Permezel M, Brennecke SP. Predicting Preterm Labour: Current Status and Future Prospects. *Dis Markers*. 2015;2015:435014. doi:10.1155/2015/435014
15. Balany J, Bhandari V. Understanding the Impact of Infection, Inflammation, and Their Persistence in the Pathogenesis of Bronchopulmonary Dysplasia. *Front Med (Lausanne)*. 2015;2:90. doi:10.3389/fmed.2015.00090
16. Guttentag S, Ballard PL. Lung Development: Embryology, Growth, Maturation, and Developmental Biology. In: H. William Taeusch M., Roberta A. Ballard M., Christine A. Gleason MD, eds. *Avery's Diseases of the Newborn (Eighth Edition)*. W.B. Saunders; 2005:601-615. doi:10.1016/B978-072169347-7.50044-5
17. Sayres WG. Preterm labor. *Am Fam Physician*. 2010;81(4):477-484. doi:10.1016/S0002-9378(01)80062-4
18. Mowitz ME, Ayyagari R, Gao W, Zhao J, Mangili A, Sarda SP. Health Care Burden of Bronchopulmonary Dysplasia Among Extremely Preterm Infants. *Front Pediatr*. 2019;7:510. doi:10.3389/fped.2019.00510
19. Hallman M, Saarela T, Zimmermann LJI. Respiratory Distress Syndrome: Predisposing

Factors, Pathophysiology, and Diagnosis. In: *Neonatology*. Springer International Publishing; 2018:823-842. doi:10.1007/978-3-319-29489-6_289
20. Doyle LW, Carse E, Adams A-M, Ranganathan S, Opie G, Cheong JLY. Ventilation in Extremely Preterm Infants and Respiratory Function at 8 Years. *Obstet Gynecol Surv*. 2017;72(12):694-696. doi:10.1097/OGX.0000000000000516
21. Bahman-Bijari B, Malekiyan A, Niknafs P, Baneshi M-R. Bubble-CPAP vs. Ventilatory-CPAP in Preterm Infants with Respiratory Distress. *Iranian journal of pediatrics*. 2011;21(2):151-158.
22. Herting E, Ha rtel C, Go pel W. Less invasive surfactant administration (LISA): chances and limitations. *Arch Dis Child Fetal Neonatal Ed*. 2019;104(6):F655-F659. doi:10.1136/archdischild-2018-316557
23. Kribs A, Roll C, Göpel W, et al. Nonintubated Surfactant Application vs Conventional Therapy in Extremely Preterm Infants: A Randomized Clinical Trial. *JAMA Pediatrics*. 2015;169(8):723-730. doi:10.1001/jamapediatrics.2015.0504
24. Trevisanuto D, Grazzina N, Ferrarese P, Micaglio M, Verghese C, Zanardo V. Laryngeal Mask Airway Used as a Delivery Conduit for the Administration of Surfactant to Preterm Infants with Respiratory Distress Syndrome. *Biol Neonate*. 2005;87(4):217-220. doi:10.1159/000083370
25. Katz M. Preventing preterm birth. *J Perinat Med*. 2016;44(5). doi:10.1515/jpm-2016-0202
26. Gibson AM, Doyle LW. Respiratory outcomes for the tiniest or most immature infants. *Semin Fetal Neonatal Med*. 2014;19(2):105-111. doi:10.1016/j.siny.2013.10.006
27. Principi N, Di Pietro GM, Esposito S. Bronchopulmonary dysplasia: clinical aspects and preventive and therapeutic strategies. *J Transl Med*. 2018;16(1):36. doi:10.1186/s12967-018-1417-7
28. Davidson LM, Berkelhamer SK. Bronchopulmonary Dysplasia: Chronic Lung Disease of Infancy and Long-Term Pulmonary Outcomes. *J Clin Med*. 2017;6(1). doi:10.3390/jcm6010004
29. Bhandari V. *Bronchopulmonary Dysplasia*. Humana; 2016.
30. Jensen, Wright. Bronchopulmonary Dysplasia: The Ongoing Search for One Definition to Rule Them All. *J Pediatr*. 2018;197:8-10. doi:10.1016/j.jpeds.2018.02.047
31. Ibrahim J, Bhandari V. The definition of bronchopulmonary dysplasia: an evolving dilemma. *Pediatr Res*. 2018;84(5):586-588. doi:10.1038/s41390-018-0167-9
32. Abman SH, Bancalari E, Jobe A. The Evolution of Bronchopulmonary Dysplasia after 50 Years. *Am J Respir Crit Care Med*. 2017;195(4):421-424. doi:10.1164/rccm.201611-2386ED
33. D e l v e I n s i g h t. Bronchopulmonary Dysplasia Market Insight, Epidemiology and Market Forecast 2030. 2021. 2021.
34. Jensen EA, Schmidt B. Epidemiology of bronchopulmonary dysplasia: Epidemiology of Bronchopulmonary Dysplasia. *Birth Defects Res A Clin Mol Teratol*. 2014;100(3):145-157. doi:10.1002/bdra.23235
35. Israel Neonatal Network, Klinger G, Sokolover N, et al. Perinatal risk factors for bronchopulmonary dysplasia in a national cohort of very-low-birthweight infants. *Am J Obstet Gynecol*. 2013;208(2):115. doi:10.1016/j.ajog.2012.11.026
36. Shahzad T, Radajewski S, Chao C-M, Bellusci S, Ehrhardt H. Pathogenesis of bronchopulmonary dysplasia: when inflammation meets organ development. *Mol Cell Pediatr*. 2016;3(1):1-8. doi:10.1186/s40348-016-0051-9
37. Steinhorn, Davis, Göpel, et al. Chronic Pulmonary Insufficiency of Prematurity: Developing Optimal Endpoints for Drug Development. *J Pediatr*. 2017;191:15-21. doi:10.1016/j.jpeds.2017.08.006
38. Higgins, Jobe, Koso-Thomas, et al. Bronchopulmonary Dysplasia: Executive Summary of a Workshop. *J Pediatr*. 2018;197:300-308. doi:10.1016/j.jpeds.2018.01.043

39. Hilgendorff A, Reiss I, Ehrhardt H, Eickelberg O, Alvira CM. Chronic lung disease in the preterm infant. Lessons learned from animal models. *Am J Respir Cell Mol Biol*. 2014;50(2):233-245. doi:10.1165/rcmb.2013-0014TR
40. Manuck TA, Levy PT, Gyamfi-Bannerman C, Jobe AH, Blaisdell CJ. Prenatal and Perinatal Determinants of Lung Health and Disease in Early Life. *JAMA Pediatrics*. 2016;170(5):E154577. doi:10.1001/jamapediatrics.2015.4577
41. Britt RD, Faksh A, Vogel E, Martin RJ, Pabelick CM, Prakash Y. Perinatal factors in neonatal and pediatric lung diseases. *Expert Rev Respir Med*. 2013;7(5):515-531. doi:10.1586/17476348.2013.838020
42. Papagianis, Pillow, Moss. Bronchopulmonary dysplasia: Pathophysiology and potential anti-inflammatory therapies. *Paediatr Respir Rev*. 2019;30:34-41. doi:10.1016/j.prrv.2018.07.007
43. Jobe AH. The New BPD. *Neoreviews*. 2006;7(10):E531-E545. doi:10.1542/NEO.7-10-E531
44. Hütten M, Wolfs T, Kramer B. Can the preterm lung recover from perinatal stress? *Mol Cell Pediatr*. 2016;3(1):1-7. doi:10.1186/s40348-016-0043-9
45. Schmitz T, Alberti C, Ursino M, Baud O, Aupiais C. Full versus half dose of antenatal betamethasone to prevent severe neonatal respiratory distress syndrome associated with preterm birth: study protocol for a randomised, multicenter, double blind, placebo-controlled, non-inferiority trial (BETADOSE). *BMC Pregnancy Childbirth*. 2019;19(1). doi:10.1186/s12884-019-2206-x
46. Jobe, Steinhorn. Can We Define Bronchopulmonary Dysplasia? *J Pediatr*. 2017;188:19-23. doi:10.1016/j.jpeds.2017.06.064
47. Jobe AH. Antenatal factors and the development of bronchopulmonary dysplasia. *Semin Neonatol*. 2003;8(1):9-17. doi:10.1016/S1084-2756(02)00188-4
48. Lall A, Prendergast M, Greenough A. Risk factors for the development of bronchopulmonary dysplasia: the role of antenatal infection and inflammation. *Expert Rev Respir Med*. 2007;1(2):247-254. doi:10.1586/17476348.1.2.247
49. Lacaze-Masmonteil T. That Chorioamnionitis is a Risk Factor for Bronchopulmonary Dysplasia - The case against. *Paediatr Respir Rev*. 2014;15(1):53-55. doi:10.1016/j.prrv.2013.09.005
50. Kramer B W. Antenatal inflammation and lung injury: prenatal origin of neonatal disease. *Journal of Perinatology*. 2008;(S1):S21-S27. doi:10.1038/jp.2008.46
51. Suhag A, Berghella V. Intrauterine Growth Restriction (IUGR): Etiology and Diagnosis. *Curr Obstet Gynecol Rep*. 2013;2(2):102-111. doi:10.1007/s13669-013-0041-z
52. Kalikkot Thekkeveedu, Guaman, Shivanna. Bronchopulmonary dysplasia: A review of pathogenesis and pathophysiology. *Respir Med*. 2017;132:170-177. doi:10.1016/j.rmed.2017.10.014
53. Check J, Gotteiner N, Liu X, et al. Fetal growth restriction and pulmonary hypertension in premature infants with bronchopulmonary dysplasia. *Journal of Perinatology*. 2013;33(7):553-557. doi:10.1038/jp.2012.164
54. McEvoy, Spindel. Pulmonary Effects of Maternal Smoking on the Fetus and Child: Effects on Lung Development, Respiratory Morbidities, and Life Long Lung Health. *Paediatr Respir Rev*. 2017;21:27-33. doi:10.1016/j.prrv.2016.08.005
55. Antonucci R, Contu P, Porcella A, Atzeni C, Chiappe S. Intrauterine smoke exposure: a new risk factor for bronchopulmonary dysplasia? *J Perinat Med*. 2004;32(3). doi:10.1515/JPM.2004.051
56. Hadchouel A, Delacourt C. Bronchopulmonary dysplasia and genetics. *Med Sci (Paris)*. 2013;29(10):821-823. doi:10.1051/medsci/20132910002
57. Somaschini M, Resta CD, Volonteri C, et al. Genetic factors predisposing to bronchopulmonary dysplasia. A pilot study by exome sequencing and pathways analysis. *Riv Ital Pediatr*. 2015;41(S1). doi:10.1186/1824-7288-41-S1-A42

58. Romejko-Wolniewicz E, Teliga-Czajkowska J, Czajkowski K. Antenatal steroids: can we optimize the dose? *Curr Opin Obstet Gynecol*. 2014;26(2):77-82. doi:10.1097/GCO.0000000000000047
59. Olaloko O, Mohammed R, Ojha U. Evaluating the use of corticosteroids in preventing and treating bronchopulmonary dysplasia in preterm neonates. *Int J Gen Med*. 2018;11:265-274. doi:10.2147/IJGM.S158184
60. Hütten MC, Kramer BW. Patterns and etiology of acute and chronic lung injury: insights from experimental evidence. *Zhongguo Dang Dai Er Ke Za Zhi*. 2014;16(5):448-459.
61. Arigliani M, Spinelli AM, Liguoro I, Cogo P. Nutrition and Lung Growth. *Nutrients*. 2018;10(7). doi:10.3390/nu10070919
62. Slutsky AS, Ranieri VM. Ventilator-induced lung injury. *N Engl J Med*. 2014;370(10):980. doi:10.1056/NEJMc1400293
63. Speer CP. Chorioamnionitis, Postnatal Factors and Proinflammatory Response in the Pathogenetic Sequence of Bronchopulmonary Dysplasia. *Neonatology*. 2009;95(4):353-361. doi:10.1159/000209301
64. Pryhuber GS. Postnatal Infections and Immunology Affecting Chronic Lung Disease of Prematurity. *Clin Perinatol*. 2015;42(4):697-718. doi:10.1016/j.clp.2015.08.002
65. Dong Y, Speer CP. Late-onset neonatal sepsis: recent developments. *Arch Dis Child Fetal Neonatal Ed*. 2015;100(3):F257-F263. doi:10.1136/archdischild-2014-306213
66. Simonsen KA, Anderson-Berry AL, Delair SF, Davies HD. Early-Onset Neonatal Sepsis. *Clin Microbiol Rev*. 2014;27(1):21-47. doi:10.1128/CMR.00031-13
67. Anderson C, Hillman NH. Bronchopulmonary Dysplasia: When the Very Preterm Baby Comes Home. *Missouri medicine*. 2019;116(2):117-122.
68. McEvoy CT, Jain L, Schmidt B, Abman S, Bancalari E, Aschner JL. Bronchopulmonary dysplasia: NHLBI Workshop on the Primary Prevention of Chronic Lung Diseases. *Ann Am Thorac Soc*. 2014;11(Suppl 3):S146-S153. doi:10.1513/AnnalsATS.201312-424LD
69. Lista G, Meneghin F, Bresesti I, Cavigioli F. Nutritional problems of children with bronchopulmonary dysplasia after hospital discharge. *Pediatr Med Chir*. 2017;39(4):183. doi:10.4081/pmc.2017.183
70. Pasha AB, Chen X-Q, Zhou G-P. Bronchopulmonary dysplasia: Pathogenesis and treatment. *Exp Ther Med*. 2018;16(6):4315-4321. doi:10.3892/etm.2018.6780
71. Speer CP. Inflammation and bronchopulmonary dysplasia: a continuing story. *Semin Fetal Neonatal Med*. 2006;11(5):354-362. doi:10.1016/j.siny.2006.03.004
72. Thomas Salaets, Andre Gie, Bieke Tack, Jan Deprest, Jaan Toelen. Modelling Bronchopulmonary Dysplasia in Animals: Arguments for the Preterm Rabbit Model. *Curr Pharm Des*. 2017;23. doi:10.2174/1381612823666170926123550
73. Niedermaier S, Hilgendorff A. Bronchopulmonary dysplasia - an overview about pathophysiologic concepts. *Mol Cell Pediatr*. 2015;2(1):1-7. doi:10.1186/s40348-015-0013-7
74. Mižíková I, Morty RE. The Extracellular Matrix in Bronchopulmonary Dysplasia: Target and Source. *Front Med (Lausanne)*. 2015;2:91. doi:10.3389/fmed.2015.00091
75. Albertine KH. Utility of large-animal models of BPD: chronically ventilated preterm lambs. *Am J Physiol Lung Cell Mol Physiol*. 2015;308(10):L983-L1001. doi:10.1152/ajplung.00178.2014
76. Buczynski BW, Maduekwe ET, O'Reilly MA. The role of hyperoxia in the pathogenesis of experimental BPD. *Semin Perinatol*. 2013;37(2):69-78. doi:10.1053/j.semperi.2013.01.002
77. Manzano R. A Hyperoxic Lung Injury Model in Premature Rabbits: The Influence of Different Gestational Ages and Oxygen Concentrations. *PLoS One*. 2014;9(4):1069-1076. doi:10.1371/JOURNAL.PONE.0095844
78. Albertine KH, Jones GP, Starcher BC, et al. Chronic lung injury in preterm lambs. Disordered

respiratory tract development. *Am J Respir Crit Care Med*. 1999;159(3):945-958. doi:10.1164/ajrccm.159.3.9804027
79. Kindermann A, Binder L, Baier J, et al. Correction to: Severe but not moderate hyperoxia of newborn mice causes an emphysematous lung phenotype in adulthood without persisting oxidative stress and inflammation. *BMC Pulm Med*. 2020;20(1). doi:10.1186/s12890-020-1051-z
80. Mascaretti RS, Mataloun MMGB, Dolhnikoff M, Rebello CM. Lung morphometry, collagen and elastin content: changes after hyperoxic exposure in preterm rabbits. *Clinics (Sao Paulo)*. 2009;64(11):1099-1104. doi:10.1590/S1807-59322009001100010
81. Daniela Fanni, Vassilios Fanos, Clara Gerosa, et al. Bronchopulmonary dysplasia: understanding of the underlying pathological mechanisms. *Journal of Pediatric and Neonatal Individualized Medicine*. 2014;3(2):E30259. doi:10.7363/030259
82. Ganguly, Martin. Vulnerability of the developing airway. *Respir Physiol Neurobiol*. 2019;270. doi:10.1016/j.resp.2019.103263
83. Kinsella JP, Greenough A, Abman SH. Bronchopulmonary dysplasia. *Lancet*. 2006;367(9520):1421-1431. doi:10.1016/S0140-6736(06)68615-7
84. Bhandari A. Pathogenesis pathology and pathophysiology of pulmonary sequelae of bronchopulmonary dysplasia in premature infants. *Front Biosci*. 2003;8(5):E370-E380. doi:10.2741/1060
85. El Mazloum D, Moschino L, Bozzetto S, Baraldi E. Chronic Lung Disease of Prematurity: Long-Term Respiratory Outcome. *Neonatology*. 2014;105(4):352-356. doi:10.1159/000360651
86. Baker CD, Alvira CM. Disrupted lung development and bronchopulmonary dysplasia: opportunities for lung repair and regeneration. *Curr Opin Pediatr*. 2014;26(3):306-314. doi:10.1097/MOP.0000000000000095
87. Tracy MK, Berkelhamer SK. Bronchopulmonary Dysplasia and Pulmonary Outcomes of Prematurity. *Pediatr Ann*. 2019;48(4). doi:10.3928/19382359-20190325-03
88. Rennard, Drummond. Early chronic obstructive pulmonary disease: definition, assessment, and prevention. *Lancet*. 2015;385(9979):1778-1788. doi:10.1016/S0140-6736(15)60647-X
89. Singer L, Yamashita T, Lilien L, Collin M, Baley J. A longitudinal study of developmental outcome of infants with bronchopulmonary dysplasia and very low birth weight. *Pediatrics*. 1997;100(6):987-993. doi:10.1542/peds.100.6.987
90. Twilhaar ES, Wade RM, de Kieviet JF, van Goudoever JB, van Elburg RM, Oosterlaan J. Cognitive Outcomes of Children Born Extremely or Very Preterm Since the 1990s and Associated Risk Factors: A Meta-analysis and Meta-regression. *Obstet Gynecol Surv*. 2018;73(10):562-563. doi:10.1097/01.ogx.0000547169.91377.70
91. Cheong, Doyle. An update on pulmonary and neurodevelopmental outcomes of bronchopulmonary dysplasia. *Semin Perinatol*. 2018;42(7):478-484. doi:10.1053/j.semperi.2018.09.013
92. Strueby L, Thébaud B. Novel therapeutics for bronchopulmonary dysplasia. *Curr Opin Pediatr*. 2018;30(3):378-383. doi:10.1097/MOP.0000000000000613
93. Michael Z, Spyropoulos F, Ghanta S, Christou H. Bronchopulmonary Dysplasia: An Update of Current Pharmacologic Therapies and New Approaches. *Clin Med Insights Pediatr*. 2018;12. doi:10.1177/1179556518817322
94. Couroucli X I, Placencia J L, Cates L A, Suresh G K. Should we still use vitamin A to prevent bronchopulmonary dysplasia? *Journal of Perinatology*. 2016;36(8):581-585. doi:10.1038/jp.2016.76
95. Daly JW, Bruns RF, Snyder SH. Adenosine receptors in the central nervous system: Relationship to the central actions of methylxanthines. *Life Sci*. 1981;28(19):2083-2097. doi:10.1016/0024-3205(81)90614-7

96. Taha D, Kirkby S, Nawab U, et al. Early caffeine therapy for prevention of bronchopulmonary dysplasia in preterm infants. *J Matern Fetal Neonatal Med*. 2014;27(16):1698-1702. doi:10.3109/14767058.2014.885941
97. Bairam A, Uppari N, Mubayed S, Joseph V. An Overview on the Respiratory Stimulant Effects of Caffeine and Progesterone on Response to Hypoxia and Apnea Frequency in Developing Rats. *Adv Exp Med Biol*. 2015;860:211-220. doi:10.1007/978-3-319-18440-1_23
98. Abdel-Hady H, Nasef N, Shabaan AE, Nour I. Caffeine therapy in preterm infants. *World J Clin Pediatr*. 2015;4(4):81-93. doi:10.5409/wjcp.v4.i4.81
99. Moschino L, Zivanovic S, Hartley C, Trevisanuto D, Baraldi E, Roehr CC. Caffeine in preterm infants: where are we in 2020? *ERJ Open Res*. 2020;6(1). doi:10.1183/23120541.00330-2019
100. Cuna A, Lewis T, Dai H, Nyp M, Truog WE. Timing of postnatal corticosteroid treatment for bronchopulmonary dysplasia and its effect on outcomes. *Pediatr Pulmonol*. 2019;54(2):165-170. doi:10.1002/ppul.24202
101. Doyle LW, Cheong JL, Ehrenkranz RA, Halliday HL. Early (< 8 days) systemic postnatal corticosteroids for prevention of bronchopulmonary dysplasia in preterm infants. *Cochrane Libr*. prepub. doi:10.1002/14651858.CD001146.pub5
102. Gupta S, Prasanth K, Chen C-M, Yeh TF. Postnatal corticosteroids for prevention and treatment of chronic lung disease in the preterm newborn. *Int J Pediatr*. 2012;2012:315642. doi:10.1155/2012/315642
103. Doyle, Cheong. Postnatal corticosteroids to prevent or treat bronchopulmonary dysplasia – Who might benefit? *Semin Fetal Neonatal Med*. 2017;22(5):290-295. doi:10.1016/j.siny.2017.07.003
104. Jensen EA, Foglia EE, Schmidt B. Evidence-Based Pharmacologic Therapies for Prevention of Bronchopulmonary Dysplasia: Application of the Grading of Recommendations Assessment, Development, and Evaluation Methodology. *Clin Perinatol*. 2015;42(4):755-779. doi:10.1016/j.clp.2015.08.005
105. Graham L. AAP revises policy statement on the use of postnatal corticosteroids for bronchopulmonary dysplasia. *Am Fam Physician*. 2011;83(12):1501.
106. Hwang J, Rehan V. Recent Advances in Bronchopulmonary Dysplasia: Pathophysiology, Prevention, and Treatment. *Lung*. 2018;196(2):129-138. doi:10.1007/s00408-018-0084-z
107. Bassler D, Shinwell ES, Hallman M, et al. Long-Term Effects of Inhaled Budesonide for Bronchopulmonary Dysplasia. *N Engl J Med*. 2018;378(2):148-157. doi:10.1056/NEJMoa1708831
108. Samiee-Zafarghandy S, van den Anker JN. Use of inhaled steroids to prevent bronchopulmonary dysplasia: a matter of great debate. *Arch Dis Child*. 2019;104(9):924-925. doi:10.1136/archdischild-2018-316132
109. Boel, Banerjee, Chakraborty. Postnatal steroids in extreme preterm infants: Intra-tracheal instillation using surfactant as a vehicle. *Paediatr Respir Rev*. 2018;25:78-84. doi:10.1016/j.prrv.2017.05.002
110. Yeh TF, Lin HC, Chang CH, et al. Early intratracheal instillation of budesonide using surfactant as a vehicle to prevent chronic lung disease in preterm infants: a pilot study. *Pediatrics*. 2008;121(5):E1310-E1318. doi:10.1542/peds.2007-1973
111. Yeh TF, Chen CM, Wu SY, et al. Intratracheal Administration of Budesonide/Surfactant to Prevent Bronchopulmonary Dysplasia. *Am J Respir Crit Care Med*. 2016;193(1):86-95. doi:10.1164/rccm.201505-0861OC
112. Kuo HT, Lin HC, Tsai CH, Chouc IC, Yeh TF. A Follow-up Study of Preterm Infants Given Budesonide Using Surfactant as a Vehicle to Prevent Chronic Lung Disease in Preterm Infants. *J Pediatr*. 2010;156(4):537-541. doi:10.1016/j.jpeds.2009.10.049
113. Biesalski HK, Nohr D. Importance of vitamin-A for lung function and development. *Mol Aspects Med*. 2003;24(6):431-440. doi:10.1016/S0098-2997(03)00039-6

114. Niederreither Karen, Dollé Pascal. Retinoic acid in development: towards an integrated view. *Nat Rev Genet*. 2008;9(7):541-553. doi:10.1038/nrg2340
115. Schwartz E, Zelig R, Parker A, Johnson S. Vitamin A Supplementation for the Prevention of Bronchopulmonary Dysplasia in Preterm Infants: An Update. *Nutr Clin Pract*. 2017;32(3):346-353. doi:10.1177/0884533616673613
116. Jensen EA, Schmidt B. Pharmacological Therapies for the Prevention of Bronchopulmonary Dysplasia. In: *Updates on Neonatal Chronic Lung Disease*. Elsevier; 2020:245-256. doi:10.1016/B978-0-323-68353-1.00016-6
117. Shenk EE, Bondi DS, Pellerite MM, Sriram S. Evaluation of Timing and Dosing of Caffeine Citrate in Preterm Neonates for the Prevention of Bronchopulmonary Dysplasia. *J Pediatr Pharmacol Ther*. 2018;23(2):139-145. doi:10.5863/1551-6776-23.2.139
118. Hercilia Guimaraes, Maria Beatriz Guedes, Gustavo Rocha, Teresa Tome, Antonio Albino-Teixeira. Vitamin A in Prevention of Bronchopulmonary Dysplasia. *Curr Pharm Des*. 2012;18(21):3101-3113. doi:10.2174/138161281120902310l
119. Rakshasbhuvankar A, Patole S, Simmer K, Pillow JJ. Enteral vitamin A for reducing severity of bronchopulmonary dysplasia in extremely preterm infants: a randomised controlled trial. *BMC Pediatr*. 2017;17(1). doi:10.1186/s12887-017-0958-x
120. Tyson J, Wright L, Oh W, Kennedy K, Mele L, Ehrenkranz R. Vitamin A supplementation for extremely-low-birth-weight infants. *J Pediatr*. 2000;136(1):124-125. doi:10.1016/S0022-3476(00)90065-9
121. Thébaud B. Stem cell-based therapies in neonatology: a new hope. *Arch Dis Child Fetal Neonatal Ed*. 2018;103(6):F583-F588. doi:10.1136/archdischild-2017-314451
122. Namba F. Mesenchymal stem cells for the prevention of bronchopulmonary dysplasia. *Pediatr Int*. 2019;61(10):945-950. doi:10.1111/ped.14001
123. Strueby L, Thébaud B. Emerging Therapies in BPD. In: *Updates on Neonatal Chronic Lung Disease*. Elsevier; 2020:307-316. doi:10.1016/B978-0-323-68353-1.00021-X
124. Álvarez-Fuente M, Moreno L, Mitchell JA, et al. Preventing bronchopulmonary dysplasia: new tools for an old challenge. *Pediatr Res*. 2019;85(4):432-441. doi:10.1038/s41390-018-0228-0
125. Collins A. Stem-cell therapy for bronchopulmonary dysplasia. *Curr Opin Pediatr*. 2020;32(2):210-215. doi:10.1097/MOP.0000000000000862
126. Mandell EW, Kratimenos P, Abman SH, Steinhorn RH. Drugs for the Prevention and Treatment of Bronchopulmonary Dysplasia. *Clin Perinatol*. 2019;46(2):291-310. doi:10.1016/j.clp.2019.02.011
127. Ley, Hallberg, Hansen-Pupp, et al. rhIGF-1/rhIGFBP-3 in Preterm Infants: A Phase 2 Randomized Controlled Trial. *J Pediatr*. 2019;206:56-65. doi:10.1016/j.jpeds.2018.10.033
128. Seedorf G, Kim C, Wallace B, et al. rhIGF-1/BP3 Preserves Lung Growth and Prevents Pulmonary Hypertension in Experimental Bronchopulmonary Dysplasia. *Am J Respir Crit Care Med*. 2020;201(9):1120-1134. doi:10.1164/rccm.201910-1975OC
129. Ambalavanan N, Morty RE. Searching for better animal models of BPD: a perspective. *Am J Physiol Lung Cell Mol Physiol*. 2016;311(5):L924-L927. doi:10.1152/ajplung.00355.2016
130. Jobe AH. Animal Models, Learning Lessons to Prevent and Treat Neonatal Chronic Lung Disease. *Front Med (Lausanne)*. 2015;2:49. doi:10.3389/fmed.2015.00049
131. Nardiello C, Mižíková I, Silva DM, et al. Standardisation of oxygen exposure in the development of mouse models for bronchopulmonary dysplasia. *Dis Model Mech*. 2017;10(2):185-196. doi:10.1242/dmm.027086
132. D'Angio CT, Ryan RM. Animal models of bronchopulmonary dysplasia. The preterm and term rabbit models. *Am J Physiol Lung Cell Mol Physiol*. 2014;307(12):L959-L969. doi:10.1152/ajplung.00228.2014
133. O'Reilly M, Thébaud B. Animal models of bronchopulmonary dysplasia. The term rat models.

Am J Physiol Lung Cell Mol Physiol. 2014;307(12):L948-L958. doi:10.1152/ajplung.00160.2014
134. Berger J, Bhandari V. Animal models of bronchopulmonary dysplasia. The term mouse models. *Am J Physiol Lung Cell Mol Physiol*. 2014;307(12):L936-L947. doi:10.1152/ajplung.00159.2014
135. Yoder BA, Coalson JJ. Animal models of bronchopulmonary dysplasia. The preterm baboon models. *Am J Physiol Lung Cell Mol Physiol*. 2014;307(12):L970-L977. doi:10.1152/ajplung.00171.2014
136. Mataloun MMGB, Leone CR, Mascaretti RS, Dohlnikoff M, Rebello CM. Effect of postnatal malnutrition on hyperoxia-induced newborn lung development. *Braz J Med Biol Res*. 2009;42(7):606-613. doi:10.1590/S0100-879X2009000700004
137. Salaets T, Aertgeerts M, Gie A, et al. Preterm birth impairs postnatal lung development in the neonatal rabbit model. *Respir Res*. 2020;21(1). doi:10.1186/s12931-020-1321-6
138. Richter J, Toelen J, Vanoirbeek J, et al. Functional assessment of hyperoxia-induced lung injury after preterm birth in the rabbit. *Am J Physiol Lung Cell Mol Physiol*. 2014;306(3):L277-L283. doi:10.1152/ajplung.00315.2013
139. Jiménez J, Richter J, Nagatomo T, et al. Progressive Vascular Functional and Structural Damage in a Bronchopulmonary Dysplasia Model in Preterm Rabbits Exposed to Hyperoxia. *Int J Mol Sci*. 2016;17(10). doi:10.3390/ijms17101776
140. Casamassimi A, Federico A, Rienzo M, Esposito S, Ciccodicola A. Transcriptome Profiling in Human Diseases: New Advances and Perspectives. *Int J Mol Sci*. 2017;18(8). doi:10.3390/ijms18081652
141. Piersigilli F, Bhandari V. Biomarkers in neonatology: the new "omics" of bronchopulmonary dysplasia. *J Matern Fetal Neonatal Med*. 2016;29(11):1758-1764. doi:10.3109/14767058.2015.1061495
142. Bhandari V, Gruen JR. The genetics of bronchopulmonary dysplasia. *Semin Perinatol*. 2006;30(4):185-191. doi:10.1053/j.semperi.2006.05.005
143. Wang H, St Julien KR, Stevenson DK, et al. A genome-wide association study (GWAS) for bronchopulmonary dysplasia. *Pediatrics*. 2013;132(2):290-297. doi:10.1542/peds.2013-0533
144. Mahlman M, Karjalainen MK, Huusko JM, et al. Genome-wide association study of bronchopulmonary dysplasia: a potential role for variants near the CRP gene. *Sci Rep*. 2017;7(1). doi:10.1038/s41598-017-08977-w
145. Hadchouel A, Durrmeyer X, Bouzigon E, et al. Identification of SPOCK2 as a susceptibility gene for bronchopulmonary dysplasia. *Am J Respir Crit Care Med*. 2011;184(10):1164-1170. doi:10.1164/rccm.201103-0548OC
146. Torgerson DG, Ballard PL, Keller RL, et al. Ancestry and genetic associations with bronchopulmonary dysplasia in preterm infants. *Am J Physiol Lung Cell Mol Physiol*. 2018;315(5):L858-L869. doi:10.1152/ajplung.00073.2018
147. Oji-Mmuo CN, Siddaiah R, Montes DT, et al. Tracheal aspirate transcriptomic and miRNA signatures of extreme premature birth with bronchopulmonary dysplasia. *Journal of Perinatology*. 2021;41(3):551-561. doi:10.1038/s41372-020-00868-9
148. Ng S, Strunk T, Lee AH, et al. Whole blood transcriptional responses of very preterm infants during late-onset sepsis. *PLoS One*. 2020;15(6):E233841. doi:10.1371/journal.pone.0233841
149. Pietrzyk J. Gene Expression Profiling in Preterm Infants: New Aspects of Bronchopulmonary Dysplasia Development. *PLoS One*. 2013;8(10):1284-1294.
150. Sahoo D, Zaramela LS, Hernandez GE, et al. Transcriptional profiling of lung macrophages identifies a predictive signature for inflammatory lung disease in preterm infants. *Commun Biol*. 2020;3(1). doi:10.1038/s42003-020-0985-2
151. Förster K, Sass S, Ehrhardt H, et al. Early Identification of Bronchopulmonary Dysplasia Using Novel Biomarkers by Proteomic Screening. *Am J Respir Crit Care Med*.

2018;197(8):1076-1080. doi:10.1164/rccm.201706-1218LE
152. Ballard PL, Oses-Prieto J, Chapin C, Segal MR, Ballard RA, Burlingame AL. Composition and origin of lung fluid proteome in premature infants and relationship to respiratory outcome. *PLoS One*. 2020;15(12):E243168. doi:10.1371/journal.pone.0243168
153. Piersigilli F, Lam T, Vernocchi P, et al. Identification of new biomarkers of bronchopulmonary dysplasia using metabolomics. *Metabolomics*. 2019;15(2):1-11. doi:10.1007/s11306-019-1482-9
154. Lu J, Zhu X, Shui JE, et al. Rho/SMAD/mTOR triple inhibition enables long-term expansion of human neonatal tracheal aspirate-derived airway basal cell-like cells. *Pediatr Res*. 2021;89(3):502-509. doi:10.1038/s41390-020-0925-3
155. Salaets T, Richter J, Brady P, et al. Transcriptome Analysis of the Preterm Rabbit Lung after Seven Days of Hyperoxic Exposure. *PLoS One*. 2015;10(8):E136569. doi:10.1371/journal.pone.0136569
156. Perkowski S, Sun J, Singhal S, Santiago J, Leikauf GD, Albelda SM. Gene Expression Profiling of the Early Pulmonary Response to Hyperoxia in Mice. *Am J Respir Cell Mol Biol*. 2003;28(6):682-696. doi:10.1165/rcmb.4692
157. Wagenaar G. Gene expression profile and histopathology of experimental bronchopulmonarydysplasia induced by prolonged oxidative stress. *Free Radic Biol Med*. 2003;35:S76.
158. Wang J, Yin J, Wang X, et al. Changing expression profiles of mRNA, lncRNA, circRNA, and miRNA in lung tissue reveal the pathophysiological of bronchopulmonary dysplasia (BPD) in mouse model. *J Cell Biochem*. 2019;120(6):9369-9380. doi:10.1002/jcb.28212
159. Jean J-C, George E, Kaestner KH, Brown LAS, Spira A, Joyce-Brady M. Transcription factor Klf4, induced in the lung by oxygen at birth, regulates perinatal fibroblast and myofibroblast differentiation. *PLoS One*. 2013;8(1):E54806. doi:10.1371/journal.pone.0054806
160. Lingappan K, Srinivasan C, Jiang W, Wang L, Couroucli XI, Moorthy B. Analysis of the transcriptome in hyperoxic lung injury and sex-specific alterations in gene expression. *Analysis of the transcriptome in hyperoxic lung injury and sex-specific alterations in gene expression*. 2014;9(7):E101581. doi:10.1371/journal.pone.0101581
161. Emery JL, Mithal A. The Number of Alveoli in the Terminal Respiratory Unit of Man During Late Intrauterine Life and Childhood. *Arch Dis Child*. 1960;35(184):544-547. doi:10.1136/adc.35.184.544
162. Cooney TP, Thurlbeck WM. The radial alveolar count method of Emery and Mithal: a reappraisal 1--postnatal lung growth. *Thorax*. 1982;37(8):572-579. doi:10.1136/thx.37.8.572
163. Tsunoda S, Fukaya H, Sugihara T, Martin CJ, Hildebrandt J. Lung volume, thickness of alveolar walls, and microscopic anisotropy of expansion. *Respir Physiol*. 1974;22(3):285-296. doi:10.1016/0034-5687(74)90078-4
164. Fu Z, Heldt GP, West JB. Thickness of the blood-gas barrier in premature and 1-day-old newborn rabbit lungs. *Am J Physiol Lung Cell Mol Physiol*. 2003;285(1):L130-L136. doi:10.1152/ajplung.00366.2002
165. Birks EK, Mathieu-Costello O, Fu Z, Tyler WS, West JB. Comparative aspects of the strength of pulmonary capillaries in rabbit, dog, and horse. *Respir Physiol*. 1994;97(2):235-246. doi:10.1016/0034-5687(94)90029-9
166. Roubliova XI, Deprest JA, Biard JM, et al. Morphologic changes and methodological issues in the rabbit experimental model for diaphragmatic hernia. *Histol Histopathol*. 2010;25(9):1105-1116. doi:10.14670/HH-25.1105
167. Matute-Bello G, Downey G, Moore BB, et al. An official American Thoracic Society workshop report: features and measurements of experimental acute lung injury in animals. *Am J Respir Cell Mol Biol*. 2011;44(5):725-738. doi:10.1165/rcmb.2009-0210ST
168. Afgan E, Baker D, Batut B, et al. The Galaxy platform for accessible, reproducible and

collaborative biomedical analyses: 2018 update. *Nucleic Acids Res*. 2018;46(W1):W537-W544. doi:10.1093/nar/gky379
169. Jolliffe IT, Cadima J. Principal component analysis: a review and recent developments. *Philos Trans A Math Phys Eng Sci*. 2016;374(2065):20150202. doi:10.1098/rsta.2015.0202
170. Metsalu T, Vilo J. ClustVis: a web tool for visualizing clustering of multivariate data using Principal Component Analysis and heatmap. *Nucleic Acids Res*. 2015;43(W1):W566-W570. doi:10.1093/nar/gkv468
171. Zhou Yingyao, Zhou Bin, Pache Lars, et al. Metascape provides a biologist-oriented resource for the analysis of systems-level datasets. *Nature Communications*. 2019;10(1):1523. doi:10.1038/s41467-019-09234-6
172. Subramanian A, Kuehn H, Gould J, Tamayo P, Mesirov JP. GSEA-P: a desktop application for Gene Set Enrichment Analysis. *Bioinformatics*. 2007;(23):3251-3253. doi:10.1093/bioinformatics/btm369
173. Bhattacharya S, Go D, Krenitsky DL, et al. Genome-wide transcriptional profiling reveals connective tissue mast cell accumulation in bronchopulmonary dysplasia. *Am J Respir Crit Care Med*. 2012;186(4):349-358. doi:10.1164/rccm.201203-0406OC
174. Bhattacharya S, Zhou Z, Yee M, et al. The genome-wide transcriptional response to neonatal hyperoxia identifies Ahr as a key regulator. *Am J Physiol Lung Cell Mol Physiol*. 2014;307(7):L516-L523. doi:10.1152/ajplung.00200.2014
175. Dong J, Carey WA, Abel S, et al. MicroRNA-mRNA interactions in a murine model of hyperoxia-induced bronchopulmonary dysplasia. *BMC Genomics*. 2012;13(1). doi:10.1186/1471-2164-13-204
176. Pietrzyk JJ, Kwinta P, Wollen EJ, et al. Gene expression profiling in preterm infants: new aspects of bronchopulmonary dysplasia development. *PLoS One*. 2013;8(10):E78585. doi:10.1371/journal.pone.0078585
177. Revhaug C, Bik-Multanowski M, Zasada M, et al. Immune System Regulation Affected by a Murine Experimental Model of Bronchopulmonary Dysplasia: Genomic and Epigenetic Findings. *Neonatology*. 2019;116(3):269-277. doi:10.1159/000501461
178. Sucre JMS, Vickers KC, Benjamin JT, et al. Hyperoxia Injury in the Developing Lung Is Mediated by Mesenchymal Expression of Wnt5A. *Am J Respir Crit Care Med*. 2020;201(10):1249-1262. doi:10.1164/rccm.201908-1513OC
179. Linguamatics. https://www.linguamatics.com/.
180. Savani. Modulators of inflammation in Bronchopulmonary Dysplasia. *Semin Perinatol*. 2018;42(7):459-470. doi:10.1053/j.semperi.2018.09.009
181. Wright CJ, Kirpalani H. Targeting Inflammation to Prevent Bronchopulmonary Dysplasia: Can New Insights Be Translated Into Therapies? *Pediatrics*. 2011;128(1):111-126. doi:10.1542/PEDS.2010-3875
182. Ibrahim J, Garantziotis S, Savani RC. The Inflammation Superhighway. In: *Updates on Neonatal Chronic Lung Disease*. Elsevier; 2020:131-150. doi:10.1016/B978-0-323-68353-1.00009-9
183. Chess PR, D'Angio CT, Pryhuber GS, Maniscalco WM. Pathogenesis of bronchopulmonary dysplasia. *Semin Perinatol*. 2006;30(4):171-178. doi:10.1053/j.semperi.2006.05.003
184. Lingappan K. Analysis of the Transcriptome in Hyperoxic Lung Injury and Sex-Specific Alterations in Gene Expression. *PLoS One*. 2014;9(7):404-416. doi:10.1371/JOURNAL.PONE.0101581
185. Pryhuber GS, Huyck HL, Staversky RJ, Finkelstein JN, O'Reilly MA. Tumor necrosis factor-alpha-induced lung cell expression of antiapoptotic genes TRAF1 and cIAP2. *Am J Respir Cell Mol Biol*. 2000;22(2):150-156. doi:10.1165/ajrcmb.22.2.3783
186. Hayes J, Feola DJ, Murphy BS, Shook LA, Ballard HO. Pathogenesis of Bronchopulmonary Dysplasia. *Respiration*. 2010;79(5):425-436. doi:10.1159/000242497

187. Perkins Neil D. Integrating cell-signalling pathways with NF-?B and IKK function. *Nature Reviews Molecular Cell Biology*. 2007;(1):49-62. doi:10.1038/nrm2083
188. Todd DA, Earl M, Lloyd J, Greenberg M, John E. Cytological changes in endotracheal aspirates associated with chronic lung disease. *Early Hum Dev*. 1998;51(1):13-22. doi:10.1016/S0378-3782(97)00069-8
189. Speer C P. Pulmonary inflammation and bronchopulmonary dysplasia. *Journal of Perinatology*. 2006;(S1):S57-S62. doi:10.1038/sj.jp.7211476
190. Suganuma T, Workman JL. MAP kinases and histone modification. *Journal of Molecular Cell Biology*. 2012;4(5):348-350. doi:10.1093/jmcb/mjs043
191. Jung E, Lee BS. Late-Onset Sepsis as a Risk Factor for Bronchopulmonary Dysplasia in Extremely Low Birth Weight Infants: A Nationwide Cohort Study. *Sci Rep*. 2019;9(1). doi:10.1038/s41598-019-51617-8
192. Van Marter, Dammann, Allred, et al. Chorioamnionitis, mechanical ventilation, and postnatal sepsis as modulators of chronic lung disease in preterm infants. *J Pediatr*. 2002;140(2):171-176. doi:10.1067/mpd.2002.121381
193. Shah J, Jefferies AL, Yoon EW, Lee SK, Shah PS. Risk Factors and Outcomes of Late-Onset Bacterial Sepsis in Preterm Neonates Born at < 32 Weeks' Gestation. *Am J Perinatol*. 2015;32(7):675-682. doi:10.1055/s-0034-1393936
194. Landry JS, Menzies D. Occurrence and severity of bronchopulmonary dysplasia and respiratory distress syndrome after a preterm birth. *Paediatr Child Health*. 2011;16(7):399-403. doi:10.1093/pch/16.7.399
195. Doyle LW. Postnatal Corticosteroids to Prevent or Treat Bronchopulmonary Dysplasia. *Neonatology*. 2021;118(2):244-251. doi:10.1159/000515950
196. Heo M, Jeon GW. Intratracheal administration of budesonide with surfactant in very low birth weight infants to prevent bronchopulmonary dysplasia. *Turk J Pediatr*. 2020;62(4):551-559. doi:10.24953/turkjped.2020.04.004
197. PAGANO A, BARAZZONE-ARGIROFFO C. Alveolar Cell Death in Hyperoxia-Induced Lung Injury. *Annals of the New York Academy of Sciences*. 2006;1010(1):405-416. doi:10.1196/annals.1299.074
198. Riccio VD, Van Tuyl M, Post M. Apoptosis in Lung Development and Neonatal Lung Injury. *Pediatr Res*. 2004;55(2):183-189. doi:10.1203/01.PDR.0000103930.93849.B2
199. Hargitai B, Szabó V, Hajdú J, et al. Apoptosis in various organs of preterm infants: histopathologic study of lung, kidney, liver, and brain of ventilated infants. *Pediatr Res*. 2001;50(1):110-114. doi:10.1203/00006450-200107000-00020
200. Das KC, Ravi D, Holland W. Increased Apoptosis and Expression of p21 and p53 in Premature Infant Baboon Model of Bronchopulmonary Dysplasia. *Antioxid Redox Signal*. 2004;6(1):109-116. doi:10.1089/152308604771978417
201. Martina JA, Chen Y, Gucek M, Puertollano R. MTORC1 functions as a transcriptional regulator of autophagy by preventing nuclear transport of TFEB. *Autophagy*. 2012;8(6):903-914. doi:10.4161/auto.19653
202. Sureshbabu A, Syed M, Das P, et al. Inhibition of Regulatory-Associated Protein of Mechanistic Target of Rapamycin Prevents Hyperoxia-Induced Lung Injury by Enhancing Autophagy and Reducing Apoptosis in Neonatal Mice. *Am J Respir Cell Mol Biol*. 2016;55(5):722-735. doi:10.1165/rcmb.2015-0349OC
203. Conrad M, Kagan VE, Bayir H, et al. Regulation of lipid peroxidation and ferroptosis in diverse species. *Genes Dev*. 2018;32(9-10):602-619. doi:10.1101/gad.314674.118
204. Xu W, Deng H, Hu S, et al. Role of Ferroptosis in Lung Diseases. *J Inflamm Res*. 2021;14:2079-2090. doi:10.2147/JIR.S307081
205. Sun L, Dong H, Zhang W, et al. Lipid Peroxidation, GSH Depletion, and SLC7A11 Inhibition Are Common Causes of EMT and Ferroptosis in A549 Cells, but Different in Specific

Mechanisms. *DNA*. 2021;40(2):172-183. doi:10.1089/dna.2020.5730
206. Rashidipour, Karami-Mohajeri, Mandegary, et al. Where ferroptosis inhibitors and paraquat detoxification mechanisms intersect, exploring possible treatment strategies. *Toxicology*. 2020;433. doi:10.1016/j.tox.2020.152407
207. Matsushita M, Freigang S, Schneider C, Conrad M, Bornkamm GW, Kopf M. T cell lipid peroxidation induces ferroptosis and prevents immunity to infection. *Journal of experimental medicine, The*. 2015;212(4):555-568. doi:10.1084/jem.20140857
208. Wenzel, Tyurina, Zhao, et al. PEBP1 Wardens Ferroptosis by Enabling Lipoxygenase Generation of Lipid Death Signals. *Cell*. 2017;171(3):628-641. doi:10.1016/j.cell.2017.09.044
209. Di Fiore JM, MacFarlane PM, Martin RJ. Intermittent Hypoxemia in Preterm Infants. *Clin Perinatol*. 2019;46(3):553-565. doi:10.1016/j.clp.2019.05.006
210. Martin RJ, Di Fiore JM, Macfarlane PM, Wilson CG. Physiologic basis for intermittent hypoxic episodes in preterm infants. *Adv Exp Med Biol*. 2012;758:351-358. doi:10.1007/978-94-007-4584-1_47
211. Abman SH. Bronchopulmonary dysplasia: "a vascular hypothesis." *Am J Respir Crit Care Med*. 2001;164(10 Part 1):1755-1756. doi:10.1164/ajrccm.164.10.2109111c
212. Coalson JJ, Bland RD. Pathology of Chronic Lung Disease of Early Infancy. In: Coalson JJ, Bland RD, eds. *Chronic Lung Disease in Early Infancy*. 00137 ed. ; 2000:85-124. doi:10.1201/b14831-6
213. Revhaug C, Zasada M, Rognlien AGW, et al. Pulmonary vascular disease is evident in gene regulation of experimental bronchopulmonary dysplasia. *J Matern Fetal Neonatal Med*. 2020;33(12):2122-2130. doi:10.1080/14767058.2018.1541081
214. Hurskainen M, Mižíková I, Cook DP, et al. Single cell transcriptomic analysis of murine lung development on hyperoxia-induced damage. *Nature Communications*. 2021;12(1). doi:10.1038/s41467-021-21865-2
215. del Cerro MJ, Sabaté Rotés A, Cartón A, et al. Pulmonary hypertension in bronchopulmonary dysplasia: Clinical findings, cardiovascular anomalies and outcomes. *Pediatr Pulmonol*. 2013;49(1):49-59. doi:10.1002/ppul.22797
216. Baker CD, Abman SH, Mourani PM. Pulmonary Hypertension in Preterm Infants with Bronchopulmonary Dysplasia. *Pediatr Allergy Immunol Pulmonol*. 2014;27(1):8-16. doi:10.1089/ped.2013.0323
217. Bush D, Mandell EW, Abman SH, Baker CD. Pulmonary Hypertension and Cardiac Changes in BPD. In: *Updates on Neonatal Chronic Lung Disease*. Elsevier; 2020:113-129. doi:10.1016/B978-0-323-68353-1.00008-7
218. Baker CD, Alvira CM. Disrupted lung development and bronchopulmonary dysplasia. *Curr Opin Pediatr*. 2014;26(3). doi:10.1097/MOP.0000000000000095
219. Jobe AJ. The new BPD: an arrest of lung development. *Pediatr Res*. 1999;46(6):641-643. doi:10.1203/00006450-199912000-00007
220. Akram Khondoker, Yates Laura, Mongey Róisín, et al. Live imaging of alveologenesis in precision-cut lung slices reveals dynamic epithelial cell behaviour. *Nature Communications*. 2019;10(1):1178. doi:10.1038/s41467-019-09067-3
221. Popova AP. Mesenchymal Cells and Bronchopulmonary Dysplasia: New Insights about the Dark Side of Oxygen. *Am J Respir Cell Mol Biol*. 2019;60(5):501-502. doi:10.1165/rcmb.2019-0010ED
222. Collins JJP, Lithopoulos MA, dos Santos CC, et al. Impaired Angiogenic Supportive Capacity and Altered Gene Expression Profile of Resident CD146+ Mesenchymal Stromal Cells Isolated from Hyperoxia-Injured Neonatal Rat Lungs. *Stem Cells Dev*. 2018;27(16):1109-1124. doi:10.1089/scd.2017.0145
223. Popova AP, Bentley JK, Cui TX, et al. Reduced platelet-derived growth factor receptor

expression is a primary feature of human bronchopulmonary dysplasia. *Am J Physiol Lung Cell Mol Physiol*. 2014;307(3):L231-L239. doi:10.1152/ajplung.00342.2013
224. Nardiello C, Morty R. MicroRNA in late lung development and bronchopulmonary dysplasia: the need to demonstrate causality. *Mol Cell Pediatr*. 2016;3(1):1-7. doi:10.1186/s40348-016-0047-5
225. Ebrahimi, Sadroddiny. MicroRNAs in lung diseases: Recent findings and their pathophysiological implications. *Pulm Pharmacol Ther*. 2015;34:55-63. doi:10.1016/j.pupt.2015.08.007
226. Zhang X, Peng W, Zhang S, et al. MicroRNA expression profile in hyperoxia-exposed newborn mice during the development of bronchopulmonary dysplasia. *Respir Care*. 2011;56(7):1009-1015. doi:10.4187/respcare.01032
227. Ranjan R, Lee YG, Karpurapu M, et al. p47phox and reactive oxygen species production modulate expression of microRNA-451 in macrophages. *Free Radical Research*. 2015;49(1):25-34. doi:10.3109/10715762.2014.974037
228. Si M-L, Zhu S, Wu H, Lu Z, Wu F, Mo Y-Y. miR-21-mediated tumor growth. *Oncogene*. 2007;26(19):2799-2803. doi:10.1038/sj.onc.1210083
229. Chan JA, Krichevsky AM, Kosik KS. MicroRNA-21 Is an Antiapoptotic Factor in Human Glioblastoma Cells. *Cancer Res*. 2005;65(14):6029-6033. doi:10.1158/0008-5472.CAN-05-0137
230. Bhaskaran M, Xi D, Wang Y, et al. Identification of microRNAs changed in the neonatal lungs in response to hyperoxia exposure. *Physiol Genomics*. 2012;44(20):970-980. doi:10.1152/physiolgenomics.00145.2011
231. Hu Y, Xie L, Yu J, Fu H, Zhou D, Liu H. Inhibition of microRNA-29a alleviates hyperoxia-induced bronchopulmonary dysplasia in neonatal mice via upregulation of GAB1. *Mol Med*. 2020;26(1). doi:10.1186/s10020-019-0127-9
232. Wang K, Qin S, Liang Z, et al. Epithelial disruption of Gab1 perturbs surfactant homeostasis and predisposes mice to lung injuries. *Am J Physiol Lung Cell Mol Physiol*. 2016;311(6):L1149-L1159. doi:10.1152/ajplung.00107.2016
233. Fulci V, Scappucci G, Sebastiani GD, et al. miR-223 is overexpressed in T-lymphocytes of patients affected by rheumatoid arthritis. *Hum Immunol*. 2010;71(2):206-211. doi:10.1016/j.humimm.2009.11.008
234. Neudecker V, Brodsky KS, Clambey ET, et al. Neutrophil transfer of miR-223 to lung epithelial cells dampens acute lung injury in mice. *Sci Transl Med*. 2017;9(408):EAAH5360. doi:10.1126/scitranslmed.aah5360
235. Zhu H, Leung S. Identification of microRNA biomarkers in type 2 diabetes: a meta-analysis of controlled profiling studies. *Diabetologia*. 2015;58(5):900-911. doi:10.1007/s00125-015-3510-2
236. Neudecker V, Haneklaus M, Jensen O, et al. Myeloid-derived miR-223 regulates intestinal inflammation via repression of the NLRP3 inflammasome. *Journal of experimental medicine, The*. 2017;214(6):1737-1752. doi:10.1084/jem.20160462
237. Feng Zunyong, Qi Shimei, Zhang Yue, et al. Ly6G+ neutrophil-derived miR-223 inhibits the NLRP3 inflammasome in mitochondrial DAMP-induced acute lung injury. *Cell Death Dis*. 2017;8(11):E3170. doi:10.1038/cddis.2017.549
238. Syed Mansoor, Das Pragnya, Pawar Aishwarya, et al. Hyperoxia causes miR-34a-mediated injury via angiopoietin-1 in neonatal lungs. *Nature Communications*. 2017;8(1):1173. doi:10.1038/s41467-017-01349-y
239. Li D, Cheng H, Chen L, Wu B. Research Article Differential expression of microRNAs in a hyperoxia-induced rat bronchopulmonary dysplasia model revealed by deep sequencing. *Genet Mol Res*. 2021;20(2). doi:10.4238/gmr18751
240. XING Y, FU J, YANG H, et al. MicroRNA expression profiles and target prediction in

neonatal Wistar rat lungs during the development of bronchopulmonary dysplasia. *International Journal of Molecular Medicine*. 2015;36(5):1253-1263. doi:10.3892/ijmm.2015.2347

241. Du Y, Ding Y, Chen X, et al. MicroRNA-181c inhibits cigarette smoke–induced chronic obstructive pulmonary disease by regulating CCN1 expression. *Respir Res*. 2017;18(1). doi:10.1186/s12931-017-0639-1
242. Kayton A, Timoney P, Vargo L, Perez JA. A Review of Oxygen Physiology and Appropriate Management of Oxygen Levels in Premature Neonates. *Adv Neonatal Care*. 2018;18(2):98-104. doi:10.1097/ANC.0000000000000434
243. Velten M, Heyob KM, Rogers LK, Welty SE. Deficits in lung alveolarization and function after systemic maternal inflammation and neonatal hyperoxia exposure. *J Appl Physiol (1985)*. 2010;108(5):1347-1356. doi:10.1152/JAPPLPHYSIOL.01392.2009
244. Yee M, Chess PR, McGrath-Morrow SA, et al. Neonatal oxygen adversely affects lung function in adult mice without altering surfactant composition or activity. *Am J Physiol Lung Cell Mol Physiol*. 2009;297(4):L641-L649. doi:10.1152/AJPLUNG.00023.2009
245. Wang H, Jafri A, Martin RJ, et al. Severity of neonatal hyperoxia determines structural and functional changes in developing mouse airway. *Am J Physiol Lung Cell Mol Physiol*. 2014;307(4):L295-L301. doi:10.1152/ajplung.00208.2013
246. Menon, Shrestha, Reynolds, Barrios, Shivanna. Long-term pulmonary and cardiovascular morbidities of neonatal hyperoxia exposure in mice. *Int J Biochem Cell Biol*. 2018;94:119-124. doi:10.1016/j.biocel.2017.12.001
247. Dutta S, Sengupta P. Rabbits and men: relating their ages. *J Basic Clin Physiol Pharmacol*. 2018;29(5):427-435. doi:10.1515/jbcpp-2018-0002